This is to certify that the
dissertation entitled

Aqueous-Phase Catalytic Hydrogenation of Organic Acids and Their Mixtures

presented by

Yuqing Chen

has been accepted towards fulfillment
of the requirements for the

Ph.D. degree in Chemical Engineering and Materials Science

Dennis J. Miller
Major Professor's Signature

8/21/07
Date

Aqueous-Phase Catalytic Hydrogenation of Organic Acids and Their Mixtures

By

Yuqing Chen

A DISSERTATION

Submitted to
Michigan State University
in partial fulfillment of the requirements
for the degree of

DOCTOR OF PHILOSOPHY

Department of Chemical Engineering and Materials Science

2007

ABSTRACT

Aqueous-Phase Catalytic Hydrogenation of Organic Acids and Their Mixtures

By

Yuqing Chen

Biomass-based organic acids are attractive feedstocks for chemicals production because they are available in large quantities and can undergo a variety of reactions to useful products. Hydrogenation of organic acids yields value-added alcohol products that are important building blocks for pharmaceuticals, foods, agricultural chemicals, and polymers. Carrying out hydrogenation in water over heterogeneous metal catalysts eliminates waste generation associated with traditional hydride reagents, facilitates viable reaction rates at mild conditions, allows easy catalyst separation and reuse, and avoids organic solvents. Further, the mild aqueous environment allows transfer of chirality present in bio-derived organic acids to their alcohol products, giving high-value, optically pure materials in a single step. Development of low-cost, high-efficiency hydrogenation routes could open economically viable pathways from renewable resource-derived materials as alternatives to today's petroleum-based chemicals.

We investigated the aqueous-phase hydrogenation of lactic acid and propionic acid and their mixtures, as well as mixtures of the acids with their alcohol products propylene glycol and 1-propanol, over Ru/C and Ru sponge catalysts in a three-phase stirred batch reactor. The goals of the work are to examine the acids' relative hydrogenation reactivities, the substrates' and products' relative affinities for metal surface sites, and how one substrate's conversion is influenced by other acid or alcohol

species in solution. By relating adsorption affinity and reactivity to substrate structure and feedstock composition, we aim to provide a rational basis for design of aqueous-phase heterogeneous hydrogenation catalysts and processes.

For the study of acid hydrogenation over Ru/C catalyst, kinetic data were collected for reactions at 343-423 K, 3.4-10.3 MPa hydrogen pressure and 0.05-5 M acid feed concentrations. Mass-transfer analysis showed that acid conversion rates were not limited by mass-transport resistances over the reaction conditions studied. A two-site Langmuir-Hinshelwood (L-H) kinetic model with a single set of rate and adsorption constants fits the conversion kinetics of both individual and mixed acid hydrogenations over a wide range of condition. Competitive adsorption of acids and their alcohol products strongly affects hydrogenation rates.

Hydrogenation reactions over Ru sponge catalyst were conducted at 403 K, 3.4-7.9 MPa hydrogen pressure and 0.1-1 M acid feed concentrations. The same two-site L-H model with a new set of kinetic constants was used to characterize acid hydrogenations over Ru sponge. Hydrogenation reactivity/selectivity and competitive adsorption of the reacting species on Ru sponge are significantly different from that on Ru/C.

The activated carbon support material facilitates selective adsorption of acids or alcohols into the carbon pore structure, which results in higher local concentrations in the vicinity of the catalyst and thus influences the observed hydrogenation rates. Adsorption of reactant and product species into the activated carbon support was studied for the prediction of local pore concentrations. A global model that incorporates local pore concentrations into the hydrogenation kinetics over Ru sponge was used to predict hydrogenation rates of organic acids over Ru/C catalyst in water.

ACKNOWLEDGMENT

I would like to thank Dr. Dennis Miller for his guidance and support as my research advisor through my Ph.D. studies. I would also like to thank Dr. James Jackson, Dr. Lawrence Drzal, Dr. Milton Smith and Dr. Ramani Narayan for serving on my graduate committee. Thanks to Miller-Jackson group members Lars Peereboom, Navin Asthana, Yaoyan Xi, Ketan Pimparkar and Xi Hong for discussion and help during this project.

TABLE OF CONTENTS

LIST OF TABLES

LIST OF FIGURES

LIST OF SCHEMES

LIST OF SYMBOLS AND ABBREVIATIONS

English:

a = effective interfacial area per unit volume reaction fluid [1 / m]

a_p = external area of catalyst particles per unit volume reaction fluid [1 / m]

C_A = concentration of species A at time t

C_{A0} = initial concentration of species A

$C_{Acid,L}$ = bulk liquid concentration of the acid [kmol / m^3]

$C_{Acid,S}$ = catalyst surface concentration of the acid [kmol / m^3]

C_{H2}^* = gas-phase concentration of hydrogen [kmol / m^3]

$C_{H2,L}$ = bulk liquid concentration of hydrogen = aqueous-phase hydrogen solubility at the hydrogen partial pressure of the experiment [kmol / m^3]

$C_{H2,S}$ = catalyst surface concentration of hydrogen [kmol / m^3]

C_s = liquid phase concentration at the catalyst surface [mol / L]

C_{t1} = total catalyst site concentration for acid and alcohol adsorption [kmol / kg catalyst]

C_{t2} = total catalyst site concentration for hydrogen adsorption [kmol / kg catalyst]

D = diffusion rate [m / s^2]

$D_e = \varepsilon^2 D_j$ = effective diffusivity [m^2 / s]

D_j = diffusivity of reactant j in the liquid phase estimated using the Wilke-Chang equation

d_I = impeller diameter [m]

d_P = particle diameter [m]

d_R = reactor diameter [m]

$E_{Act.}$ = activation energy [J / mol]

ee = enantiomeric excess

g = gravitation constant [9.8066 m / s^2]

$H_A(T)$ = Henry's Law constant for A in a specific solvent [atm / (mole A/mole solution)]

K_{Acid} = adsorption constant for each acid [m^3 / kmol]

$K_{Alcohol}$ = adsorption constant for each alcohol product [m^3 / kmol]

K_{H2} = adsorption constant for hydrogen [1 / MPa]

Kow = octanol-water partition coefficient

k = reaction rate constant

k_o = pre-exponential factor

k_a = rate constant of adsorption process

k_{Acid} = composite rate constant for each acid [m^3 / kg catalyst / MPa / sec]

k_d = rate constant of desorption process

k_{sA} = surface reaction rate constant for each acid [(kg catalyst)^2 / kmol^2 / sec]

$k_{LS,Acid}a_p$ = L-S mass transfer coefficient of the acid [1 / s]

$k_{LS,H2}a_p$ = L-S mass transfer coefficient of hydrogen [1 / s]

L = characteristic length of the catalyst [m] = d_p / 6 for spherical particles

LA = lactic acid

L-H kinetic model = Langmuir-Hinshelwood kinetic model

M_B = molecular weight of solvent [g / mol]

N = number of adsorbed molecules [kmol / kg catalyst]

N_{min} = minimum stirring speed for complete catalyst suspension [rotations / sec]

P = bulk gas pressure [atm]

P_A = partial pressure of species A in the gas phase [atm]

PA = propionic acid

PG = propylene glycol; 1,2-propanediol

1-PrOH = 1-propanol

R = ideal gas constant [J / mol / K]

$-r_A$ = conversion rate of species A [kmol species A / m^3 / s]

$-r_{Acid}$ = observed reaction rate of the acid [kmol / m^3 / s]

$-r_{H2}$ = observed reaction rate of hydrogen [kmol / m^3 / s]

S = total number of available sites [kmol / kg catalyst]

S_T = surface tension [N / m]

Sh = Sherwood number [dimensionless]

T = absolute temperature [K]

u_g = superficial gas velocity [cm / s]

V_j = molar volume of j as liquid at its normal boiling point [cm^3 / g mol]

V_L = volume of the solution [cm^3]

x_A = mole fraction of species A in the liquid phase

y_A = mole fraction of species A in the gas phase

Greek:

ε = support porosity

$\eta\varphi^2$ = observable modulus

θ = fraction of surface coverage

μ_L = liquid viscosity [kg / m·s]

ρ_P = particle density [kg / m^3]

ρ_L = liquid density [kg / m^3]

ϕ_B = association parameter for solvent = 2.6 for water

w = catalyst loading [grams of catalyst / 100 grams of solution]

Chapter 1. Background

1.1. Introduction

Organic acids are attractive biorenewable intermediates because they can be produced in large quantities via fermentation of carbohydrate monomers and can undergo a variety of reactions to useful products.[1] Hydrogenation of organic acids yields alcohol products that are important building blocks for pharmaceuticals, foods, agricultural chemicals, and polymers.[2] Carrying out hydrogenation in water, the "native" solvent for fermentation-derived substrates, in the presence of heterogeneous supported metal catalysts eliminates waste generation associated with traditional hydride reagents (e.g. $LiAlH_4$), facilitates viable reaction rates at mild conditions, allows easy catalyst separation and reuse, and avoids organic solvents. Further, the mild aqueous environment allows transfer of chirality present in bio-derived organic acids to their alcohol products, giving high-value, optically pure materials in a single step.[3] The development of low-cost, high-efficiency hydrogenation routes will open economically viable pathways from renewable resource-derived materials as alternatives to today's petroleum-based chemicals.

1.2. Research objectives

Hydrogenation of organic carboxylic acids to alcohols has been extensively investigated. Most of the previous research has focused on catalyst modifications, and control of process variables as a means to improve the yield and selectivity to the desired alcohols. However, some potentially important mechanistic details are far from

understood, such as competitive adsorption of species on the catalyst surface, and the relationship between substrate-metal interactions and reactivity. Ignoring these mechanistic details leads to poor assumptions when determining the correct model describing the reaction system.

To improve our understanding of organic acid hydrogenation to alcohol products, we investigate the hydrogenation of lactic acid (2-hydroxypropanoic acid, herein LA) and propionic acid (propanoic acid, herein PA) alone, together, and in mixtures with their alcohol products propylene glycol (1,2-propanediol, herein PG) and 1-propanol (herein 1-PrOH), over ruthenium metal catalysts in a three-phase stirred batch reactor. Such competition studies illuminate the acids' relative hydrogenation reactivities, the substrates' and products' relative affinities for metal surface sites, and how one substrate's conversion is influenced (usually inhibited) by other acid or alcohol species in solution. By relating adsorption affinity and reactivity to substrate structure and feedstock composition, we aim to provide a rational basis for design of aqueous-phase heterogeneous hydrogenation catalysts and processes.

1.3. Organic acid hydrogenation

Organic acids compose a major class of renewable-resource feedstock chemicals. Some organic acids are traditionally produced via fermentation of biomass-derived glucose, including citric acid, gluconic acid, itaconic acid, lactic acid, and acetic acid. Fermentation technologies to several other organic acids are currently under development, including routes to succinic acid, propionic acid, butyric acid, fumaric acid, and poly-(3-hydroxybutyric) acid.[1] In addition, amino acids are formed predominantly by

fermentation or enzymatic conversion. Because of their multiple functional groups and high reactivity, organic acids undergo a variety of reactions to valuable products, including esterification, condensation, dehydration, oxidation, and hydrogenation.

Hydrogenation is the addition of gaseous hydrogen to saturate a double bond (e.g. C = O or C = C). Generally, hydrogenation of organic carboxylic acids to alcohols is not easy, and vigorous conditions are needed for successful reduction on a synthetic scale. Because molecular hydrogen is not reactive chemically at low temperature and it's solubility in aqueous phase is very low at low pressure, almost all hydrogenation reactions need catalysts, elevated temperature and high pressure.

The most commonly used hydrogenation catalysts are metals, metal oxides and some salts in solid state, such as Raney Ni, Ni/Al_2O_3, Pd/carbon, Ru/carbon, Ru/TiO_2, Ru/Al_2O_3, Rh_2O_3 and $CuCrO_x$. To increase the surface area, and therefore the number of active sites, solid catalysts are often finely dispersed on the surface of a supporting material. Hydrogenation selectivity is directly influenced by the choice of catalyst and the quantity of catalyst used. In spite of the hundreds of techniques available for studying catalyst surfaces, it is much more difficult to study heterogeneous reactions than it is to study reactions where all species are in solution. Also, many heterogeneous catalysts produce a wide range of products and have no single mechanism of action. Because of this, the exact mechanisms for many seemingly simple reactions catalyzed by metals are still poorly understood.

1.3.1. Literature review

Hydrogenation of organic acids and esters over metal catalysts has been the subject of numerous studies over the last several decades. In 1934, Bowden and Adkins[4] studied the hydrogenation of optically active esters and ketones to optically active alcohols over copper-chromium oxide and nickel catalysts under 15-20 MPa H_2 pressure at 250°C. The paper of Adkins and Pavlic[5] published in 1947 was about hydrogenation of amino acid esters over Raney nickel in ethanol. By using high loadings of catalyst and lower temperatures (25-75°C), they could obtain the corresponding amino alcohols at increased yields and purities. In the 1950's, Carnahan and Ford[6] used ruthenium based catalysts (RuO_2 and Ru/C) to directly hydrogenate organic acids such as acetic acid, oxalic, adipic, succinic, and hydroxyacetic acid at low temperatures (94-192°C) and high H_2 pressures (over 50 MPa) with yields ranging from 47 % to 88 %. In Broadbent's paper,[7] they described the hydrogenation of organic acids catalyzed by rhenium powder prepared *in situ* at 137-286°C and 15-33 MPa H_2 pressures, including formic, acetic, propionic, butyric, capric, lauric, stearic, lactic, maleic, succinic, and glutaric acid. Miroslav's patent[8] showed the hydrogenation of fluorine-containing alkyl, cycloalkyl, and benzene carboxylic acids using solid rhodium or iridium as the catalyst. The patent granted to Antons[9] reported their study about hydrogenation of lactic and maleic acid over ruthenium catalysts. At temperatures of 60-70°C and 10 MPa H_2 pressure, they produced optically active alcohols with enantiomeric excess over 90 %. Dumesic[10] investigated the vapor phase lactic acid hydrogenation over silica-supported copper. They produced propylene glycol with 88 % yield and high selectivity at 200°C and a hydrogen pressure of 0.7 MPa. Recently, Mao *et al*[11] published their work on hydrogenation of

carboxylic acids catalyzed by magnesia-supported poly-γ-aminopropylsiloxane-Ru complex (*MgO-NH_2-Ru*). This complex catalyst was able to catalyze the hydrogenation of acetic acid, propionic acid, lactic acid and isobutyric acid to the corresponding alcohols with 100 % yields in the presence of water at 240°C and 5 MPa H_2.

1.3.2. Previous work on organic acid hydrogenation in our research group

Worldwide production of lactic acid (LA) has increased steadily since the early 1990s, and is expected to rise still further. Propylene glycol (PG) is a valuable commodity chemical that finds many uses in foods and consumer products. Lactic acid hydrogenation to PG in aqueous solution was investigated by Zhang, Z. *et al.*[2] Ruthenium on activated carbon was identified as an active and selective catalyst for this reaction. Under optimal conditions (150°C and 10-14 MPa H_2), over 90 % PG selectivity with 95 % LA conversion was achieved in both a batch autoclave reactor and continuous trickle bed reactor. At temperatures lower than 100°C, optically active S-PG is formed from fermentation-derived L-LA with about 100 % ee. These initial studies demonstrated higher sustained PG yields at milder reaction conditions than prior studies that used either lactate esters or aqueous-phase free LA as the starting material.

Amino alcohols are important building blocks in agricultural, pharmaceutical, and peptide chemistry, and are also utilized as chiral auxiliaries. Hydrogenation of L-alanine (2-aminopropanoic acid) to the corresponding amino alcohol was studied by Jere, F. T. *et al.*[3] At 100°C and 6.9 MPa of hydrogen, aqueous L-alanine undergoes facile hydrogenation to L-alaninol over a 5 % Ru/C catalyst. In the presence of sufficient phosphoric acid, protonated L-alaninol was formed with selectivity exceeding 95% and

enantiomeric excess (ee) over 99 %. The retention of stereochemistry at the amine-bearing sp^3 C site was the most unexpected finding in this work. Understanding the configuration of alanine adsorbed on the catalyst, and thus the mode by which stereochemistry is retained represents a major technical challenge associated with this condensed-phase catalytic hydrogenation.

1.4. Competitive adsorption

1.4.1. Traditional adsorption theory

Adsorption is the binding of molecules or particles to a surface. It is usually an exothermic process. Molecules can interact with a surface via a physical process (physisorption) or a chemical process (chemisorption). A comparison of physisorption and chemisorption is shown in Table 1.1.

Table 1.1. Comparison of physisorption and chemisorption[12]

Comparison	Physisorption	Chemisorption
Attractive forces	Van der Waals; electrostatic interactions	strong chemical bonds formation; involve sharing or transfer of electrons
Adsorption energy	less than 80 kJ / mol	200 kJ / mol or more
Adsorption conditions	takes place on all surfaces provided that T and P are favorable	highly selective; occurs only between chemically active surface and certain adsorbate
Adsorption layer	multi-layer	single-layer
Reversibility	reversible	irreversible

In an adsorption process, molecules in the free gaseous state are in a dynamic equilibrium with adsorbed molecules. The relationship between the quantity of molecules adsorbed and the pressure of gas at a fixed temperature is called the adsorption isotherm.

The famous Langmuir isotherm[13] developed in 1916 was based on three assumptions: (1) monolayer adsorption; (2) all active surface sites are equivalent and only one molecule at a time can occupy a site; (3) there are no attractive or repulsive interactions between adsorbed molecules, even at high fractional coverage. Consider the reaction:

$$A\ (g) + M\ (\text{active surface site}) \leftrightarrow A\text{-}M$$

At equilibrium:

$$\theta = \frac{N}{S} = \frac{KP}{1+KP} \tag{1.1}$$

$$K = \frac{k_a}{k_d} \tag{1.2}$$

Where:

θ = fraction of surface coverage

N = number of adsorbed molecules [kmol / kg catalyst]

S = total number of available sites [kmol / kg catalyst]

P = bulk gas pressure [atm]

k_a = rate constant of adsorption process

k_d = rate constant of desorption process

1.4.2. Methods for aqueous-phase adsorption studies

To understand the mechanism of a catalytic reaction, it is advantageous to characterize the adsorbed species in detail – to have information on their structure, energetics (ΔH_{ad}) and dynamics. Over the past few decades, many advanced techniques have been developed for studying the metal catalyst surface and the absorbed molecules.

For our special aqueous-phase catalytic hydrogenation systems, the most commonly used methods are solution analysis, ATR-IR technique, and isotopic labeling.

Solution analysis is a simple and straightforward method to determine the quantity of species adsorbed on metal surfaces by measuring the difference between the initial and final concentrations in solution before and after adsorption. The major disadvantage of this method is its low sensitivity due to the relatively large quantity of solution per gram of catalyst present. The quantity adsorbed must often be determined by small differences in solution concentration.

Vibrational spectroscopy, most prominently infrared spectroscopy (IR), plays an important role in heterogeneous catalysis research. A vibrational spectrum contains detailed information about the nature of adsorbed molecules, interaction mode between the surface and the adsorbate, and intermolecular interactions within the adsorbate layer. The use of infrared spectroscopy to investigate aqueous systems has been previously hindered by the strong IR absorptions of water. Attenuated total reflection infrared spectroscopy (ATR-IR) holds promise as an effective means for probing the solid-liquid interfaces in aqueous solution. It overcomes the water adsorption because the evanescent wave selectively probes the region near the interface, so that the contribution from the liquid can be kept reasonably small.[14] Figure 1.1 depicts an ATR cell used for in situ adsorption measurements. In contrast to transmission IR spectroscopy where the IR beam passes directly through the sample, in the ATR mode the IR radiation is coupled into the internal reflection element (IRE), an IR transparent crystal of high refractive index in contact with the sample. The IR radiation propagates through the IRE at an angle of incidence larger than the critical angle, such that total reflection occurs at the IRE-sample

interface. An evanescent electromagnetic field is generated that penetrates into the sample and is attenuated by the sample, thus producing an IR spectrum. Since the earliest work in the late 1980s and early 1990s,[15,16] several research groups have implemented ATR for catalytic studies.[17,18] These researchers have presented methods for depositing thin layers of catalyst particles on ATR windows as well as detailed descriptions of background subtraction techniques. ATR-IR technique provides a starting point to gain structural and semi-quantitative adsorption data for our special reaction system.

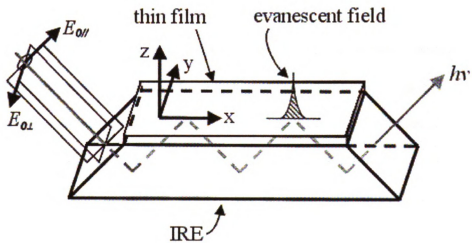

Figure 1.1. ATR cell used for in situ adsorption measurements.

Isotopic labeling (H-D exchange) provides non-destructive measure of substrate-catalyst interactions. Examining H-D exchange rate of a specific organic acid helps to determine the reactivity of hydrogen atoms on different carbons in the acid. H-D exchange between D_2O and hydrogen yields important information about water-catalyst interaction and thus the role of water in aqueous phase hydrogenation. The extent of H-D exchange can be measured by ^{1}H-NMR or indirectly (inorganic molecules) via ^{13}C-NMR.

1.4.3. Relevant results from literature and the previous work in our research group

Competitive adsorption for surface sites is created when the adsorption system involves more than one adsorbate. A few studies have probed catalyst adsorption of organic acids, particularly acetic and formic acid, relative to their configurations on the metal surface.[19] In examining the catalytic production of ethylene glycol (EG) and propylene glycol (PG) from glycerol with 5 wt% Ru/C catalyst, Lahr and Shanks[20] addressed competitive adsorption involving those three polyols, but few other analyses of substrate-catalyst interactions in heterogeneous aqueous phase catalysis have been reported. Lahr and Shanks examined the degradation of EG and PG and found that PG degraded at a slightly faster rate than EG. However, introducing the mixture of EG and PG into the reactor resulted in significantly higher fractional turnover for EG than that for PG. This result indicated that PG was less competitive for active sites than EG. The difference in adsorption behavior for EG and PG was attributed to their different structures; these polyols adsorb presumably to ruthenium through oxygen, so the presence of a hydrophobic nonoxygenated end in PG may cause it to be partially repelled by the polar catalytic surface, thus decreasing its binding energy and allowing EG to adsorb more readily on the surface sites. In the kinetic study of glycerol conversion, they found that the reaction rate of glycerol decreased in proportion to the amount of EG added while the addition of PG had a minimal effect on this reaction rate. This behavior indicated that glycerol and EG competed relatively equally for active sites on the ruthenium metal surface.

Some results from the previous work in our research group provided an important starting point in addressing the issue of competitive adsorption of species on the catalyst

from aqueous solution. D. Kovacs[21] studied C-H activation in PG over Ru by using chirality and isotopic exchange. She found that without lactic acid present, H-D exchange at C2 of optically pure S-PG in solution was accompanied by rapid racemization, but, if an equal molar quantity of L-lactic acid was added to the solution along with the S-PG, the observed rate of H-D exchange was significantly decreased and the extent of PG racemization was minimized. This behavior clearly showed that compared to lactic acid PG was weakly adsorbed onto Ru. More importantly, the reduced racemization of PG upon adding lactic acid indicates that lactic acid may exhibit a "templating" behavior that retains or generates chirality. Works by Zhang[2] and Jere[3] showed that the presence of 3 wt % (0.33M) alanine reduced lactic acid (1.3M feed concentration) conversion from 60 % to 25 %, and this effect was completely reversible. This result indicated that alanine was able to exclude lactic acid from the catalyst surface by blocking adsorption sites. Moreover, the fact that alanine conversion was only about 50 % at these conditions indicated that adsorption ability was not necessarily related to reactivity; otherwise nearly complete conversion of alanine would be expected.

1.5. Kinetic model for catalytic reactions

1.5.1. Langmuir-Hinshelwood (L-H) kinetic model

A catalytic reaction proceeds through a particular sequence of individual steps called the reaction mechanism. This series of steps serves as the basis for development of the mathematical description of the reaction kinetics, called the rate expression. The first goal of any kinetic study is to get an accurate predictive relationship between the rate of

reaction and the experimental parameters controlling it, which are primarily the temperature and concentrations (or partial pressures) of the reactants. If conversions are high enough, then consideration of the influence of the products may also be required, both in regard to competitive adsorption and to the reverse reactions if conversions are too close to the equilibrium conversion.[22] It is important that one works with kinetic data free from any significant artifacts, particularly heat and mass transfer limitations, in order that the postulated rate expression describes the intrinsic reaction kinetics.

In 1920s Langmuir[23] studied the kinetics of surface reactions and introduced what is now known as the "Langmuir isotherm" to relate the coverage, or surface concentration, of a reactant or product species with its gas-phase or liquid-phase concentration, which can be measured. This approach was further developed by Hinshelwood[24,25] into the "Langmuir-Hinshelwood mechanism" of heterogeneous reactions, and the resulting rate expressions are referred to as "Langmuir-Hinshelwood models". The Langmuir-Hinshelwood (L-H) mechanism has found use in correlating and interpreting rate data for many reactions taking place on solid surfaces. This mechanism consists of the following types of steps: (1) adsorption of the reactants on the active sites; (2) dissociation of molecules at the surface; (3) reactions between adsorbed molecules on the surface; (4) desorption of the products from the active sites. Two simplifying assumptions for the model are that: (1) one step is the rate-determining step, and (2) one surface intermediate is dominant and thus all the other intermediates are present in relatively insignificant amounts. When Langmuir-Hinshelwood kinetics are postulated, it is reasonable to expect that the rate constant will show Arrhenius temperature dependence, while the adsorption equilibrium constants will decrease with temperature.[26]

1.5.2. Relevant results from literature and the previous work in our research group

We have previously demonstrated aqueous-phase hydrogenation of lactic acid and L-alanine over 5 wt% Ru/C catalyst, and have reported reaction kinetics for each system.[27,28] For the hydrogenation of lactic acid to propylene glycol, Zhang[27] proposed a one-site Langmuir-Hinshelwood (L-H) kinetic model in which lactic acid and molecular hydrogen adsorb on the same surface catalytic site. A two-site L-H model was first used in our group by Jere[28] for stereoretentive amino acid hydrogenation, where protonated alanine and undissociated phosphoric acid compete for one set of surface sites and hydrogen dissociatively adsorbs on a second set of sites. The molecular modeling results of Neurock[29] for the hydrogenation of acetic acid over palladium support this two-site approach, as they show that the adsorbed acid is bound by carboxylate ~2 Å above catalyst surface palladium atoms while hydrogen nestles in the 3-fold coordinated interstices between surface metal atoms. Dissociative hydrogen adsorption on metal surfaces is widely accepted in the literature.[30]

1.6. References

(1) Sriram Varadarajan, S.; Miller, D. J., Catalytic upgrading of fermentation-derived organic acids. *Biotechnol. Prog.* **1999**, *15*, 845.

(2) Zhang, Z.; Jackson, J. E.; Miller, D. J., Aqueous-phase hydrogenation of lactic acid to propylene glycol. *Appl. Catal. A.* **2001**, 219, 89.

(3) Jere, F. T.; Miller, D. J.; Jackson, J. E., Stereoretentive C-H Bond Activation in the Aqueous Phase Catalytic Hydrogenation of Amino Acids to Amino Alcohols. *Org. Lett.* **2003**, 5, 527.

(4) Bowden, E.; Adkins, H., *J. Am. Chem. Soc.*, **1934**, *56*, 689.

(5) Adkins, H.; Pavlic, A.A., *J. Am. Chem. Soc.*, **1947**, *69*, 3039.

(6) Carnahan, J.E. et al., *J. Am. Chem. Soc.*, **1955**, *77*, 3766.

(7) Broadbent, H. S.; Campbell, G. C.; Bartley, W. J.; Johnson, J. H. *J. Am. Chem. Soc.* **1959**, *24*, 1847.

(8) Novotny; Miroslav. U.S. Patent 2,607,807, **1981**.

(9) Antons, S.; Tilling, A. S.; Wolters, E. U.S. Patent 6,355,848, **2002**.

(10) Cortright, R. D.; Sanchez-Castillo, M.; Dumesic J. A. *Applied Catal B: Env.* **2002**, *39*, 353.

(11) Bao-Wei Mao; Zhong-Zhan Cai, Mei-Yu Huang and Ying-Yan Jiang. *Polym. Adv. Technol.* **2003**, *14*, 278.

(12) Paul A. Webb, Introduction to Chemical Adsorption Analytical Techniques and their Applications to Catalysis. *MIC Technical Publications*, January **2003**.

(13) Michael J. Pilling and Paul W. Seakins, *Reaction Kinetics*, page 179, **1995**, New York.

(14) Davide Ferri, Thomas Bulrgi, and Alfons Baiker. *J. Phys. Chem. B*, **2001**, 105, 3187.

(15) Zippel, E.; Breiter, M. W.; Kellner, R. *J. Chem. Soc.* **1991**, 87 (4), 637.

(16) Blesa, M. A.; Weisz, A. D.; Morando, P. J.; Salfity, J. A.; Magaz, G. E.; Regazzoni, A. E. *Coordin. Chem. Rev.* **2000**, 196, 31.

(17) McQuillan, J. *Adv. Mater.* **2001**, 13, 1034.

(18) Baiker, A. *Chimia* **2001**, 55, 796.

(19) Pallassana, V.; Neurock, M. Reaction paths in the hydrogenolysis of acetic acid to ethanol over Pd (III), Re (0001), and PdRe alloys. *J. Catal.* **2002**, 209 (2), 289.

(20) Daniel G. Lahr and Brent H. Shanks. Kinetic analysis of the hydrogenolysis of lower polyhydric alcohols: glycerol to glycols. *Ind. Eng. Chem. Res.* **2003**, *42*, 5467.

(21) Kovacs, D., D. J. Miller, and J. E. Jackson, "On the mechanism of catalytic hydrogenation of lactic acid to propylene glycol", Paper #340, 221st ACS National Meeting, San Diego, CA, April, **2001**.

(22) M. Albert Vannice, *Kinetics of Catalytic Reactions*, page 106, **2005**, New York.

(23) I. Langmuir, *Trans. Faraday Soc.* **1921**, *17*, 621.

(24) C. N. Hinshelwood, "Kinetics of Chemical Change in Gaseous Systems", Clarendon, Oxford, **1926**.

(25) C. N. Hinshelwood, "The Kinetics of Chemical Change", 4th Ed., Oxford Press, Oxford, **1940**.

(26) Lee, Hong H., *Heterogeneous Reactor Design*, page 63, **1985**, Butterworth Publishers.

(27) Zhang, Z.; Jackson, J. E.; Miller, D. J. Kinetics of aqueous phase hydrogenation of lactic acid to propylene glycol. *Ind. Eng. Chem. Res.* **2002**, *41*, 691.

(28) Jere, F.; Jackson, J. E.; Miller, D. J. Kinetics of aqueous phase hydrogenation of L-alanine to L-alaninol. *Ind. Eng. Chem. Res.* **2004**, *43*, 3297.

(29) Pallassana, V.; Neurock, M. Reaction paths in the hydrogenolysis of acetic acid to ethanol over Pd (III), Re (0001), and PdRe alloys. *J. Catal.* **2002**, 209 (2), 289.

(30) Singh, U.K.; Vannice, M.A. Kinetics of liquid phase hydrogenation reactions over supported metal catalysts – A review. *Appl. Catal. A: Gen.* **2001**, 213(1), 1.

Chapter 2. Experimental Methods

2.1. Hydrogenation of organic acids over carbon-supported and unsupported ruthenium catalysts

Hydrogenation of lactic acid, propionic acid, acid mixtures, and combinations of acids with their alcohol products in aqueous solution were performed in a laboratory-scale stirred batch reactor. Liquid phase products were analyzed using high performance liquid chromatography (HPLC) and gas phase samples were analyzed on a Varian 3300 GC instrument.

2.1.1. Materials

The main reactants for hydrogenation were lactic acid, propionic acid, 1,2-propanediol (propylene glycol), 1-propanol and hydrogen. Reagent-grade D,L-lactic acid (85% solution in water) and 1-propanol (99 %) were purchased from Aldrich Chemical Co. Propionic acid (>99%) was obtained from J.T. Baker, and propylene glycol (99.5%) was ordered from Jade Scientific. Feed materials were prepared using HPLC grade water (J.T. Baker). Ultrahigh-purity hydrogen gas (99.999%, AGA) was used without further purification in all experiments.

The catalysts used in the experiments were (1) a 5 wt % ruthenium on activated carbon powder (Ru/C) or (2) a nonporous ruthenium sponge. The 5 wt % Ru/C was obtained from PMC, Inc. with a mean particle diameter of 150 μm, a N_2 BET surface area of 715.6 m^2/g, a porosity of 0.6, and a dry particle density of 800 kg/m^3. The ruthenium metal dispersion of the as-received catalyst, measured by volumetric hydrogen

chemisorption in a Micromeritics ASAP 2010 instrument, was 8.8 % corresponding to the metallic surface area of 1.6 m^2/g catalyst. The as-received catalyst is a 50.9 wt% slurry in water; The Ru sponges (-100 mesh, 99.9 %) were purchased from Aldrich Chemical Co. with a metallic surface area of 0.2-0.4 m^2/g catalyst for the old Ru sponge (with unknown batch No.) and 0.055-0.22 m^2/g catalyst for the new Ru sponge (batch No. 09814PB). Catalyst loadings and reaction rates in the thesis are reported on a dry catalyst basis.

2.1.2. Reactor system

Reactions were carried out in a Parr series 5000 multiple reactor system (Figure 2.1) equipped with a magnetically coupled stirring unit. The system contains six 75 ml reactors constructed of 316 stainless steel and rated to a maximum pressure of 20 MPa at 573 K. Each reactor is equipped with an individual heating mantle and ports for gas and liquid sampling.

Figure 2.1. Parr series 5000 multiple reactor system.

2.1.3. Operating procedure

In a typical reaction, 0.5 g of Ru/C catalyst (dry basis) or 5 g of Ru sponge was pre-reduced in a dry reactor by purging with nitrogen and heating to 423-473 K, charging with hydrogen to 3.4 MPa, and holding at these conditions for 12 hours. After cooling to room temperature, the reactor was vented and 50 ml of organic acid feed solution (0.05-5 M) was forced into the reactor from a sample cylinder under hydrogen pressure. The stirring speed was set to 1000 rpm, a value determined to be high enough to avoid external mass transport limitations in the reactor. It took 10-15 min for the reaction temperature to reach the desired value (343-423 K). When the reaction temperature stabilized at the desired value, the reactor was pressurized with hydrogen gas (3.4-10.3 MPa) to initiate the reaction and that time was recorded as "time zero". Due to adsorption and pre-reaction of the starting materials, non-zero conversions were usually observed at "time zero". Liquid samples (1-2 ml) were typically taken at one hour intervals throughout the reaction via a sampling loop system. For each sample, the loop was purged with compressed air and then flushed with reaction mixture several times to ensure that a representative composition was obtained; the ~1 ml liquid sample taken was then filtered through a syringe microfilter prior to analysis. At the end of the reaction time, which ranged from 5 to 80 hours, the reactor was cooled and the pressure was reduced. The reactor set-up for charging and sampling is shown in Figure 2.2.

The Ru sponge was recovered by separating from the final reaction solution by filtration or centrifugation and then washed thoroughly with HPLC water. The wet catalyst was put in an oven and calcined at 350 °C for 12 hours. After pre-reduction the metal catalyst was ready to use for the next experiment.

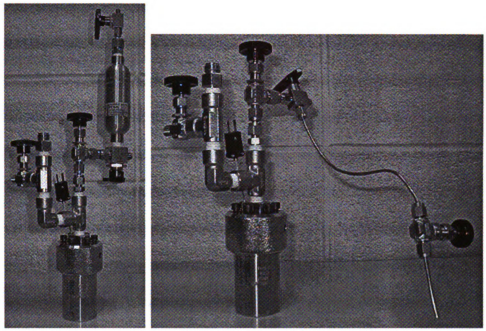

Figure 2.2. The reactor set-up for (a) charging and (b) sampling.

2.1.4. Analytical

Liquid-phase samples were analyzed on a Spectra Tech P1000 HPLC (Thermo Separation Products, Inc.) with RI detection and UV detection at 250 nm. The separation was carried out on a Biorad Aminex HPX-87H column at 323 K. The mobile phase was 0.005 M H_2SO_4 in HPLC grade water with a flow rate of 0.45 ml/min. A RI chromatogram of the typical liquid reaction species is shown in Figure 2.3. Gas-phase samples were analyzed on a 1/8" x 6 ft Spherocarb packed column in a Varian 3300 gas chromatograph with thermal conductivity detector and helium as carrier gas. For both chromatographic analyses, multipoint calibration curves were developed to obtain peak response factors. Data from the HPLC and GC were used to calculate acid conversion,

product yields and selectivities, and overall reaction material balances (the variability of HPLC data is ~5%).

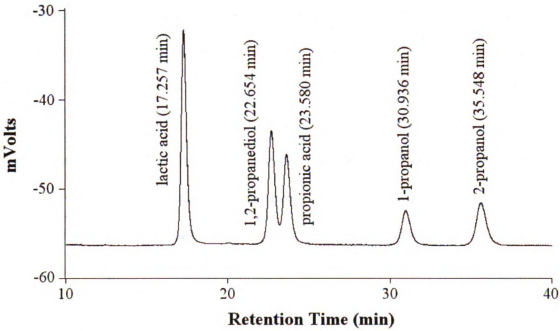

Figure 2.3. RI Chromatograph of the typical liquid reaction species. HPLC operation conditions: Aminex HPX-87H column temperature = 323 K, mobile phase = 0.005 M H_2SO_4 in HPLC grade water, flow rate of the mobile phase = 0.45 ml / min.

2.2. Catalyst characterization

Catalysts used in the experiments were characterized using a number of standard methods to determine the total (BET) surface area, average pore size and pore size distribution, micropore and total pore volume, metal surface area, as well as the metal dispersion on the catalysts. All of the gases used in these analysis were of ultra high purity (99.999%, AGA/BOC).

2.2.1. Physisorption

The BET surface area was measured by nitrogen physisorption at 77 K using the Accelerated Surface Area and Porosimetry System (Micromeritics ASAP 2010), and analyzed using the method proposed by Brunauer, Emmett and Teller. [1] Catalyst sample was loaded to a pre-weighed quartz sample tube and heated to 423 K to remove water and other potential contaminants. The sample was then reweighed to determine the actual amount of catalyst present in the sample tube. Next, the evacuated sample tube was placed in a Dewar flask of liquid nitrogen and further evacuated until equilibrium was reached. At this point, analysis commenced with dosing of the analysis gas and subsequent measurement of the adsorbed gas. The amount of nitrogen adsorbed at a given composition and pressure was used to determine the BET surface area down to the micro pore level.

2.2.2. Chemisorption

The metal surface area and metal dispersion on the catalysts were calculated using chemisorption methods. Adsorption of hydrogen or carbon monoxide on to activated metal sites provides information about the fraction of active metal that is available for reaction. Chemisorption measurements were conducted using the Micromeritics ASAP 2010 instrument. Samples were first prepared by degassing the material in a pre-weighed glass sample tube to remove water and other potential contaminants. The sample was then reweighed to determine the actual amount of catalyst present. Once complete, the sample tube was placed in the analysis port of the ASAP 2010 system. The sample tube was then placed under vacuum and heated to remove adsorbed materials on the catalyst.

Next, the catalyst was reduced under hydrogen to activate the metal sites. Then, the sample tube was cooled and evacuated again. At this point, analysis commenced with dosing of the analysis gas and subsequent measurement of the adsorbed gas. The metal surface area and metal dispersion of the catalyst were calculated using the corresponding Micromeritics software.

2.2.3. Pore volume and pore size measurement

A simple model for a porous catalyst is to assume it to be composed of a collection of cylindrical pores of radius *r*. A volume of liquid can be forced under pressure to fill the void space and thus determine pore volumes and the pore size distribution of larger pores with radii larger than 10 nm. This liquid is invariably mercury that does not wet the pore wall surface due to its high surface tension (mercury porosimetry method [2]). A nitrogen desorption technique can be used to determine the distribution of pores with diameters smaller than 20 nm by using the Kelvin equation[3] to relate pore radius to the vapor pressure. Combining these two techniques can give the overall pore size distribution. For the ruthenium catalysts used in our reaction systems, the micropore volume was determined using the *t*-plot method in nitrogen physisorption, and total pore volume was characterized as volume adsorbed at the maximum relative pressure (P/P_0) of 0.99.

2.3. Liquid phase adsorption studies

The quantity of species adsorbed onto a surface is determined by measuring the difference between the initial and final species concentrations in solution, which were measured prior to and following exposure to the surface, respectively.

2.3.1. Adsorption onto activated carbon support

Isothermal adsorption experiments at room temperature were performed using 8.5 ml glass vials with Teflon-lined plastic lids. The vials were cleaned and air-dried, and then the activated carbon powder (# 3310) was weighed and added to the vials based on the solution concentration to be examined in order to maintain a detectable change in solution concentration before and after adsorption. The vials were capped and put on a rotator overnight to ensure thorough mixing and equilibration. Upon removal from the rotator, the vials were either centrifuged or left standing to allow the suspended carbon in the solution to settle. Liquid samples were then taken and analyzed using HPLC.

Temperature dependent adsorption experiments were conducted using the 75 ml batch reactor shown in Figure 2.1. The operating procedure was about the same as that described in section 2.3.2 except that the carbon support doesn't need to be pre-reduced.

2.3.2. Adsorption onto Ru/C catalyst

Adsorption onto the 5 wt % Ru/C catalyst was carried out in the 75 ml batch reactor shown in Figure 2.1. A specified amount of catalyst was pre-reduced at 473 K and 3.4 MPa hydrogen pressure for 5-12 hours in order to activate the metal surface. Then the reactor was cooled and charged with 50 ml aqueous solution of the substrates

investigated. The reactor was purged with hydrogen to remove air present in the solution, and then sealed. To begin the temperature variation adsorption experiments, the reactor was first stirred at room temperature overnight to equilibrate and the first liquid sample was taken. The reactor temperature was then set to 30°C and increased by increments of 20°C up to 150°C. Liquid samples were taken at each temperature setting after several hours of equilibration. An in-line filter was connected to the dip tube within the reactor in order to separate the solid catalyst from the liquid solution during sampling. The samples were analyzed by HPLC and the solution concentrations were used to calculate the amount of substrates adsorbed on catalyst at each temperature. The sampling loss and the change of solution volume were taken into account during the calculation.

2.3.3. Adsorption onto Ru sponge

The quantity of substrate adsorbed onto ruthenium sponge is extremely small due to the low surface area of the catalyst (0.1-0.2 m^2/g Ru). The high cost of Ru metal led us to focus on decreasing the solution volume in order to maximize the metal to solution volume ratio and thus increase the sensitivity of detection. Lars Peereboom[4] from Miller group designed a recirculating microreactor system (Figure 2.4) consisting of a pump, packed bed reactor, thermal stabilization components, inline sampling system, and a HPLC. The system allows us to have a large amount of catalyst (1-10 g) with a minimal amount of liquid volume (10-20 ml). The inline sampling and HPLC system allows removal of a minimal amount of liquid sample (10 μl) and allows accurate measurement of concentration changes down to 10^{-5} M. The detailed operating procedure of this system can be found in the Ph.D. dissertation of Lars Peereboom.

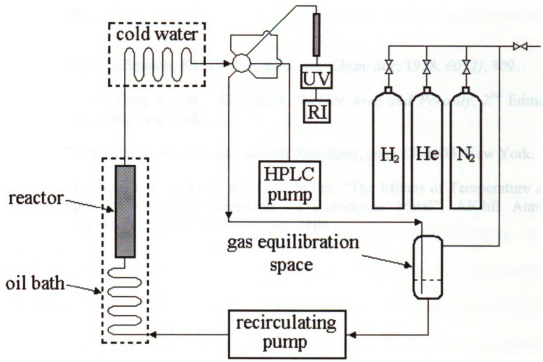

Figure 2.4. Recirculating microreactor system.

2.4. References

(1) Brunauer, S.; Emmett, P.H.; Teller, E., *J. Am. Chem. Soc*, **1938**, *60 (2)*, 309.

(2) Gregg, S.J.; Sing, K.S.W., *Adsorption, Surface Area and Porosity*, 2nd Edition, **1982**, 173-190, New York.

(3) M. Albert Vannice, *Kinetics of Catalytic Reactions*, page 18, **2005**, New York.

(4) L. Peereboom, J. E. Jackson, and D. J. Miller, "The Effects of Temperature and Hydrogen on Glycerol Adsorption on Ruthenium Metal", AIChE Annual Meeting, San Francisco, CA, November, **2006**.

Chapter 3. Aqueous-Phase Hydrogenation of Organic Acids and Their Mixtures over Carbon-Supported Ruthenium Catalyst

3.1. Introduction

Our research aims to develop an improved mechanistic understanding of the conversion from organic acids to the corresponding alcohols. We seek to investigate substrate-metal interactions in aqueous solution, and then to relate those adsorption properties to the efficacy for hydrogenation. We approach this goal by conducting adsorption and reduction studies of individual acids, acid mixtures, and combinations of acids with their alcohol products. These studies provide valuable information on the relative hydrogenation reactivity of different acids, the relative binding strength of different substrates on the metal catalyst surface, and how the presence of one species at the surface influences the reactivity of another.

The aqueous-phase hydrogenation of lactic acid (LA) and propionic acid (PA) alone, together, and in mixtures with their alcohol products propylene glycol (PG) and 1-propanol (1-PrOH), over a 5 wt % Ru/C catalyst was performed in a three-phase stirred batch reactor. Experiments were performed at several acid feed concentrations from 0.05 to 5 M, at temperatures from 343 to 423 K, and at hydrogen pressures from 3.4 to 10.3 MPa. To maintain reasonable reaction rates in the kinetic regime of reaction, a hydrogen pressure of 6.9 MPa (1000 psi) and a temperature of 403 K were used for most experiments. Catalyst loading was 0.5 g (dry basis) in 50 ml aqueous solution for all

experiments. The reactions are depicted in Scheme 3.1 and a summary of the reaction conditions investigated is reported in Table 3.1.

Scheme 3.1. Catalytic hydrogenation of lactic acid and propionic acid

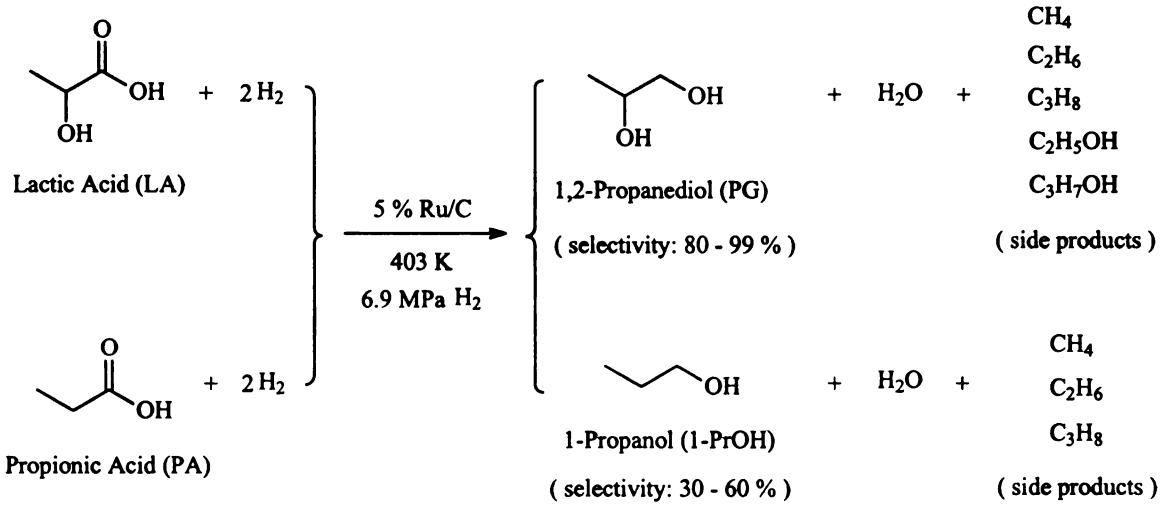

Table 3.1. Summary of reaction conditions for the hydrogenation of lactic acid and propionic acid over 5 wt % Ru/C catalyst

T (K)	P_{H2} (MPa)	t (hour)	Concentrations of the starting materials (M)				Conversion of acids (%)		Selectivity to alcohols (%)	
			LA	PA	PG	1-PrOH	LA	PA	PG	1-PrOH
343	6.9	24	0.5				24		90	
363	6.9	8	0.5				30		85	
383	6.9	8	0.5				64		87	
383	6.9	7	0.5				60		89	
403	6.9	8	0.1				100		85	
403	6.9	7	0.5				97		86	
403	6.9	6	0.5				88		97	
403	6.9	8	2				77		90	
403	6.9	5	2				50		78	
403	6.9	8	5				50		66	
403	3.4	30	0.5				99		78	
403	3.4	30	2				96		77	
403	10.3	12	0.5				99		100	
403	10.3	12	2				93		86	
423	6.9	4	0.5				83		85	
383	6.9	8		0.5				20		56
393	6.9	28		0.5				69		54
403	6.9	8		0.1				80		44
403	6.9	8		0.5				41		54
403	6.9	6		0.5				26		65
403	6.9	6		2				13		48
403	6.9	8		5				12		33
403	8.3	11		0.5				61		55
403	8.3	11		2				26		50
403	3.4	31		0.5				69		33
403	3.4	31		2				45		43
413	6.9	12		0.5				77		40
423	6.9	12		0.5				91		39
383	6.9	8	0.5	0.5			53	11	80	57
403	6.9	8	0.1	0.1			100	60	100	75
403	6.9	8	0.5	0.5			90	28	84	60
403	6.9	8	2	2			59	18	73	29
403	6.9	8	0.05	0.5			100	41	68	42
403	6.9	8	0.5	2			59	9	82	87
403	6.9	8	0.5	5			55	11	68	29
403	6.9	8	2	0.5			62	17	84	60
403	6.9	8	5	0.5			52	21	59	35
403	10.3	12	2	2			83	24	81	44
403	3.4	30	0.5	0.5			100	73	100	44
403	3.4	31	2	2			83	26	75	44
403	6.9	3	0.5		0.5		58		79	
403	6.9	7	0.5		0.1		93		85	
403	6.9	7	0.5			0.5	90		87	
403	6.9	10	0.5			solvent	68		20	
403	6.9	8		0.5		0.5		29		0
403	6.9	8		0.5		0.36		29		0
403	6.9	7		0.5	0.5			35		56
403	6.9	8	0.5	0.5	0.5		89	28	74	56
403	6.9	8	0.5	0.5	0.5	0.5	81	23	80	0
T (K)	P_{H2} (MPa)	t (hour)	LA	PA	PG	1-PrOH	LA	PA	PG	1-PrOH
			Concentrations of the starting materials (M)				Conversion of acids (%)		Selectivity to alcohols (%)	

3.2. Hydrogenation of single lactic acid and propionic acid over Ru/C catalyst

The conversion rates of LA and PA are influenced dramatically by temperature and hydrogen pressure, with LA reacting nearly four times faster than PA over the range of conditions examined. Selectivity to PG from LA ranged from 80 to 99%, while selectivity to 1-PrOH from PA was less than 60% under most conditions. Methane, ethane, and propane were detected as the chief side products for these reactions.

3.2.1. Effect of temperature

The effects of hydrogenation temperature on acid conversion rates are shown in Figures 3.1 and 3.2. The rate of conversion for both LA and PA increase dramatically with temperature. Lower temperatures, as shown in Table 3.2, favored selectivity to the alcohol products.

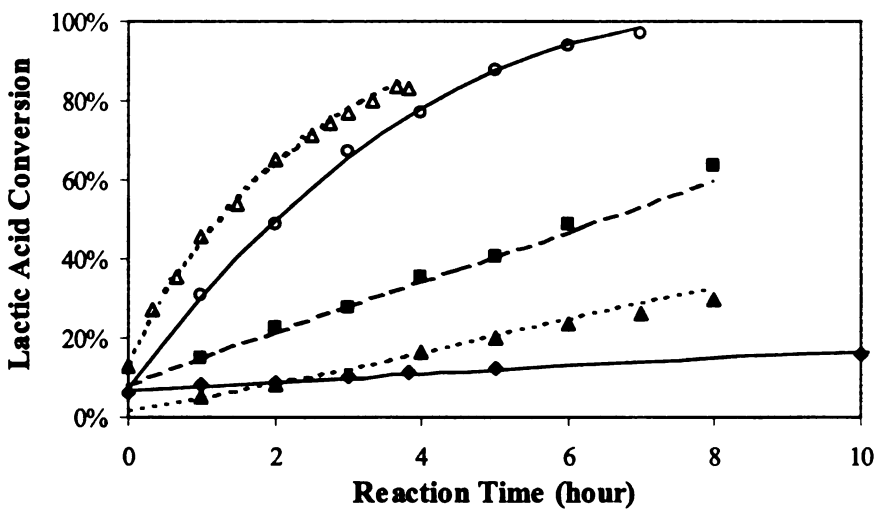

Figure 3.1. Effect of temperature on lactic acid hydrogenation rate over Ru/C. Conditions: LA concentration = 0.5 M; P_{H2} = 6.9 MPa; 0.5 g (5 wt % Ru/C) /50 ml aqueous solution; 1000 rpm. (◆) 343 K; (▲) 363 K; (■) 383 K; (○) 403 K; (△) 423 K.

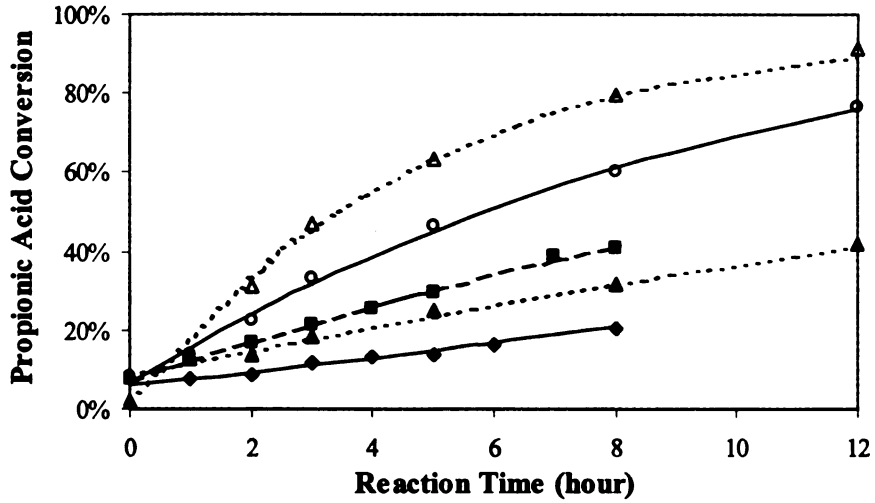

Figure 3.2. Effect of temperature on propionic acid hydrogenation rate over Ru/C. Conditions: PA concentration = 0.5 M; P_{H2} = 6.9 MPa; 0.5 g (5 wt % Ru/C) /50 ml aqueous solution; 1000 rpm. (◆) 383 K; (▲) 393 K; (■) 403 K; (○) 413 K; (△) 423 K.

Table 3.2. Effect of temperature on the hydrogenation selectivity

Lactic acid hydrogenation			Propionic acid hydrogenation		
T (K)	LA conv. (%)	PG sele. (%)	T (K)	PA conv. (%)	1-PrOH sele. (%)
343	24	90	383	20	56
363	30	85	393	69	54
383	64	87	403	41	54
403	97	86	413	77	40
423	83	85	423	91	39

Conditions: Acid feed concentration = 0.5 M, P_{H2} = 6.9 MPa, 0.5 g (5 wt % Ru/C)/50 ml solution, 1000 rpm.

3.2.2. Effect of hydrogen pressure

Due to the low solubility of hydrogen (Table 3.3)[1,2] in aqueous solution, elevated hydrogen pressure should be used to achieve reasonable reaction rates. Conversion rates of LA and PA at three different hydrogen pressures (3.4, 6.9, and 10.3 MPa for LA; 3.4, 6.9, and 8.3 MPa for PA) and two different acid concentrations (0.5 and 2 M) are

reported in Figures 3.3 and 3.4. Higher hydrogen pressures favored the conversion of LA and PA, and the selectivity (Table 3.4) to alcohol products.

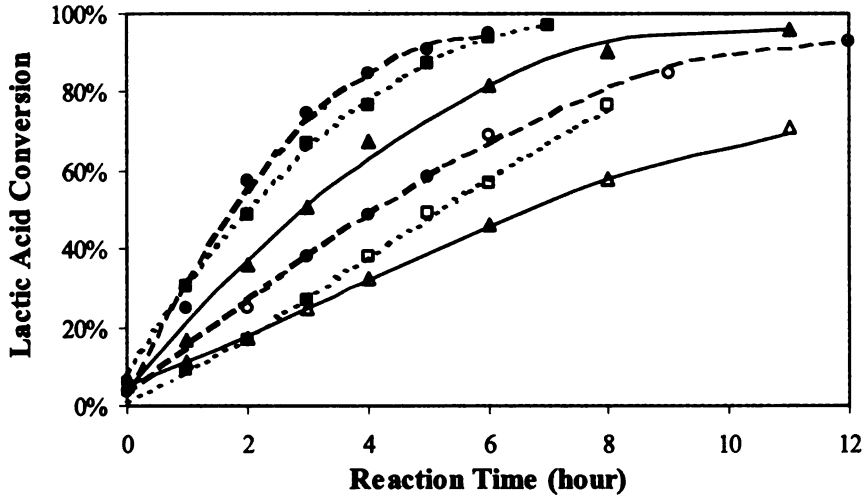

Figure 3.3. Effect of hydrogen pressure on lactic acid hydrogenation rate over Ru/C. Conditions: T = 403 K; 0.5 g (5 wt % Ru/C) /50 ml aqueous solution; 1000 rpm. (▲) 0.5M LA, 3.4 MPa; (■) 0.5M LA, 6.9 MPa; (●) 0.5M LA, 10.3 MPa; (△) 2M LA, 3.4 MPa; (□) 2M LA, 6.9 MPa; (○) 2M LA, 10.3 MPa.

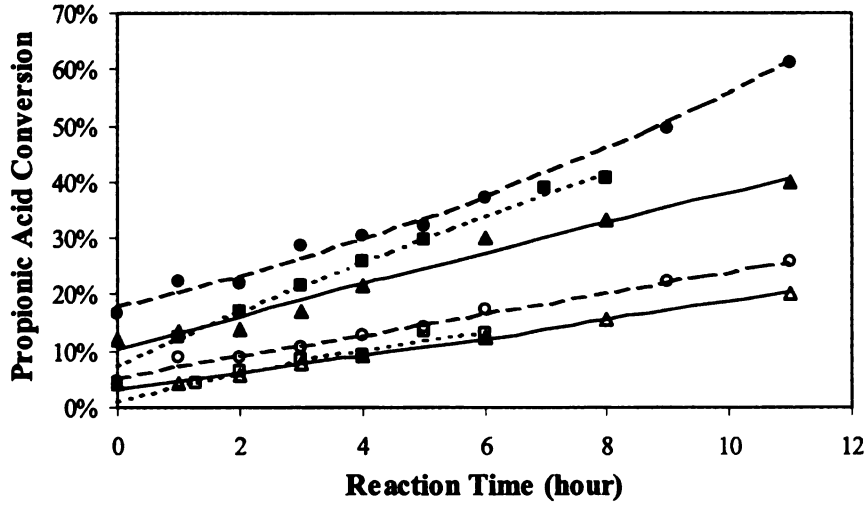

Figure 3.4. Effect of hydrogen pressure on propionic acid hydrogenation rate over Ru/C. Conditions: T = 403 K; 0.5 g (5 wt % Ru/C) /50 ml aqueous solution; 1000 rpm. (▲) 0.5M PA, 3.4 MPa; (■) 0.5M PA, 6.9 MPa; (●) 0.5M PA, 8.3 MPa; (△) 2M PA, 3.4 MPa; (□) 2M PA, 6.9 MPa; (○) 2M PA, 8.3 MPa.

Table 3.3. The solubility of hydrogen in water[1,2]

Solubility [ml H_2 (STD)/ml H_2O]	0 °C	10 °C	20 °C	25 °C	30 °C	40 °C	50 °C	60 °C	80 °C	100 °C	150 °C
0.1 MPa	0.021	0.019	0.018	0.017	0.016	0.015	0.014	0.013	0.008	0.006	
1 MPa				0.19							
2 MPa				0.38							
2.5 MPa	0.54	0.19	0.42		0.43	0.41	0.41	0.40	0.42	0.46	
3 MPa				0.57							
4 MPa				0.76							
5 MPa	1.07	0.97	0.89	0.95	0.82	0.82	0.81	0.81	0.84	0.91	
6 MPa				1.14							
6.9 MPa											
7 MPa				1.33							1.64
7.6 MPa	1.60	1.45	1.34		1.27	1.23	1.21	1.21	1.25	1.35	
7.7 MPa											1.67
8 MPa				1.52							
9 MPa				1.71							
10 MPa	2.13	1.93	1.78	1.90	1.69	1.64	1.61	1.61	1.67	1.80	
11 MPa				2.09							
12 MPa				2.28							
13 MPa				2.47							
14 MPa				2.66							
15 MPa	3.17	2.87	2.65	2.85	2.51	2.43	2.39	2.39	2.48	2.68	

Table 3.4. Effect of hydrogen pressure on the hydrogenation selectivity

Lactic acid hydrogenation			**Propionic acid hydrogenation**		
P_{H2} (MPa)	LA conv. (%)	PG sele. (%)	P_{H2} (MPa)	PA conv. (%)	1-PrOH sele. (%)
3.4	99	78	3.4	69	33
6.9	97	86	6.9	41	54
10.3	99	100	8.3	61	55

Conditions: Initial concentration of the acid = 0.5 M, T = 403 K, 0.5 g (5 wt % Ru/C)/50 ml solution, 1000 rpm.

3.2.3. Effect of acid feed concentration

Conversion rates of LA and PA at four different feed concentrations (0.1, 0.5, 2 and 5 M) with otherwise identical reaction conditions are reported in Figures 3.5 and 3.6. Higher acid feed concentration results in lower conversion after the same reaction time

although the absolute reaction rate increases with the concentration. The dependence of rate on concentration is minimized when the acid concentration is over 2 M, indicating that the catalyst surface is nearly saturated with acids at this concentration.

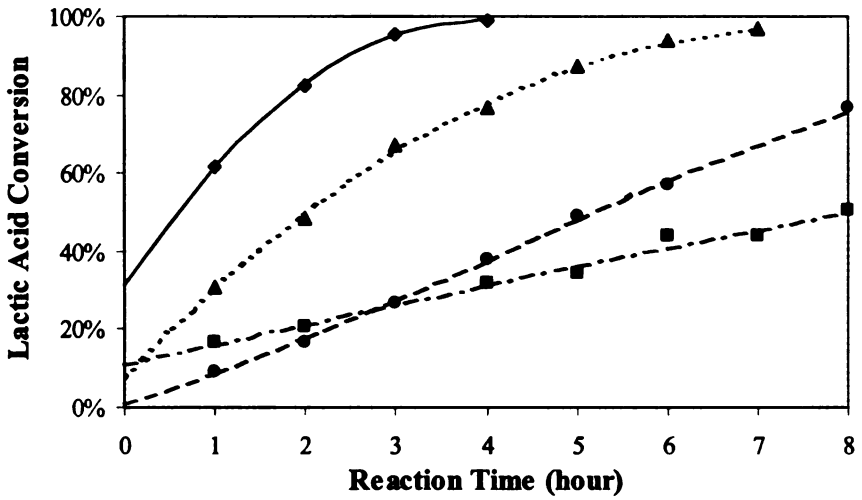

Figure 3.5. Effect of initial acid concentration on lactic acid hydrogenation rate over Ru/C.
Conditions: T = 403 K; P_{H2} = 6.9 MPa; 0.5 g (5 wt % Ru/C) /50 ml aqueous solution; 1000 rpm. (◆) 0.1M LA; (▲) 0.5M LA; (●) 2M LA; (■) 5M LA.

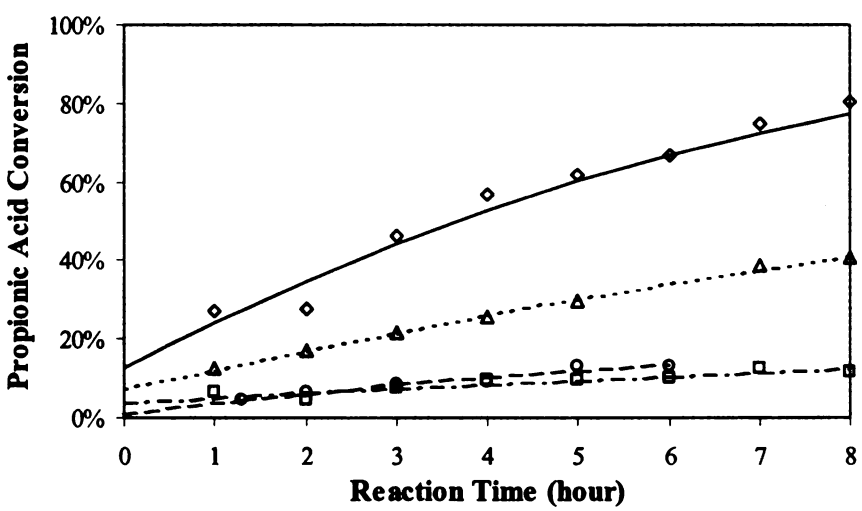

Figure 3.6. Effect of initial acid concentration on propionic acid hydrogenation rate over Ru/C.
Conditions: T = 403 K; P_{H2} = 6.9 MPa; 0.5 g (5 wt % Ru/C) /50 ml aqueous solution; 1000 rpm. (◇) 0.1M PA; (△) 0.5M PA; (○) 2M PA; (□) 5M PA.

3.2.4. Effect of catalyst loading

Initial hydrogenation rates of LA at three different catalyst loadings (0.25, 0.5, and 1 g Ru/C) with otherwise identical reaction conditions are represented in Figure 3.7. The observation that the acid conversion rate increases in proportion to the catalyst loading indicates that mass transport resistances across phase boundaries are negligible at these experimental conditions. This would not be the case if phase boundary mass transfer resistances limited reaction rate (Chapter 6).

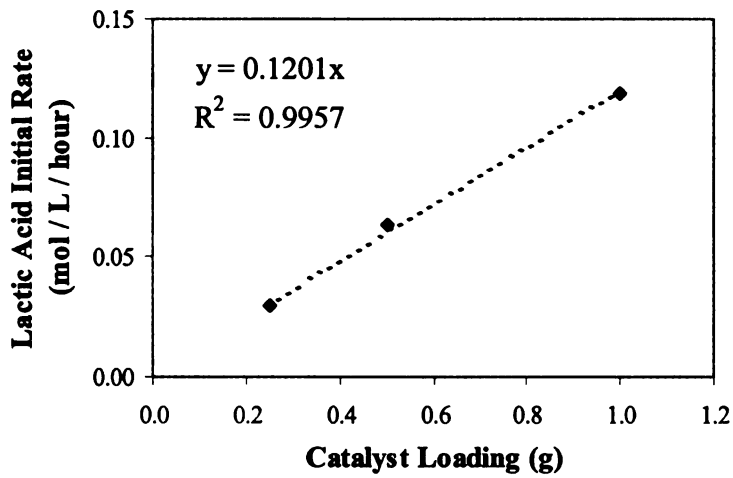

Figure 3.7. Effect of catalyst loading on lactic acid hydrogenation rate over Ru/C. Conditions: The catalyst is 5 wt % Ru/C; 50 ml 0.2 M LA aqueous solution; T = 403 K; P_{H2} = 6.9 MPa; 1000 rpm.

3.2.5. Degradation of the alcohol products of hydrogenation

The alcohol products (PG and 1-PrOH) of hydrogenation react further under the hydrogenation conditions. Degradation of the alcohol products of hydrogenation was investigated under typical reaction conditions. As shown in Table 3.5, for 0.5 M solutions of the alcohols, 11% of the PG and 25% of the 1-PrOH were degraded after 8.5 hours of

reaction at 403 K and 6.9 MPa. Examination of 1-PrOH degradation over a concentration range of 0.5 to 2 M showed zero-order behavior with a constant rate of 0.012 mol/liter/hour (Table 3.6). Degradation of PG was also studied by Shanks *et al*,[3] and was found to be zero order reaction for the concentration range of 0.3 to 1.5 M. Degradation products included methane, ethane, and propane from both 1-PrOH and PG, along with significant quantities of ethanol and 1-PrOH from PG. The relatively rapid degradation of 1-PrOH, coupled with the slow hydrogenation rate of PA, together contribute to the low selectivity to 1-PrOH from PA relative to that of PG from LA. In new studies probing adsorption of acids and alcohols on the catalyst Ru metal and carbon support components (Chapter 5), we have found that 1-PrOH adsorbs more strongly than PG into the carbon, creating locally high pore concentrations of 1-PrOH near catalytic Ru sites that contribute to its elevated degradation rate.

Table 3.5. Degradation of 1,2-propanediol and 1-propanol under the hydrogenation conditions

Starting materials	Alcohol conv. (carbon %)	Yield of liquid phase products (carbon %)	Yield of gas phase products (carbon %)
0.5M PG	11 %	ethanol and 1-propanol (2.7 %)	methane, ethane, and propane (2.4 %)
0.5M 1-PrOH	25 %	None	methane, ethane, and propane (4.9 %)

Conditions: T = 403 K, P_{H2} = 6.9 MPa, t = 8.5 hour, 0.5 g (5 wt % Ru/C)/50 ml solution, 1000 rpm.

Table 3.6. Degradation rates of 1-propanol at different initial concentrations

Initial concentration of 1-PrOH (M)	0.5	2	5
Degradation rate of 1-PrOH (mol/L/hour)	0.0123	0.0120	0.0111

Conditions: T = 403 K, P_{H2} = 6.9 MPa, 0.5 g (5 wt % Ru/C)/50 ml solution, 1000 rpm.

3.2.6. Determination of reaction rate, reaction order and rate constant

Acid hydrogenation rates were calculated via differential analysis: acid concentration vs. time data were fit to an *nth*-order polynomial (n = 2-4), which was then differentiated and evaluated at various times over the course of reaction. Initial rates were calculated by extrapolating the rate curve to time zero without forcing it through the origin. By incorporating the acid concentration and the quantity and properties of the catalyst, reaction rates on a catalyst mass basis (kmol acid/kg catalyst/s) or on a reactor fluid volume basis (kmol acid/m^3 solution/s) were determined. Initial rate data were used to estimate the activation energy and the dependence of rates on acid feed concentrations. This initial rate evaluation avoids possible complications from side reactions and catalyst deactivation.

For a batch reactor, the plot of $\ln(-r_A)$ vs. $\ln(C_A)$ yields the reaction order (n) from the slope and the rate constant (k) from the intercept based on equations 3.1 and 3.2:

$$-r_A = -\frac{dC_A}{dt} = kC_A^{\,n} \tag{3.1}$$

$$\ln(-r_A) = n\ln(C_A) + \ln k \tag{3.2}$$

For a 1st order reaction (n = 1), the rate constant can be determined by the slope of $\ln(C_{A0}/C_A)$ vs. t:

$$-r_A = kC_A \tag{3.3}$$

$$\ln\left(\frac{1}{1-x_A}\right) = \ln\frac{C_{A0}}{C_A} = kt \tag{3.4}$$

The method of data analysis was illustrated by the following example (experimental conditions: 50 ml 0.5 M LA, 423 K, 6.9 MPa hydrogen pressure, and 0.5 g

Ru/C catalyst.): the data of concentration vs. time were fit to a 4th order polynomial (Figure 3.8); the equation of $C_{LA} = f(t)$ from the polynomial was then differentiated to yield the reaction rates at various times over the course of reaction (Figure 3.9); the plot of $\ln(-r_{LA})$ vs. $\ln(C_{LA})$ (Figure 3.10) indicated that the reaction was nearly 1st order (n = 1.01) at this experimental conditions, and the rate constant was calculated from the intercept ($\ln k = -0.78$, $k = 0.46$); plotting $\ln(C_{LA0}/C_{LA})$ vs. t (Figure 3.11) gave a straight line through the origin, which confirmed that the reaction was 1st order, and the rate constant was determined from the slope ($k = 0.45$).

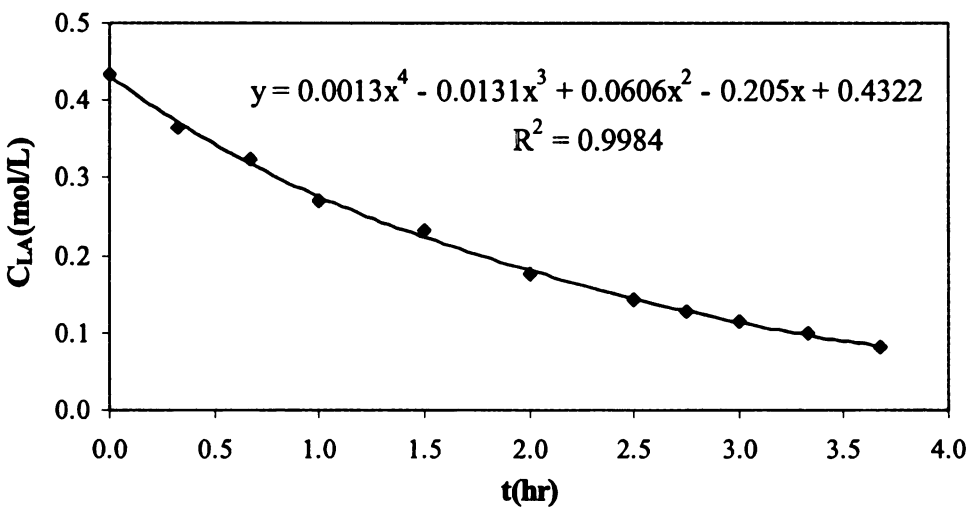

Figure 3.8. The plot of concentrations vs. reaction time for the hydrogenation of lactic acid over Ru/C at 423 K.
Conditions: LA feed concentration = 0.5 M, T = 423K, P_{H2} = 6.9 MPa, 0.5 g (5 wt % Ru/C)/50 ml solution, 1000 rpm.

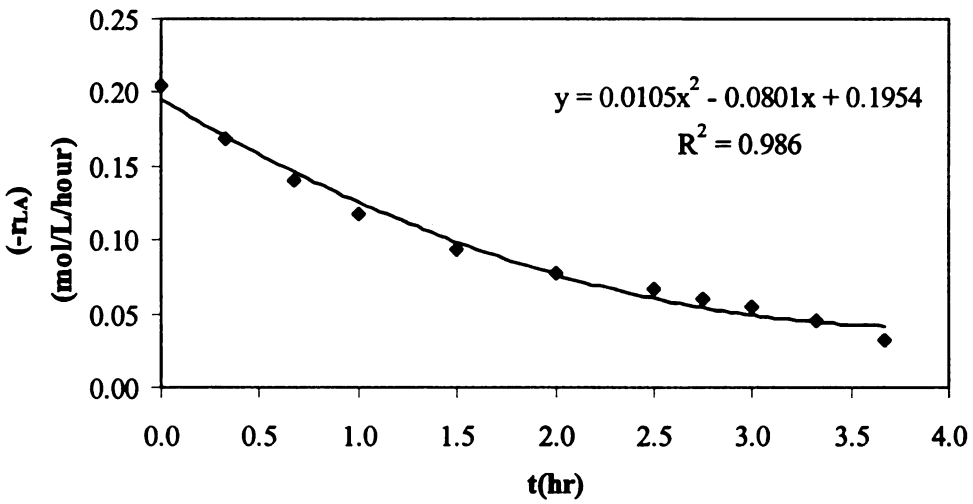

Figure 3.9. The plot of reaction rates vs. reaction time for the hydrogenation of lactic acid over Ru/C at 423 K.
Conditions: LA feed concentration = 0.5 M, T = 423K, P_{H2} = 6.9 MPa, 0.5 g (5 wt % Ru/C)/50 ml solution, 1000 rpm.

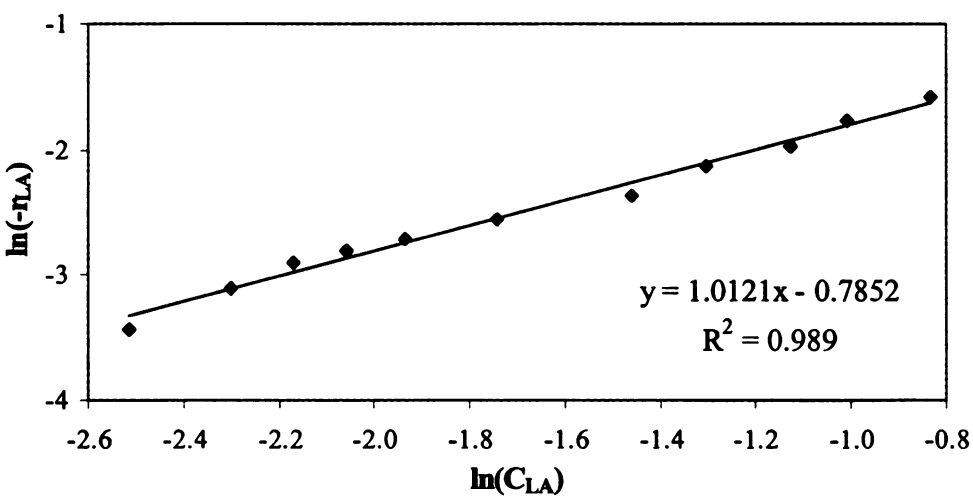

Figure 3.10. Determination of the reaction order and rate constant for the hydrogenation of lactic acid over Ru/C at 423 K.
Conditions: LA feed concentration = 0.5 M, T = 423K, P_{H2} = 6.9 MPa, 0.5 g (5 wt % Ru/C)/50 ml solution, 1000 rpm.

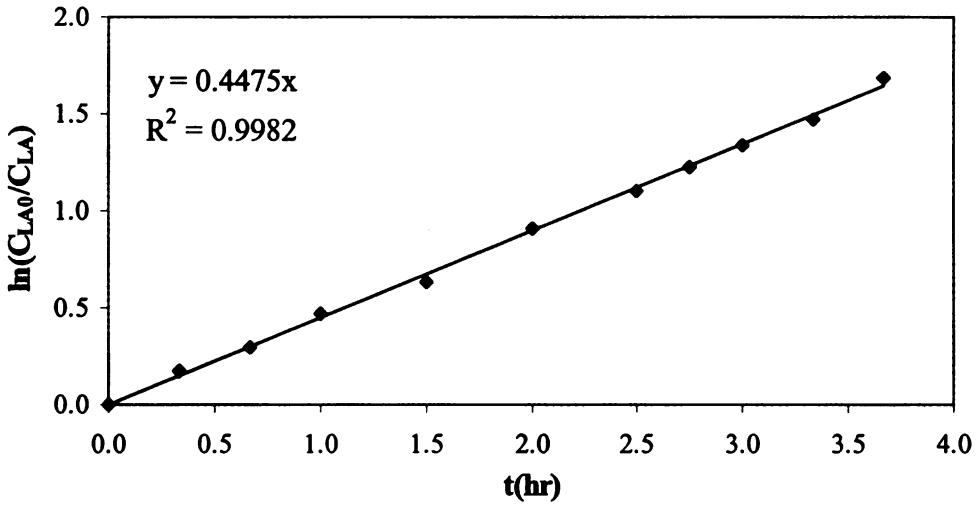

Figure 3.11. Determination of the rate constant for a first order reaction. Conditions: LA feed concentration = 0.5 M, T = 423K, P_{H2} = 6.9 MPa, 0.5 g (5 wt % Ru/C)/50 ml solution, 1000 rpm.

Initial LA and PA hydrogenation rates at four different feed concentrations (approximately 0.1, 0.5, 2 and 5 M) with otherwise identical reaction conditions are reported in Figure 3.12. The non-linear dependence of initial rate on initial concentration indicates that at the higher concentrations (≥ 2 M) the hydrogenation reactions are not simply first order with respect to LA or PA, and suggests that a Langmuir-Hinshelwood type of rate expression would better describe the reaction kinetics. Figure 3.13 shows the data of concentration vs. time for the hydrogenation of 2 M LA. The linear dependence of LA concentration on reaction time indicates that the hydrogenation reaction is nearly zero order at this concentration with a constant rate of 0.2 mol/L/hour.

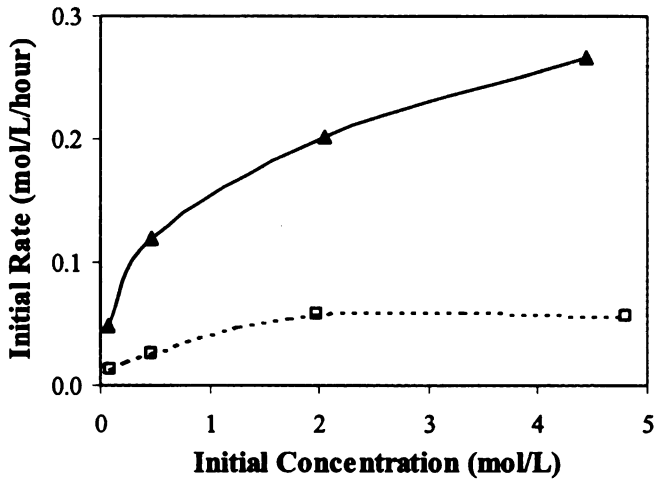

Figure 3.12. Concentration dependence of the initial hydrogenation rate.
Conditions: T = 403 K; P_{H2} = 6.9 MPa; 0.5 g (5 wt % Ru/C)/50 ml aqueous solution; 1000 rpm. (▲) LA; (□) PA.

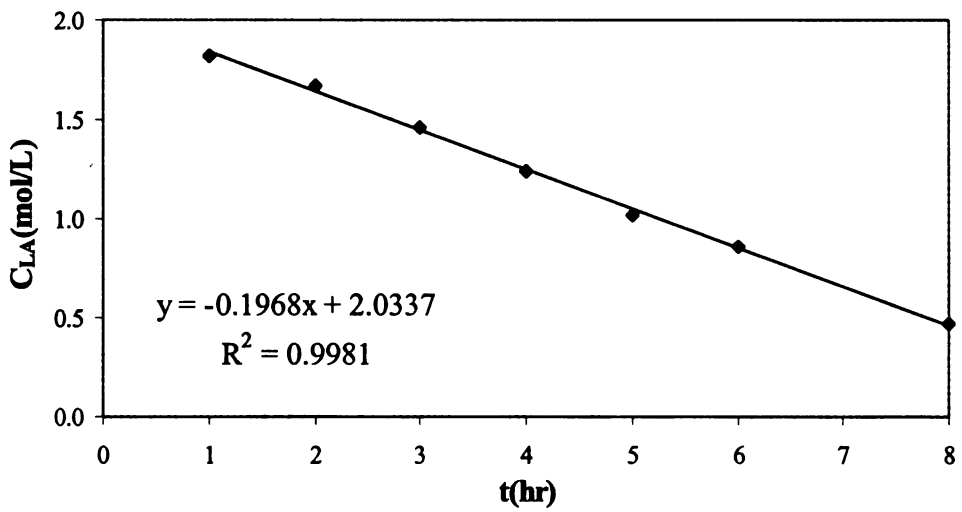

Figure 3.13. The plot of concentrations vs. reaction time for the hydrogenation of 2M lactic acid over Ru/C at 403 K.
Conditions: LA feed concentration = 2 M, T = 403K, P_{H2} = 6.9 MPa, 0.5 g (5 wt % Ru/C)/50 ml solution, 1000 rpm.

3.2.7. Activation energy calculation

The activation energy ($E_{Act.}$) is related to the reaction rate constant (k) by Arrhenius' law[4]:

$$k = k_0 exp\left(\frac{-E_{Act.}}{RT}\right) \tag{3.5}$$

Transforming the equation:

$$\ln k = -\left(\frac{E_{Act.}}{R}\right)\frac{1}{T} + \ln k_0 \tag{3.6}$$

where:

k = reaction rate constant [hour $^{-1}$]

k_o = pre-exponential factor [hour $^{-1}$]

$E_{Act.}$ = activation energy [J / mol]

R = ideal gas constant [J / mol / K]

T = Temperature [K]

The activation energy for acid hydrogenation was estimated by plotting the natural log of the initial rate versus reciprocal absolute temperature. The data points were fitted with a linear trendline, and the activation energy was then calculated from the slope of the trendline ($-E_{Act.}/R$). Plots are shown in Figure 3.14 for PA at 0.5 M and for LA at 0.5 M and 2.0 M. The initial activation energies for LA (average) and PA hydrogenation are 51 kJ/mol and 68 kJ/mol, respectively. The data used for the calculation of activation energies were shown in Table 3.7.

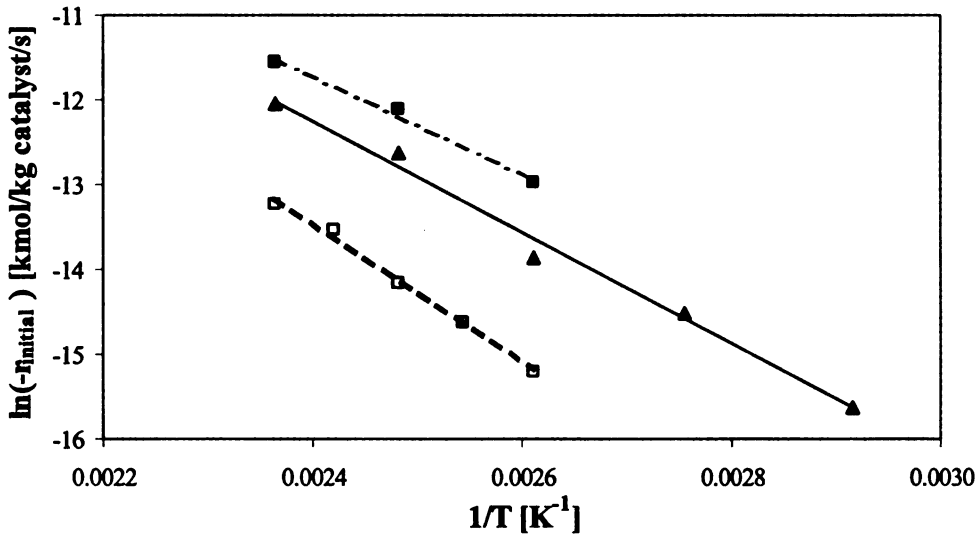

Figure 3.14. Arrhenius plot for activation energy of hydrogenation. Conditions: 0.5 g (5 wt% Ru/C)/50 ml solution; P_{H2} = 6.9 MPa. (▲) 0.5 M LA; (■) 2 M LA; (□) 0.5 M PA.

Table 3.7. Results of activation energy calculation for acid hydrogenation over 5 wt % Ru/C catalyst

Initial conc. of the acid	T (K)	Initial rate x 10^6 (kmol/kg catalyst/s)	Equation of the Arrhenius plot	$E_{Act.}$ (kJ/mol)
0.5M LA	343	0.16	y = -6555.4x + 3.4749 R^2 = 0.9895	54
	363	0.50		
	383	0.95		
	403	3.32		
	423	5.80		
2M LA	383	2.31	y = -5798.7x + 2.199 R^2 = 0.992	48
	403	5.47		
	423	9.65		
0.5M PA	383	0.25	y = -8198.9x + 6.2173 R^2 = 0.9944	68
	393	0.44		
	403	0.70		
	413	1.32		
	423	1.81		

Conditions: P_{H2} = 6.9 MPa, 0.5 g (5 wt % Ru/C)/50 ml solution, 1000 rpm.

3.3. Mixed acid/alcohol hydrogenation over Ru/C catalyst – Effect of competitive adsorption

The simultaneous hydrogenation of two acids and combinations of acids with product alcohols provides insight into the interactions of the reaction species with the catalyst surface that cannot be ascertained from single acid hydrogenation. These studies provide valuable information on the relative hydrogenation reactivity of acids and alcohols, the relative binding strength of different substrates on the metal catalyst surface, and how the presence of one acid or alcohol species in solution influences hydrogenation rate of another species.[5]

Hydrogenation of acid mixtures and combinations of acids with product alcohols was performed at several concentration ratios. The results of these experiments are represented in Figures 3.15-3.18 (lines represent polynomial fits for rate calculations). As seen in Figures 3.15 and 3.16, adding a second acid significantly decreases the conversion rate of a given acid, and this inhibitory effect increases with the concentration of the added acid. This observation indicates that LA and PA compete for active sites on the catalyst surface, and, consistent with the above concentration study (Figure 3.12), suggests that surface hydrogenation of the adsorbed acid is the rate-limiting step in the reaction. The inhibitory effect becomes nearly constant at added acid concentrations over 2 M, suggesting that the catalyst is saturated with acids at this concentration.

The influence of the alcohol products on acid reaction rates is shown in Figures 3.17 and 3.18. The presence of PG in the starting solution has little effect on the hydrogenation rates of either acid, indicating that PG adsorption on the catalyst surface is weak. Adding 1-PrOH to the initial reaction solution decreases PA conversion rate

(Figure 3.18), while the effect of 1-PrOH on LA is less significant (Figure 3.17). All of these observations suggest that competitive adsorption of the reaction species on the catalyst surface affects acid hydrogenation rates, and that any kinetic model describing the reaction system must include these inhibitory effects in order to properly describe the reaction.

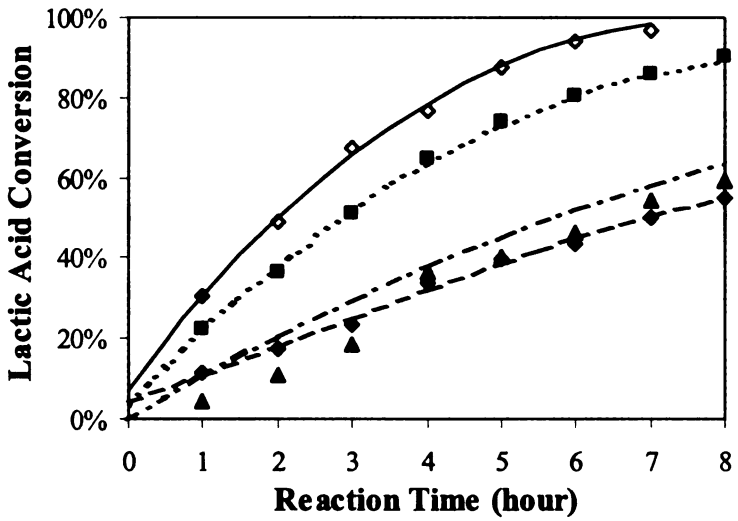

Figure 3.15. Effect of propionic acid on lactic acid hydrogenation rate over Ru/C. Conditions: T = 403 K; P_{H2} = 6.9 MPa; 0.5 g (5 wt % Ru/C)/50 ml aqueous solution; 1000 rpm. (◇) 0.5 M LA; (■) 0.5 M LA and 0.5 M PA; (▲) 0.5 M LA and 2 M PA; (◆) 0.5 M LA and 5 M PA.

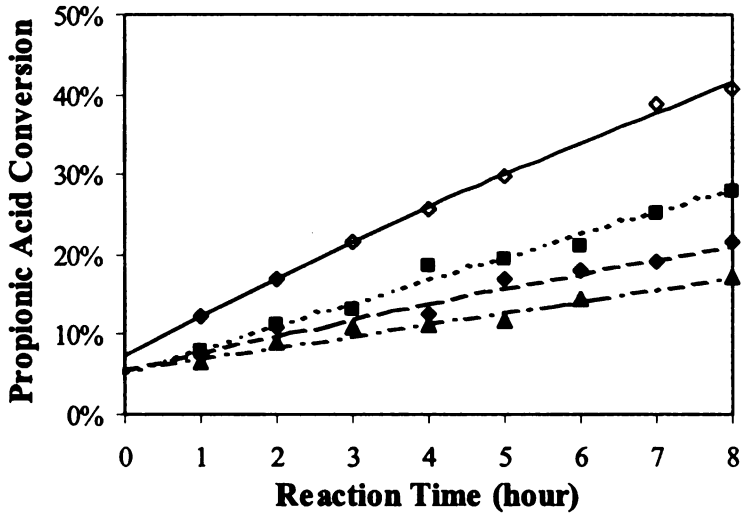

Figure 3.16. Effect of lactic acid on propionic acid hydrogenation rate over Ru/C. Conditions: T = 403 K; P_{H2} = 6.9 MPa; 0.5 g (5 wt % Ru/C)/50 ml aqueous solution; 1000 rpm. (◇) 0.5 M PA; (■) 0.5 M PA and 0.5 M LA; (▲) 0.5 M PA and 2 M LA; (◆) 0.5 M PA and 5 M LA.

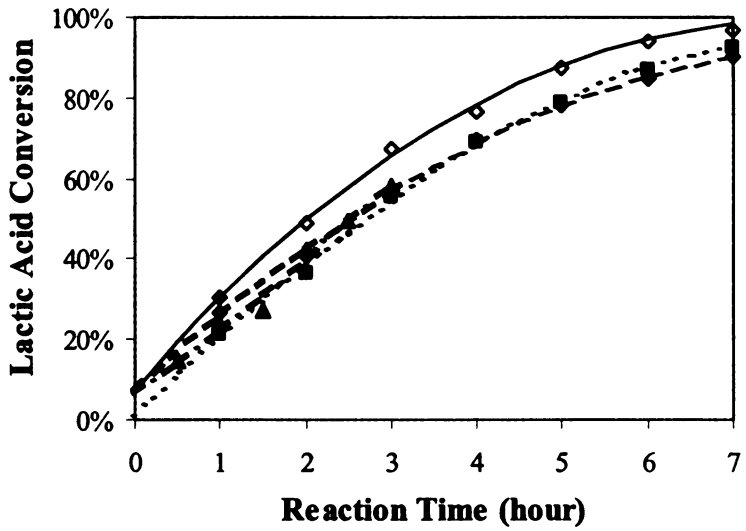

Figure 3.17. Effect of 1,2-propanediol and 1-propanol on lactic acid hydrogenation rate over Ru/C.
Conditions: T = 403 K; P_{H2} = 6.9 MPa; 0.5 g (5 wt % Ru/C)/50 ml aqueous solution; 1000 rpm. (◇) 0.5 M LA; (■) 0.5 M LA and 0.1 M PG; (▲) 0.5 M LA and 0.5 M PG; (◆) 0.5 M LA and 0.5 M 1-PrOH.

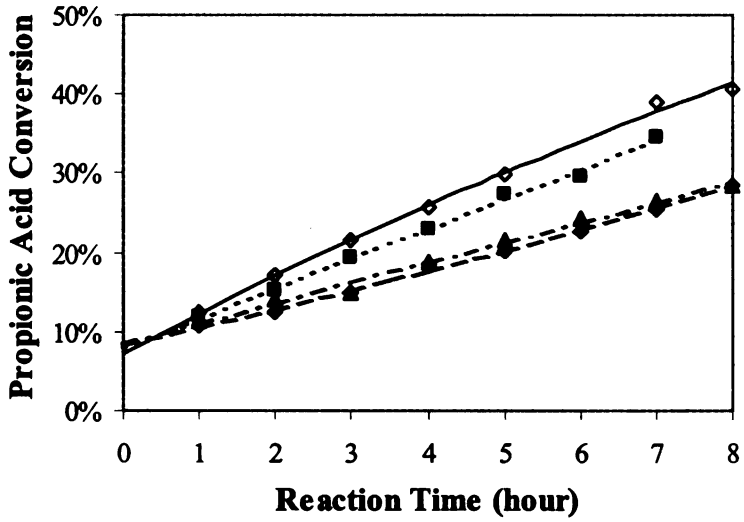

Figure 3.18. Effect of 1,2-propanediol and 1-propanol on propionic acid hydrogenation rate over Ru/C.
Conditions: T = 403 K; P_{H2} = 6.9 MPa; 0.5 g (5 wt % Ru/C)/50 ml aqueous solution; 1000 rpm. (◇) 0.5 M PA; (■) 0.5 M PA and 0.5 M PG; (▲) 0.5 M PA and 0.36 M 1-PrOH; (◆) 0.5 M PA and 0.5 M 1-PrOH.

3.4. Uncertainty and error

The experimental uncertainties were estimated by performing replicate reactions over the course of the experiments and checking the consistency of the data collected. Shown in Figures 3.19-3.22 are conversion data from replicate runs for the hydrogenation of LA and PA over Ru/C at different reaction conditions. The errors of these conversion data are within 10 %. The variability of concentration data from the HPLC is ~ 5 %.

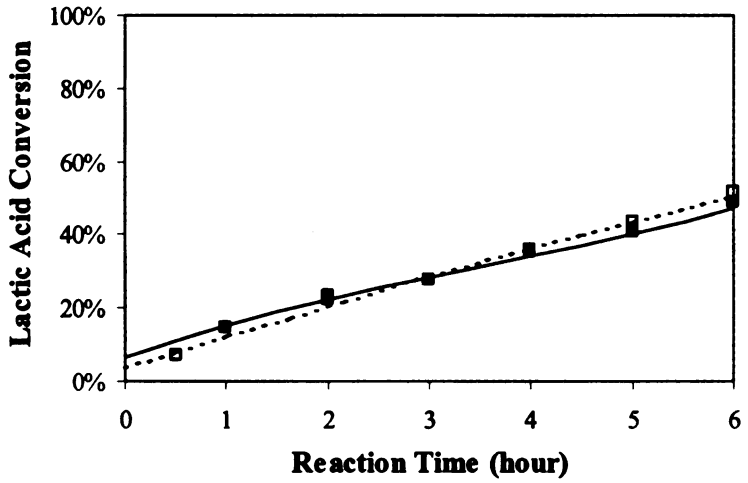

Figure 3.19. Replicate experiments for lactic acid hydrogenation over Ru/C - Experiments 23 and 50.
Conditions: 0.5M LA; T = 383 K; P_{H2} = 6.9 MPa; 0.5 g (5 wt % Ru/C)/50 ml aqueous solution. (■) Experiment 50; (□) Experiment 23.

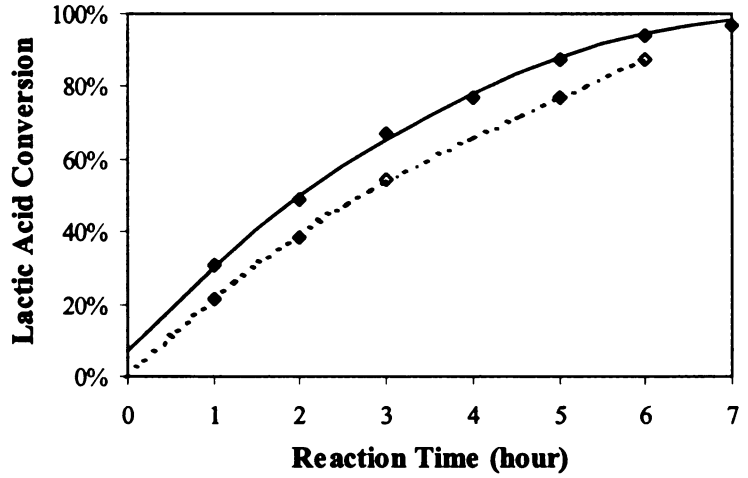

Figure 3.20. Replicate experiments for lactic acid hydrogenation over Ru/C - Experiments 15 and 38.
Conditions: 0.5M LA; T = 403 K; P_{H2} = 6.9 MPa; 0.5 g (5 wt % Ru/C)/50 ml aqueous solution. (◆) Experiment 38; (◇) Experiment 15.

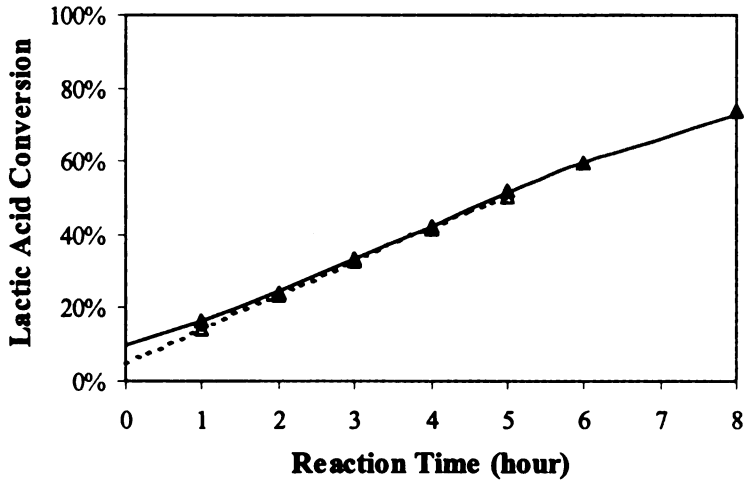

Figure 3.21. Replicate experiments for lactic acid hydrogenation over Ru/C - Experiments 26 and 116.
Conditions: 2M LA; T = 403 K; P_{H2} = 6.9 MPa; 0.5 g (5 wt % Ru/C)/50 ml aqueous solution. (▲) Experiment 26; (△) Experiment 116.

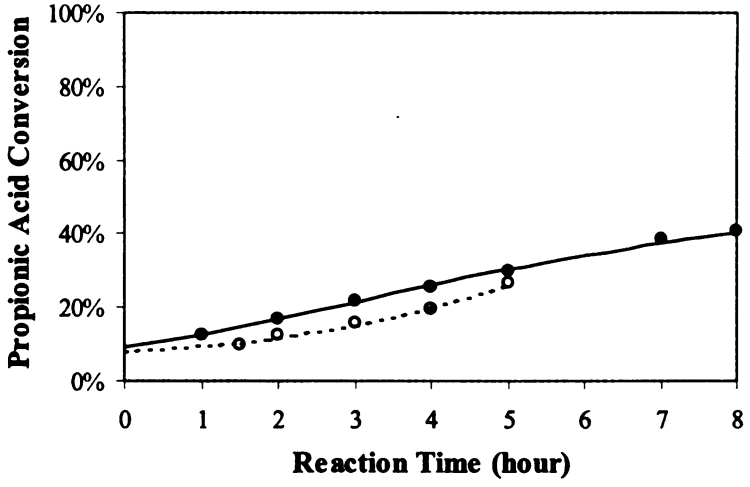

Figure 3.22. Replicate experiments for propionic acid hydrogenation over Ru/C - Experiments 22 and 42.
Conditions: 0.5M PA; T = 403 K; P_{H2} = 6.9 MPa; 0.5 g (5 wt % Ru/C)/50 ml aqueous solution. (●) Experiment 42; (○) Experiment 22.

3.5. References

(1) Hydrogen and Deuterium; Young, C. L., Ed.; *Solubility Data Series*; IUPAC, Pergamon Press; New York, **1981**; Vol. 5/6.

(2) Stephan, H., *The solubility of inorganic and organic compounds*, The Macmillan company, New York, **1963**.

(3) Daniel G. Lahr and Brent H. Shanks. Kinetic analysis of the hydrogenolysis of lower polyhydric alcohols: glycerol to glycols. *Ind. Eng. Chem. Res.* **2003**, *42*, 5467.

(4) Levenspiel, O., *Chemical Reaction Engineering*, 3rd Edition, page 27, Wiley, New York, **1999**.

(5) Yuqing Chen, Dennis J. Miller and James E. Jackson. Kinetics of Aqueous-Phase Hydrogenation of Organic Acids and Their Mixtures over Carbon Supported Ruthenium Catalyst. *Ind. Eng. Chem. Res.* **2007**, *46*, 3334-3340.

Chapter 4. Aqueous-Phase Hydrogenation of Organic Acids and Their Mixtures over Ruthenium Sponge

4.1. Introduction

The aqueous-phase hydrogenation of LA and PA alone, together, and in mixtures with their alcohol products PG and 1-PrOH, over bulk ruthenium metal catalyst (un-supported Ru sponge) was performed in a three-phase stirred batch reactor. This group of experiments was conducted to help understand the effects of the activated carbon support on hydrogenation reactivity and selectivity, by comparing the results of acid adsorption and hydrogenation over carbon supported (5 wt % Ru/C) and un-supported (Ru sponge) ruthenium catalysts. Since the role of the activated carbon support is often to facilitate selective adsorption of organic species out of aqueous solution, it may be that selective adsorption of acids or alcohols into the carbon pore structure results in higher local concentrations in the vicinity of the catalyst and thus affects the observed rates of organic acid hydrogenation.

Hydrogenation experiments were performed at temperature of 403 K, at several acid feed concentrations from 0.1 to 1 M, and at hydrogen pressures from 3.4 to 7.9 MPa. Catalyst loading was 5 g Ru sponge in 50 ml aqueous solution for most experiments. A summary of the reaction conditions investigated is reported in Table 4.1.

Table 4.1. Summary of reaction conditions for the hydrogenation of lactic acid and propionic acid over Ru sponge

T (K)	P_{H2} (MPa)	Catalyst[a]	Catalyst Loading (g/50 ml solution)	Concentrations of the Starting Materials (M)				t (hour)	LA Conv. (%)	PA Conv. (%)
				LA	PA	PG	1-PrOH			
403	6.9	old Ru sponge	2.7	0.1				5	75	
403	6.9	old Ru sponge	2.7		0.1			5		17
403	6.9	old Ru sponge	2.7		0.5			52.5		57
403	6.9	old Ru sponge	2.7		2			52		37
403	6.9	old Ru sponge	2.7	0.1	0.1			5	74	8.7
403	6.9	Ru-I-0	2.5	0.1				51	35	
403	6.9	Ru-I-0	5	0.1				51	73	
403	6.9	Ru-I-0	10	0.1				51	99	
403	3.4	Ru-II-0	5	0.1				5	47	
403	6.9	Ru-I-5	5	0.1				5	69	
403	6.9	Ru-I-4	5	0.1		0.5		5	71	
403	6.9	Ru-I-4	5	0.1			0.1	5	68	
403	6.9	Ru-I-4	5	0.1			0.5	5	78	
403	7.9	Ru-II-1	5	0.1				5	59	
403	3.4	Ru-I-6	5		0.1			6		4.7
403	6.9	Ru-I-5	5		0.1			46.25		82
403	6.9	Ru-I-3	5		0.1	0.5		77		95
403	6.9	Ru-I-3	5		0.1		0.1	53.5		92
403	6.9	Ru-I-3	5		0.1		0.5	77		95
403	7.9	Ru-II-1 and 2	5		0.1			5		18
403	3.4	Ru-II-0	5	0.1	0.1			6	34	2.9
403	6.9	Ru-I-5	5	0.1	0.1			5	66	8.2
403	6.9	Ru-I-2	5	0.5	0.1			52	84	13
403	6.9	Ru-I-2	5	1	0.1			52	71	3.5
403	6.9	Ru-I-1	5	0.1	0.5			74.5	85	22
403	6.9	Ru-I-1	5	0.1	1			74.5	88	20
403	7.9	Ru-I-6 and 7	5	0.1	0.1			5	47	4.2
T (K)	P_{H2} (MPa)	Catalyst[a]	Catalyst Loading (g/50 ml solution)	LA	PA	PG	1-PrOH	t (hour)	LA Conv. (%)	PA Conv. (%)
				Concentrations of the Starting Materials (M)						

[a]Catalyst: "Ru" means Ru sponge; "I, II" are the catalyst batch numbers; "0,1,.....7" are the numbers of times the catalyst is reused.
For example: "Ru-I-6" means the Ru sponge with batch number "I" has been reused for six times".

4.2. Effect of microporous carbon support on hydrogenation reactivity and selectivity

The aqueous-phase hydrogenation of LA, PA and their mixtures were performed in a Parr series 5000 batch reactor at 403 K and 6.9 MPa hydrogen pressure. Both 5 wt % ruthenium supported on 3310 activated carbon and nonporous ruthenium bulk sponge were used as catalysts to determine the effect of microporosity on reactivity. The metallic surface area of each catalyst, measured by volumetric hydrogen chemisorption in a Micromeritics ASAP 2010 instrument, is 1.6 m^2/g for the Ru/C, 0.2 ~ 0.4 m^2/g for the old Ru sponge (with unknown batch No.), and 0.055 ~ 0.22 m^2/g for the new Ru sponge (batch No. 09814PB). For direct comparison of results from these catalysts, all ruthenium catalysts were pre-reduced at the same conditions (473 K and 3.4 MPa hydrogen pressure for 12 hours). The acid conversion rates were calculated on a metallic surface area basis (mol acid / m^2 metallic surface area / s).

The initial hydrogenation rates of LA, PA, and their mixtures are summarized in Table 4.2. The rates per unit metal area are, within experimental uncertainty (± 40%) of measuring the active surface area, the same for the old and new ruthenium sponges. Both acids react faster on the carbon-supported ruthenium catalyst than on the ruthenium sponges. The LA initial rate on Ru/C is 1.4 times the initial rate on Ru sponge, and the PA initial rate on Ru/C is three times that on Ru sponge. Hydrogenation of an equimolar LA / PA mixture gives an initial rate of LA ten times that of PA over the un-supported ruthenium sponge catalyst, while on the carbon-supported ruthenium catalyst the initial rate of LA is only five times that of PA. The difference in hydrogenation reactivity of acids over carbon-supported and un-supported ruthenium catalysts indicates that the

activated carbon support may play a role in influencing relative rates of organic acid hydrogenation. Since the role of activated carbon is often to selectively adsorb organic species out of aqueous solution, the selective adsorption of acids into the carbon pore structure may result in higher local concentrations inside the carbon micropores and thus increase the observed hydrogenation rates.

Table 4.2. Comparison of the acid hydrogenation rates over carbon-supported and un-supported ruthenium catalysts

Catalysts	Metal surface area (m^2/g catalyst)	Starting materials	Initial rate × 10^7 (mol/m^2 metal surface area/s)		Initial rate ratio (LA/PA)
			LA	PA	
0.5 g (5 wt% Ru/C)	1.6	0.1M LA	7.1		
		0.1M PA		2.1	
		(0.1M LA) and (0.1M PA)	7.3	1.4	5.1
2.7 g old Ru sponge (unknown batch No.; reused for many times)	0.3 (0.2~0.4)	0.1M LA	5.0 (± 2.0)		
		0.1M PA		0.53 (± 0.21)	
		(0.1M LA) and (0.1M PA)	4.2 (± 1.7)	0.39 (± 0.16)	11
5 g new Ru sponge (batch No. 09814PB; Ru-I-5)	0.16 (0.055~0.22)	0.1M LA	4.7 (± 1.9)		
		0.1M PA		0.59 (± 0.24)	
		(0.1M LA) and (0.1M PA)	4.0 (± 1.6)	0.43 (± 0.17)	9.2

Conditions: T = 403 K, P_{H2} = 6.9 MPa, 50 ml reaction solution, 1000 rpm.

Adsorption experiments with LA and PA were performed on the 3310 activated carbon support by L. Peereboom[1] from the Miller group. Representative results of these adsorption studies are shown in Figure 4.1, as the quantity of each acid adsorbed as a function of temperature at 0.25 M solution concentration. The results indicate that PA is more strongly adsorbed into the carbon pore structure than is LA. Based on a micrcopore volume of 0.17 cm^3/g for 3310 carbon, the calculated local concentration of PA at 100-150 °C, which is the typical range of reaction temperatures for hydrogenation, is 7-8

times that of the bulk concentration of 0.25 M. In contrast, the pore concentration of LA is only 2.5 – 3 times the bulk concentration at those temperatures. These observations are consistent with the results of reactivity studies discussed previously: The ratio of initial rates (LA/PA) on the carbon-supported ruthenium is much lower than that on the nonporous Ru sponge because of the local enhancement of PA concentration inside the carbon micropores, resulting in its enhanced reaction rate. The rates measured on the nonporous Ru sponge represent real reaction kinetics because local and bulk concentrations are the same. We thus conclude that the actual ratio of reactivity of LA to PA is about ten (see Table 4.2), but that value is disguised over Ru/C catalyst because of pore concentration enhancement.

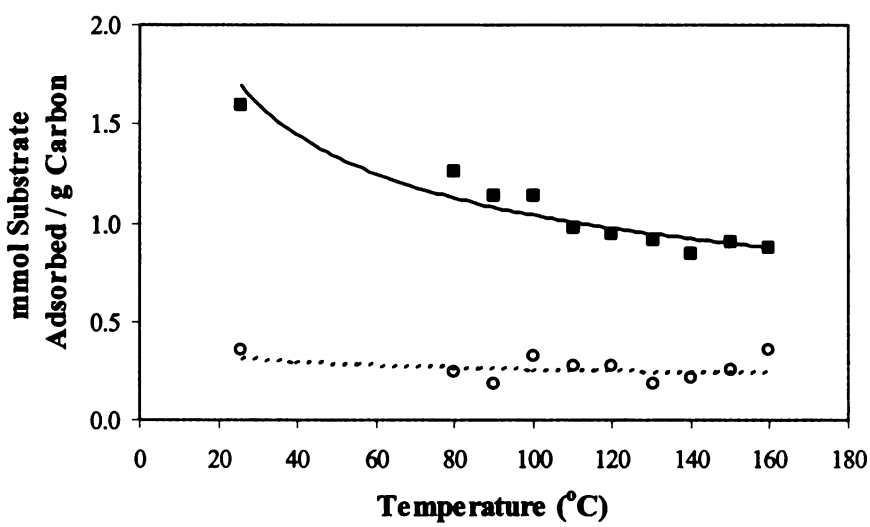

Figure 4.1. Temperature dependent adsorption of lactic acid and propionic acid on activated carbon 3310.
Conditions: mixture of (0.25 M LA) and (0.25 M PA); 50 ml aqueous solution; 3 g carbon 3310; (○) LA; (■) PA.

Selectivity to the alcohol products of hydrogenation was observed over carbon supported and un-supported ruthenium catalysts. The selectivity to PG in LA hydrogenation is similar on Ru/C and Ru sponge catalysts (80 - 90 % selectivity). The selectivity to 1-PrOH in PA hydrogenation, as shown in Table 4.3, is obviously higher when using Ru sponge as the catalyst. In adsorption studies of acids and alcohols on the carbon support (Chapter 5), we have found that 1-PrOH adsorbs more strongly than PG into the carbon micropore, creating locally high pore concentrations of 1-PrOH near catalytic Ru sites that contribute to its elevated degradation rate and lower selectivity on Ru/C.

Table 4.3. Comparison of the 1-propanol selectivity over carbon-supported and un-supported ruthenium catalysts

Starting materials	2.7g Ru sponge			0.5g 5 wt% Ru/C		
	t (hour)	PA conv. (%)	1-PrOH sele. (%)	t (hour)	PA conv. (%)	1-PrOH sele. (%)
0.1 M PA	5	17	99	8	80	44
0.5 M PA	52.5	57	73	8	41	54
2 M PA	52	37	63	6	13	48
(0.1M LA) and (0.1M PA)	5	13	96	8	60	75

Conditions: T = 403 K, P_{H2} = 6.9 MPa, 50 ml reaction solution, 1000 rpm.

4.3. Hydrogenation of single lactic acid and propionic acid over Ru sponge

4.3.1. Effect of catalyst loading

Initial hydrogenation rates of 0.1 M LA at three different catalyst loadings (2.5, 5, and 10 g new Ru sponge) with otherwise identical reaction conditions (403 K and 6.9 MPa hydrogen pressure) are represented in Figure 4.2. The acid conversion rate increased

linearly with the catalyst loading, indicating that the reaction was controlled by the availability of catalytic surface sites. Selectivity to PG was not affected by catalyst loading at the temperature and pressure investigated.

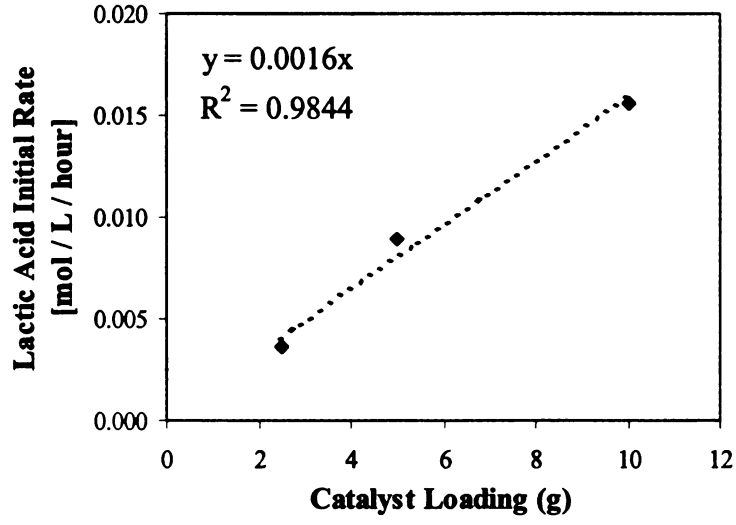

Figure 4.2. Effect of catalyst loading on lactic acid hydrogenation rate over Ru sponge. Conditions: The catalyst is new Ru sponge with a metallic surface area of 0.1 m^2/g; 50 ml 0.1 M LA aqueous solution; T = 403 K; P_{H2} = 6.9 MPa; 1000 rpm.

4.3.2. Effect of acid feed concentration

PA conversion rates at three different feed concentrations (approximately 0.1, 0.5, and 2 M) but otherwise identical reaction conditions are reported in Figure 4.3. Initial PA hydrogenation rates at these concentrations are represented in Figure 4.4. The non-linear dependence of initial rate on initial concentration in PA is similar to the observation on Ru/C catalyst (Figure 3.12), which indicates that the hydrogenation over Ru sponge is not simply first order in PA, and suggests that the reaction kinetics on Ru sponge would be better described using a Langmuir-Hinshelwood type of rate expression.

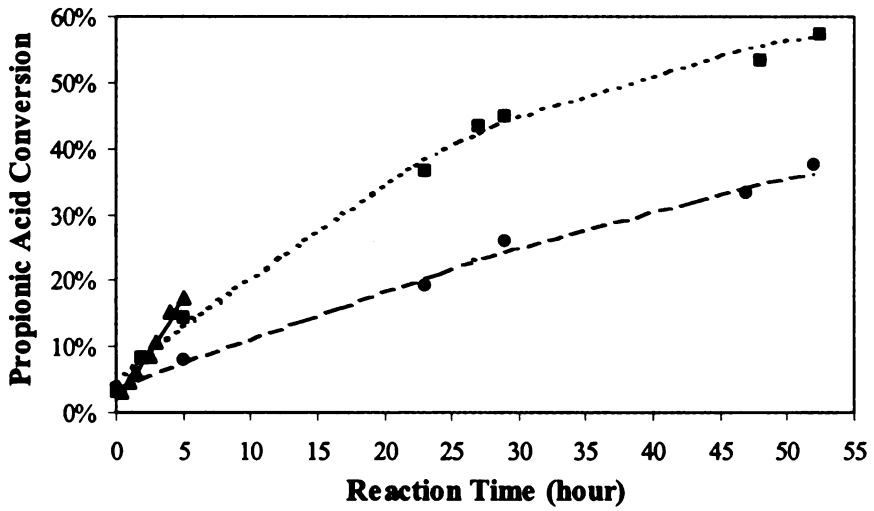

Figure 4.3. Effect of initial acid concentration on propionic acid hydrogenation rate over Ru sponge.
Conditions: The catalyst is 2.7g old Ru sponge with a metal surface area of 0.2-0.4 m^2/g; T = 403 K; P_{H2} = 6.9 MPa; 1000 rpm. (▲) 0.1M PA; (■) 0.5M PA; (●) 2M PA.

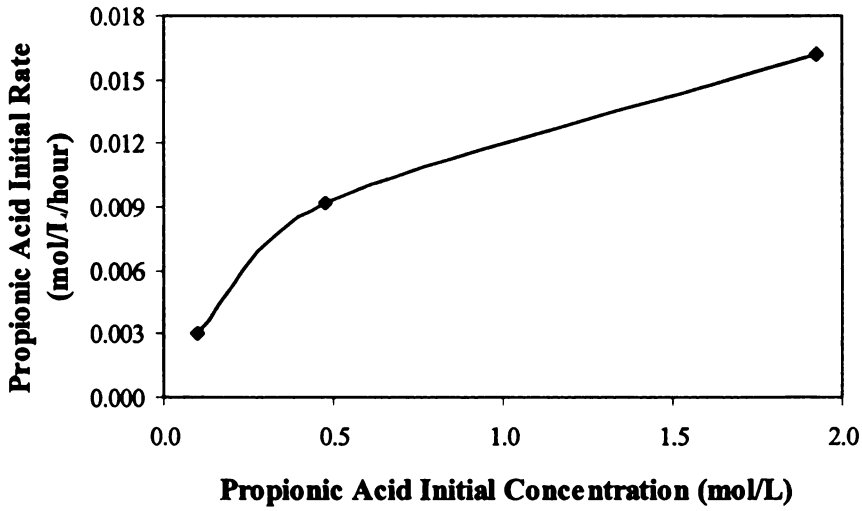

Figure 4.4. Concentration dependence of the propionic acid hydrogenation rate over Ru sponge.
Conditions: The catalyst is 2.7g old Ru sponge with a metal surface area of 0.2-0.4 m^2/g; T = 403 K; P_{H2} = 6.9 MPa; 1000 rpm.

4.3.3. Effect of hydrogen pressure

Conversion rates of LA and PA at three different hydrogen pressures (3.4, 6.9, and 7.9 MPa) are reported in Figure 4.5. Higher hydrogen pressures favored the conversion of LA and PA, and hydrogen pressure has little effect on the selectivity to product alcohols on Ru sponge.

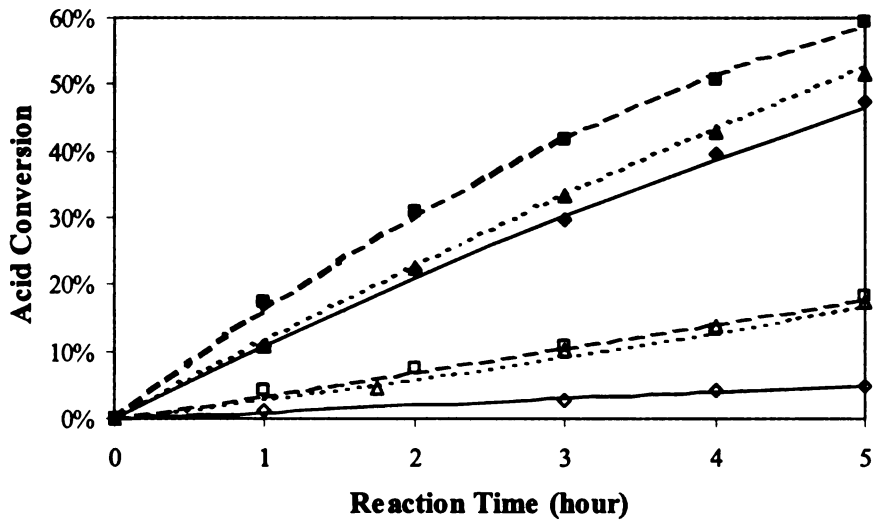

Figure 4.5. Effect of hydrogen pressure on acid hydrogenation rate over Ru sponge. Conditions: Starting materials = 0.1M LA or 0.1M PA; T = 403 K; 5 g Ru sponge/50 ml aqueous solution; 1000 rpm.

For LA: (◆) 3.4 Mpa, Ru-II-0; (▲) 6.9 Mpa, Ru-II-1; (■) 7.9 Mpa, Ru-II-1.

For PA: (◇) 3.4 Mpa, Ru-I-6; (△) 6.9 Mpa, Ru-I-5; (□) 7.9 Mpa, Ru-II-1 and Ru-II-2.

4.3.4. Effect of catalyst reuse

The expensive ruthenium sponge catalyst for hydrogenation reactions can be reused for many times without obvious decrease in catalytic activity. To recover the catalyst, the Ru sponge was first separated from the final reaction solution by filtration or centrifugation, washed thoroughly with HPLC water, and then calcined at 350-400 °C for

12 hours. The recovered catalyst was pre-reduced in situ at 200 °C and 500 psi hydrogen pressure for 12 hours before the next use. Although the activity of a Ru sponge catalyst did not decrease following its repeated use in hydrogenation, an increase in catalytic activity was observed in the used Ru sponge when compared with the new Ru sponge. Shown in Table 4.4 is the characterization of several Ru sponges with different number of times of reuse. The BET surface area and metallic surface area in Table 4.4 were measured by nitrogen physisorption and hydrogen chemisorption, respectively, in a Micromeritics ASAP 2010 instrument. The BET surface area does not change after repeated use of the catalyst. The metallic surface area of new and used Ru sponge, however, are quite different. To test the catalytic activity of new and used Ru sponge, hydrogenation of LA and PA were conducted with several different Ru sponges at otherwise identical reaction conditions. The conversion curves of LA and PA for these experiments are reported in Figures 4.6 and 4.7. As can be seen, the acid hydrogenation reactivity is higher on the used Ru sponge, and the catalytic activity tends to stabilize after the catalyst has been reused for more than three times. The degree of activity increase is dependent on the reaction conditions, catalyst recovery conditions, and the number of times the catalyst is reused. The possible cause for the increase in catalytic activity is a physical change of the active site of the catalyst itself caused by reaction circumstances such as reaction temperature and pressure, or the accumulation of a foreign metal (XPS analysis showed that the used Ru sponge was contaminated by Chromium that presumably from the stainless steel reactor vessel).

Table 4.4. Characterization of the Ruthenium Sponge

Ru Sponge	BET Surface Area (m^2/g Ru)	Metal Dispersion (%)	Metallic Surface Area (m^2/g Ru)
Ru-I-0 (Batch No. I; New sponge)	0.31, 0.33	0.028, 0.029	0.10, 0.11
Ru-I-6 (Batch No. I; Reused for six times)	0.43	0.015	0.054
Ru-I-7 (Batch No. I; Reused for seven times)	0.39	0.016	0.060
Ru-II-0 (Batch No. II; New sponge)	0.42	0.043, 0.029	0.12, 0.11
Ru-II-1 (Batch No. II; Reused for once)	0.34	0.060, 0.048	0.22, 0.17

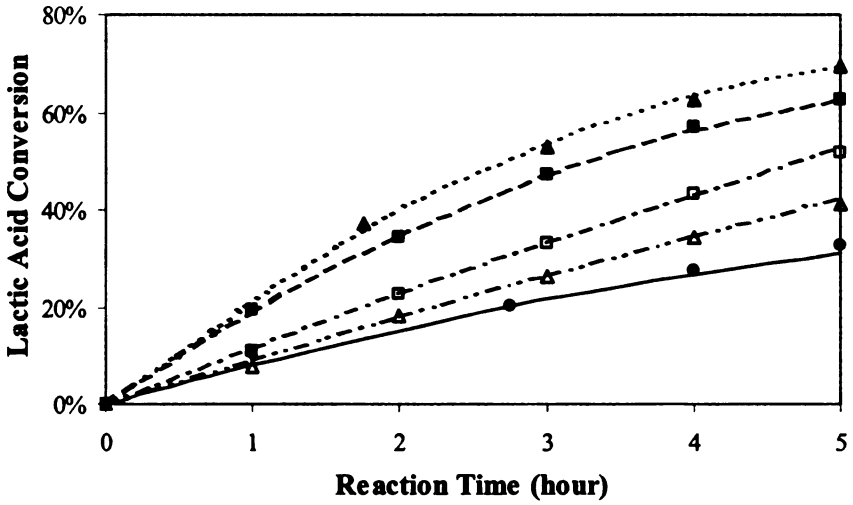

Figure 4.6. Change in the catalytic activity of Ru sponge for lactic acid hydrogenation. Conditions: 0.1 M LA; T = 403 K; P_{H2} = 6,9 MPa; 5 g Ru sponge/50 ml aqueous solution; 1000 rpm. (●) Ru-I-0; (▲) Ru-I-5; (■) Ru-I-7; (△) Ru-II-0; (□) Ru-II-1.

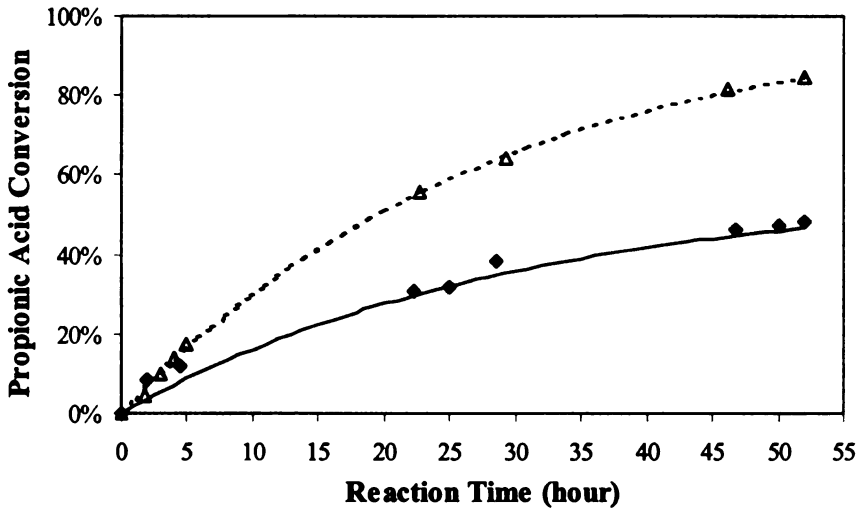

Figure 4.7. Change in the catalytic activity of Ru sponge for propionic acid hydrogenation.
Conditions: 0.1 M PA; T = 403 K; P_{H2} = 6.9 MPa; 5 g Ru sponge/50 ml aqueous solution; 1000 rpm. (◆) Ru-I-2; (△) Ru-I-5.

Since the activity of ruthenium sponge changes with the catalyst age, it is necessary to normalize the rate data collected, before using them for kinetic model development, based on the stabilized catalytic activity (the number of times for catalyst reuse ≥ 3). The method of normalization is described as follows: the catalysts Ru-I-3, Ru-I-4, Ru-I-5, Ru-I-6, and Ru-I-7 have the same activity that is directly proportional to the total concentration (C_t) of active sites; the activity of Ru-I-0, Ru-I-1, Ru-I-2, Ru-II-0, Ru-II-1, or Ru-II-2 was calculated according to the initial rate data available in Table 4.5, and was represented as a certain fraction of C_t (shown in Table 4.6); for example, the observed initial rate of LA hydrogenation was 0.0088 mol/L/hour over the catalyst Ru-I-0 (its activity was represented as $0.4C_t$), then the rate used for kinetic modeling should be

0.022 mol/L/hour (= 0.0088/0.4) after being normalized to the stabilized catalytic activity (represented as C_t).

Table 4.5. Initial rates of acid hydrogenation over Ru sponges with different age

Ru Sponge	LA Initial Rate (mol/L/hour)	PA Initial Rate (mol/L/hour)
Ru-I-0	0.0088	
Ru-I-1		
Ru-I-2		0.0018
Ru-I-3		
Ru-I-4		
Ru-I-5	0.024	0.0034
Ru-I-6		
Ru-I-7	0.020	
Ru-II-0	0.009	
Ru-II-1	0.012	
Ru-II-2		

Conditions: 0.1 M LA or PA; T = 403 K; P_{H2} = 6.9 MPa; 5 g Ru sponge/50 ml aqueous solution; 1000 rpm.

Table 4.6. Catalytic activity of Ru sponges with different age (the basis for rate data normalization)

Ru Sponge	Total Concentration of Active Sites (for LA hydrogenation)	Total Concentration of Active Sites (for PA hydrogenation)
Ru-I-0	$0.40C_t$	$0.40C_t$
Ru-I-1	$0.51C_t$	$0.51C_t$
Ru-I-2	$0.56C_t$	$0.56C_t$
Ru-I-3	C_t	C_t
Ru-I-4	C_t	C_t
Ru-I-5	C_t	C_t
Ru-I-6	C_t	C_t
Ru-I-7	C_t	C_t
Ru-II-0	$0.43C_t$	$0.43C_t$
Ru-II-1	$0.55C_t$	$0.55C_t$
Ru-II-2	$0.61C_t$	$0.61C_t$

4.4. Mixed acid/alcohol hydrogenation over Ru sponge – Effect of competitive adsorption

The simultaneous hydrogenation of two acids and combinations of acids with product alcohols were performed over Ru sponge catalyst at several concentration ratios. These studies provide insight into the interactions of the reaction species with the Ru metal, and how these species compete for active sites on the metal surface. By comparing the competition behavior of reaction species on Ru sponge with that on Ru/C, we expect to understand the role of the activated carbon support in acid adsorption and hydrogenation.

The results of these experiments are shown in Figures 4.8-4.11 (lines represent polynomial or exponential fits for rate calculations). As seen in Figures 4.8 and 4.9, LA conversion rates are not obviously affected by adding PA (consider the fact that Ru-I-5 has higher catalytic activity than Ru-I-1); while adding LA significantly decreases the conversion rate of PA, and this inhibitory effect increases with the concentration of the added LA. This observation indicate that PA is less competitive for active sites than LA on the Ru metal surface. The influence of the alcohol products on acid reaction rates is shown in Figures 4.10 and 4.11. The presence of PG and 1-PrOH in the starting solution has little effect on the hydrogenation rates of either acid, indicating that the adsorption of PG and 1-PrOH on the Ru metal surface is much weaker compared to the acids.

The results of competitive adsorption and hydrogenation over Ru sponge shown here are quite different from the previous results over Ru/C (Figures 3.15-3.18): LA and PA compete relatively equally for surface reaction sites on Ru/C; PG is weakly adsorbed on the Ru/C surface and it has little effect on the hydrogenation rates of either acid;

adding 1-PrOH to the initial reaction solution decreases PA conversion rate on Ru/C, while the effect of 1-PrOH on LA is less significant. We attribute these differences in observed relative reactivity of hydrogenation to the different adsorption affinity of reaction species on activated carbon support and on ruthenium metal surface: LA adsorbs more strongly than PA onto the ruthenium metal sites, while it adsorbs to a much lesser extent onto the support material compared to PA - consistent with the fact that PA competes relatively equally with LA over Ru/C while it has little effect on decreasing the LA conversion rates over Ru sponge; PG is weakly adsorbed onto both the metal active sites and the carbon micropores; the decreased PA conversion rates on Ru/C upon adding 1-PrOH is evidence of strong adsorption of 1-PrOH onto the activated carbon support.

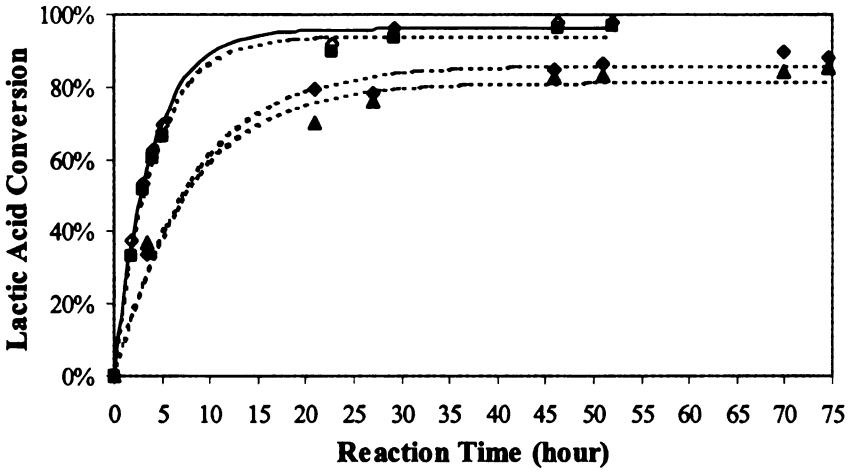

Figure 4.8. Effect of propionic acid on lactic acid hydrogenation rate over Ru sponge. Conditions: T = 403 K; P_{H2} = 6.9 MPa; 5 g Ru sponge/50 ml aqueous solution; 1000 rpm. (◇) 0.1 M LA; Ru-I-5; (■) 0.1 M LA and 0.1 M PA; Ru-I-5; (▲) 0.1 M LA and 0.5 M PA; Ru-I-1; (◆) 0.1 M LA and 1 M PA; Ru-I-1.

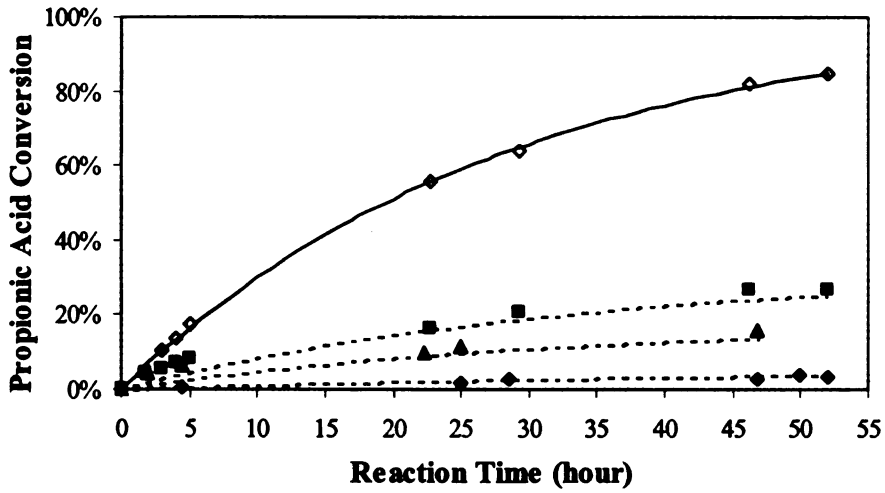

Figure 4.9. Effect of lactic acid on propionic acid hydrogenation rate over Ru sponge. Conditions: T = 403 K; P_{H2} = 6.9 MPa; 5 g Ru sponge/50 ml aqueous solution; 1000 rpm. (◇) 0.1 M PA; Ru-I-5; (■) 0.1 M PA and 0.1 M LA; Ru-I-5; (▲) 0.1 M PA and 0.5 M LA; Ru-I-2; (◆) 0.1 M PA and 1 M LA; Ru-I-2.

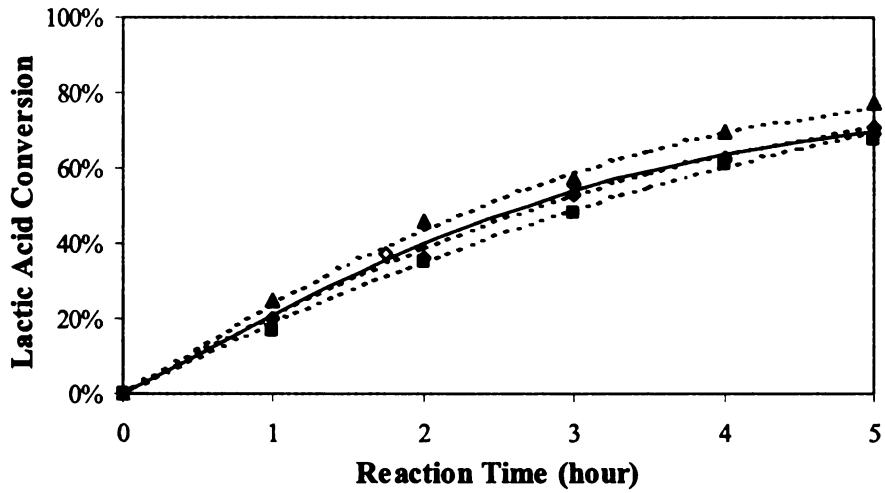

Figure 4.10. Effect of 1,2-propanediol and 1-propanol on lactic acid hydrogenation rate over Ru sponge.
Conditions: T = 403 K; P_{H2} = 6.9 MPa; 5 g Ru sponge/50 ml aqueous solution; 1000 rpm. (◇) 0.1 M LA; Ru-I-5; (■) 0.1 M LA and 0.1 M 1-PrOH; Ru-I-4; (▲) 0.1 M LA and 0.5 M 1-PrOH; Ru-I-4; (◆) 0.1 M LA and 0.5 M PG; Ru-I-4.

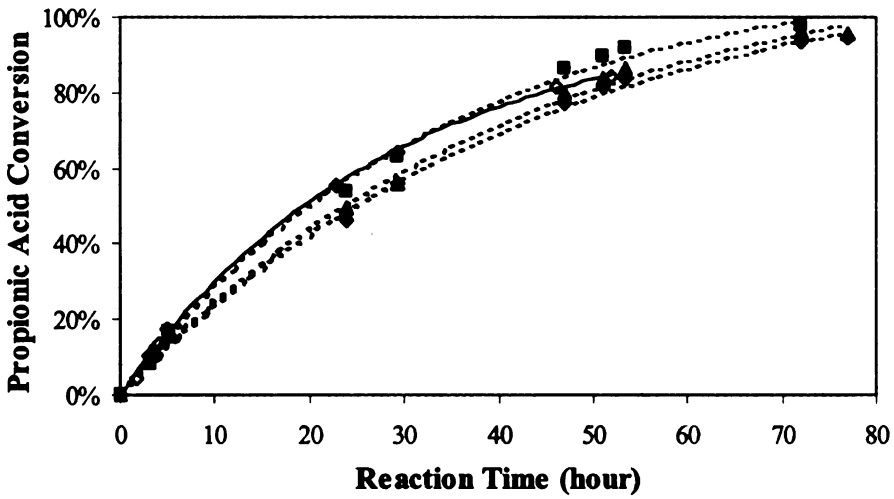

Figure 4.11. Effect of 1,2-propanediol and 1-propanol on propionic acid hydrogenation rate over Ru sponge.
Conditions: T = 403 K; P_{H2} = 6.9 MPa; 5 g Ru sponge/50 ml aqueous solution; 1000 rpm. (◇) 0.1 M PA; Ru-I-5; (■) 0.1 M PA and 0.1 M 1-PrOH; Ru-I-3; (▲) 0.1 M PA and 0.5 M 1-PrOH; Ru-I-3; (◆) 0.1 M PA and 0.5 M PG; Ru-I-3.

The above observations on adsorption affinity and hydrogenation reactivity over carbon supported and un-supported ruthenium catalysts demonstrate the importance of catalyst support material on the observed rate of acid hydrogenation. In order to properly characterize kinetics of acid conversion over Ru/C catalyst, particularly when mixtures of materials are present, it is necessary to consider the adsorption behavior of reaction species onto the activated carbon micropores in kinetic modeling and reactor design.

4.5. References

(1) L. Peereboom, Y. Chen, J. E. Jackson, and D. J. Miller, "Polyols and Organic Acids Adsorption onto Activated Carbon, and Its Role in Aqueous-Phase Catalytic Hydrogenation Rates", AIChE Annual Meeting, San Francisco, CA, November, **2006**.

Chapter 5. Adsorption Study on Activated Carbon

5.1. Introduction

Selective adsorption of reactant and product species onto the porous catalyst support materials can have a major effect on hydrogenation rates by causing difference in concentration between solution and pore. The adsorption of acids (LA and PA) and product alcohols (PG and 1-PrOH) on the 3310 activated carbon support was studied by Lars Peereboom[1,2] in the Miller group. The objective of his work is to develop adsorption models to characterize local concentrations in the catalyst pores and eventually incorporate local pore concentrations into kinetic modeling and reactor design of organic acid hydrogenation. In this Chapter, we briefly describe the adsorption work done by Lars Peereboom as a basis for the later development of a global model for organic acid hydrogenations over Ru/C catalyst (Chapter 7: Section 7.3).

5.2. Carbon characterization

The # 3310 activated carbon powder is the support material for ruthenium catalyst we used in organic acid hydrogenation. The BET surface area, micropore volume and total pore volume of this carbon support were characterized in a Micrometrics ASAP 2010 instrument using nitrogen physisorption method described in Section 2.2.

5.3. Isothermal adsorption

Adsorption experiments were conducted at room temperature (25 °C) using the method described in Section 2.3.1 for LA, PA, PG, and 1-PrOH with solution

concentration ranging from 0.01 M to 2 M. The quantity of species adsorbed onto the carbon support was determined by the difference in initial and final species concentration in solution, which was measured by HPLC prior to and following exposure to the activated carbon, respectively (Eq. 5.1). The local pore concentrations were then calculated based on the measured micropore volume of 0.17 cm^3/g carbon.

$$C_{AS} = \frac{(C_{A0} - C_A) * V_{solution}}{m_{carbon}} \tag{5.1}$$

where:

C_A = observed solution concentration of species A in equilibrium with the carbon support [M]

C_{A0} = initial solution concentration of species A prior to adsorption [M]

C_{AS} = concentration of species A in the carbon pore structure [mol/kg carbon]

m_{carbon} = mass of carbon in solution [kg]

The adsorption data from single component experiments were modeled using the Langmuir isotherm (Eq. 5.2) to obtain adsorption constants at room temperature. A plot of experimental data as (C_A/C_{AS}) vs. C_A gives a slope of $1/C_{TA}$ and an intercept of $1/K_A C_{TA}$. Comparing the experimental quantities adsorbed with those predicted by the model indicated that Langmuir isotherm gives the best fit of individual LA and PA adsorption at concentrations below 0.5 M. Shown in Table 5.1 are the Langmuir isotherm coefficients for LA, PA, PG and 1-PrOH adsorption on the # 3310 activated carbon.

$$C_{AS} = \frac{K_A C_A C_{TA}}{1 + K_A C_A} \tag{5.2}$$

where:

C_{TA} = maximum concentration of species A in the carbon pore structure [mol/kg carbon]

K_A = equilibrium constant for adsorption of species A in Langmuir isotherm model [1/M]

Table 5.1. Langmuir isotherm coefficients for LA, PA, PG and 1-PrOH adsorption on the # 3310 activated carbon

Substrates	Maximum Concentration of the Substrate in the Carbon Pore Structure C_{TA} (mol/kg carbon)	Equilibrium Constant for Adsorption K_A (1/M)
LA	2.71	2.38E-02
PA	1.61	1.87E-02
PG	1.43	1.80E-02
1-PrOH	2.62	1.80E-02

5.4. Elevated temperature adsorption

Quantities of reaction species adsorbed onto the 3310 activated carbon were measured at concentrations from 0.1 M to 0.5 M and temperatures from 303 to 423 K, using the method described in Section 2.3.2. At each temperature, the equilibrium constant (K_A) for the Langmuir isotherm was calculated using C_{TA} determined from isothermal adsorption experiments at 25 °C. The equilibrium constant varies with temperature based on the Van't Hoff Equation (Eq. 5.3). For each substrate, the plot of $ln(K_A)$ vs. $1/T$ was fitted with a straight line via least-squares linear regression to give the heat of adsorption (ΔH) from the slope ($-\Delta H/R$) and the preexponential constant (K_0) from the intercept ($ln(K_0)$).

$$\ln(K_A) = -\frac{\Delta H}{R} * \frac{1}{T} + \ln(K_0) \tag{5.3}$$

where:

ΔH = heat of adsorption [kJ/mol]; this is a constant since Langmuir isotherm assumes all adsorption sites have equal binding energies.

K_0 = Van't Hoff constant [1/M]

K_A = equilibrium constant for adsorption of species A in Langmuir isotherm model [1/M]

R = ideal gas constant [8.31 J/mol/K]

T = absolute temperature [K]

5.5. Mixed-component adsorption

Isothermal (298 K) and temperature-dependent (303-423 K) adsorption experiments were conducted for acid mixtures and combinations of acids with their alcohol products at several concentration ratios. The extended Langmuir model (Eqs. 5.4a and 5.4b) was applied to characterize mixed-substrate adsorption on the carbon support. The denominator of the extended Langmuir isotherm accounts for competitive adsorption of the two substrates into the carbon micropores. All parameters required in the extended model were taken from the single component modeling results.

$$C_{AS} = \frac{K_A C_A C_{TA}}{1 + K_A C_A + K_B C_B} \tag{5.4a}$$

$$C_{BS} = \frac{K_B C_B C_{TB}}{1 + K_A C_A + K_B C_B} \tag{5.4b}$$

where subscripts *A* and *B* denotes different component in the mixture.

5.6. Octanol-water partition coefficient estimation

The octanol-water partition coefficient (*Kow*) is defined as the ratio of a chemical's equilibrium concentration in the octanol phase to its concentration in the aqueous phase of a two-phase octanol/water system (Equation 5.5). Measured values of *Kow* for organic chemicals have been found as low as 10^{-3} and as high as 10^{7}. In terms of *logKow*, this range is from -3 to 7. Values of *Kow* represent the tendency of the chemical to partition itself between an organic phase and an aqueous phase. Chemicals with low *Kow* values may be considered relatively hydrophilic; they tend to have high water solubilities and small adsorption coefficients into organic matter. Conversely, chemicals with high *Kow* values are very hydrophobic; they preferentially partition into organic matter rather than water. The LogKow (KowWin) program estimates the *logKow* values of organic chemicals using an atom/fragment contribution method[3] developed at SRC. The *logKow* values of LA, PA, PG, and 1-PrOH are reported in Table 5.2. The relative magnitude of these *logKow* values indicates that PA and 1-PrOH are strongly adsorbed into the activated carbon micropores and functionalized carbon surfaces, while the adsorption of LA and PG is very weak on the carbon support.

$$Kow = \frac{\text{Concentration in octanol phase}}{\text{Concentration in aqueous phase}} \tag{5.5}$$

Table 5.2. The logKow values of LA, PA, PG, and 1-PrOH

Chemicals	*logKow* values
LA	-0.72
PA	0.33
PG	-0.92
1-PrOH	0.25

5.7. References

(1) Lars Peereboom, Benjamin Koenigsknecht, Margaret Hunter, James E. Jackson, and Dennis J. Miller. Aqueous-Phase adsorption of propylene glycol onto activated carbon. *Carbon* **2007**, *45*, 579-586.

(2) L. Peereboom, Y. Chen, J. E. Jackson, and D. J. Miller, "Polyols and Organic Acids Adsorption onto Activated Carbon, and Its Role in Aqueous-Phase Catalytic Hydrogenation Rates", AIChE Annual Meeting, San Francisco, CA, November, **2006**.

(3) W. M. Meylan and P. H. Howard. Atom/fragment contribution method for estimating octanol-water partition coefficients. *J. Pharm. Sci.* **1995**, *84*, 83-92.

Chapter 6. Mass Transfer Analysis

6.1. Introduction

Aqueous phase catalytic hydrogenation is a three-phase reaction involving hydrogen gas, aqueous solution of the organic acid and its alcohol product, and the solid catalyst. For reaction to occur, the following steps must take place: (1) hydrogen transport from the gas phase to the liquid phase across the gas-liquid interface; (2) hydrogen and acid transport from the bulk liquid phase to the catalyst across the liquid-solid interface; (3) hydrogen and the acid diffusion through the porous catalyst support to the metal surface sites; (4) adsorption and conversion of the acid to its alcohol product via a sequence of surface chemical reaction steps; (5) product desorption from the catalyst surface; (6) diffusion of products through the porous catalyst support to the liquid phase. For three-phase reactions, the rate of mass transfer between phases can significantly affect overall reaction rate. Collection of experimental rate data suitable for kinetic model development requires that the reactor contents are well mixed and that the reaction rates are not limited by mass transport resistances. Correlations in the literature have been developed to estimate the minimum stirring rate necessary for complete catalyst suspension and calculate the mass-transfer coefficients across the phase boundaries. Figure 5.1 illustrates the concentration profile of a three-phase reaction.

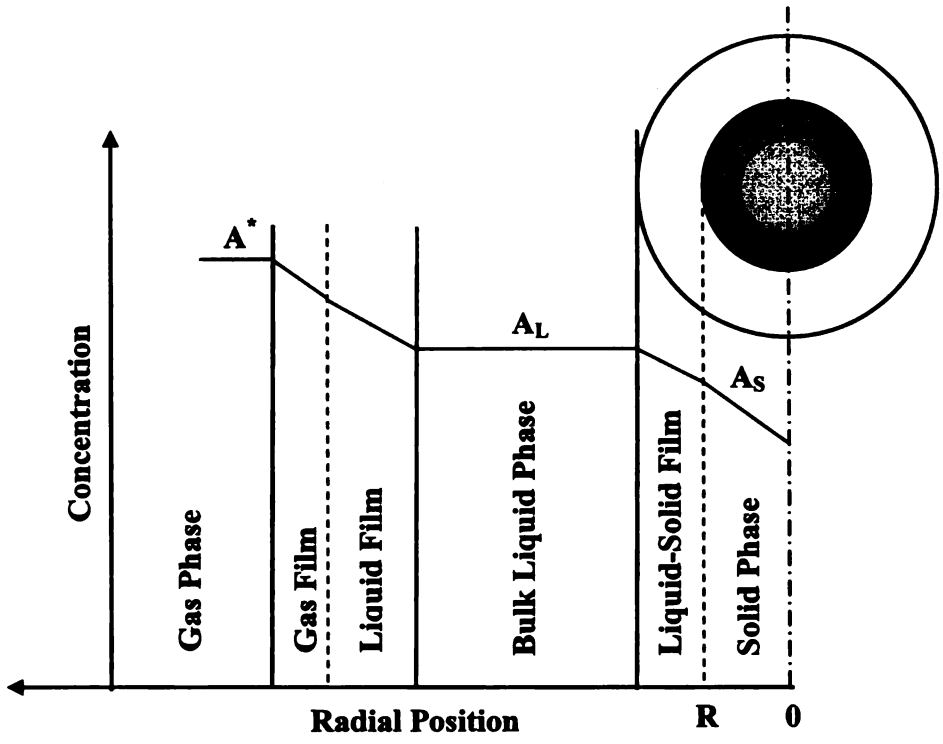

Figure 6.1. Mass transfer in a three-phase catalytic reaction

6.2. Catalyst suspension

For maximum utilization of the catalyst, it is necessary to keep the entire solid catalyst suspended and evenly distributed in the reaction solution. The Zwietering correlation[1] is used to estimate the minimum stirring rate necessary for complete catalyst suspension.

$$N_{\min} = \frac{2\left(\frac{d_R}{d_I}\right)^{1.33} d_P^{0.2} \mu_L^{0.1} g^{0.45} \left(\rho_P - \rho_L\right)^{0.45} w^{0.13}}{\rho_L^{0.55} d_I^{0.85}} \qquad (6.1)$$

where:

N_{min} = minimum stirring speed for complete catalyst suspension [rotations / sec]

d_R = reactor diameter [m]

d_I = impeller diameter [m]

d_P = particle diameter [m]

μ_L = liquid viscosity [kg / m·s]

g = gravitation constant [9.8066 m / s^2]

ρ_P = particle density [kg / m^3]

ρ_L = liquid density [kg / m^3]

w = catalyst loading [grams of catalyst / 100 grams of solution]

For this reaction system, with 0.5 g of 5 wt % Ru/carbon in 50 ml aqueous acid solution, the minimum stirring speed required for complete catalyst suspension is about 500 rpm. A stirring rate of 1000 rpm was therefore used in all experiments.

6.3. Gas-liquid mass transfer

The mass transfer rate across the gas-liquid (G-L) phase boundary is expressed by the following equation:

$$-r_{H_2} = k_{GL,H_2} a\left(C_{H_2}^{\ *} - C_{H_2,L}\right) \tag{6.2}$$

where:

$-r_{H2}$ = observed reaction rate of hydrogen [kmol / m^3 / s]

$k_{GL,H2}a$ = G-L mass transfer coefficient of H_2 [1 / s]

a = effective interfacial area per unit volume reaction fluid [1 / m]

$C_{H2}^{\ *}$ = gas-phase concentration of hydrogen [kmol / m^3]

$C_{H2,L}$ = bulk liquid concentration of hydrogen = aqueous-phase hydrogen solubility at the hydrogen partial pressure of the experiment [kmol / m^3]

The mass transfer coefficient ($k_{GL,H2}a$) across the gas-liquid (G-L) phase boundary for hydrogen was estimated using the correlations of Bern et al.[2] and of Yagi and Yoshida[3].

In 1976, Bern *et al* proposed the following correlation (Equation 6.3) for $k_{GL}a$ in an agitated slurry reactor from studies of the hydrogenation of oil in a gas-liquid mass transfer controlled regime and this correlation satisfied their data for both 30 and 500 liter reaction vessels.

$$k_{GL}a = 1.099 \times 10^{-2} N^{1.16} d_I^{1.979} u_g^{0.32} V_L^{-0.521} \tag{6.3}$$

where:

$k_{GL}a$ = G-L mass transfer coefficient [1 / s]

a = gas-liquid interfacial area per unit volume of solution [1 / cm]

d_I = impeller diameter [cm]

N = stirring speed [s^{-1}]

u_g = superficial gas velocity [cm / s]

V_L = volume of the solution [cm^3]

The correlation (Equation 6.4) from Yagi and Yoshida in 1975 was used to satisfactorily predict CO_2 adsorption in the glycerol-water system at 30°C.

$$Sh = \frac{k_{GL}ad_I^2}{D}$$

$$= 0.06\left(\frac{d_I^2 N\rho_L}{\mu_L}\right)^{1.5}\left(\frac{d_I N^2}{g}\right)^{0.19}\left(\frac{\mu_L}{\rho_L D}\right)^{0.5}\left(\frac{\mu_L u_g}{S_T}\right)^{0.6}\left(\frac{Nd_I}{u_g}\right)^{0.32} \tag{6.4}$$

where:

Sh = Sherwood number [dimensionless]

$k_{GL}a$ = G-L mass transfer coefficient [1 / s]

d_I = impeller diameter [m]

D = diffusion rate [m / s^2]

N = stirring speed [s^{-1}]

ρ_L = liquid density [kg / m^3]

μ_L = liquid viscosity [kg / m · s]

g = gravitational constant [9.8066 m / s^2]

u_g = superficial gas velocity [cm / s]

S_T = surface tension [N / m]

The gas phase concentration of hydrogen (C_{H2}^*) was calculated using the ideal gas law. The bulk liquid concentration of hydrogen ($C_{H2,L}$) can be measured[4] by a volumetric technique or determined by Henry's Law[5]:

$$P_A = y_A P = x_A H_A(T) \tag{6.5}$$

where:

P_A = partial pressure of species A in the gas phase [atm]

y_A = mole fraction of species A in the gas phase

P = total pressure in the gas phase [atm]

x_A = mole fraction of species A in the liquid phase

$H_A(T)$ = Henry's Law constant for A in a specific solvent [atm / (mole A / mole solution)]

6.4. Liquid-solid mass transfer

The mass transfer rates across the liquid-solid (L-S) phase boundary are expressed by the following equations:

$$-r_{Acid} = k_{LS,Acid} a_p \left(C_{Acid,L} - C_{Acid,S}\right) \tag{6.6}$$

$$-r_{H_2} = k_{LS,H_2} a_p \left(C_{H_2,L} - C_{H_2,S}\right) \tag{6.7}$$

where:

$-r_{Acid}$ = observed reaction rate of the acid [kmol / m^3 / s]

$-r_{H2}$ = observed reaction rate of hydrogen [kmol / m^3 / s]

$k_{LS,Acid}a_p$ = L-S mass transfer coefficient of the acid [1 / s]

$k_{LS,H2}a_p$ = L-S mass transfer coefficient of hydrogen [1 / s]

a_p = external area of catalyst particles per unit volume reaction fluid [1 / m]

$C_{Acid,L}$ = bulk liquid concentration of the acid [kmol / m^3]

$C_{Acid,S}$ = catalyst surface concentration of the acid [kmol / m^3]

$C_{H2,L}$ = bulk liquid concentration of hydrogen [kmol / m^3]

$C_{H2,S}$ = catalyst surface concentration of hydrogen [kmol / m^3]

The liquid-solid mass transfer coefficient, k_{LS}, for hydrogen and liquid phase reactants were calculated using the Boon-Long correlation[6] proposed in 1978 for agitated vessels.

$$\frac{k_{LS}d_p}{D} = 0.046\left(\frac{2\pi^2 d_p \rho_L d_T N}{\mu_L}\right)^{0.283}\left(\frac{\rho_L{}^2 g d_p{}^3}{\mu_L{}^2}\right)^{0.173}\left(\frac{w'V_L}{d_p{}^3}\right)^{-0.011}\left(\frac{d_T}{d_p}\right)^{0.019}\left(\frac{\mu_L}{\rho_L D}\right)^{0.461} \quad (6.8)$$

where:

k_{LS} = liquid-solid mass transfer coefficient [m / s]

d_p = catalyst particle diameter [m]

D = diffusion rate of species [m^2 / s]

d_T = reactor diameter [m]

N = stirring speed [s^{-1}]

μ_L = liquid viscosity [kg / m · s]

ρ_L = liquid density [kg / m^3]

g = gravitational constant [9.8 m / s^2]

w' = catalyst loading [grams of catalyst / 100 grams of solution]

V_L = liquid volume [m^3]

The mass transfer area for the liquid-solid interface is calculated using properties of the catalyst and conditions of the experiment:

$$a_p = \frac{6w'\rho_L}{d_p\rho_p} \tag{6.9}$$

where:

a_p = ratio of catalyst surface area to volume of reaction fluid [1 / m]

w' = catalyst loading [grams of catalyst / 100 grams of solution]

ρ_L = liquid density [kg / m^3]

d_p = catalyst particle diameter [m]

ρ_p = catalyst particle density [kg / m^3]

6.5. Comparison of reaction rates with mass transfer rates

For three-phase reactions, the rate of mass transfer between phases can significantly affect the overall reaction rate. The driving force for mass transfer is the difference in species concentration between phases, which can be measured directly or calculated. The maximum mass transfer rate is calculated as the product of the mass transfer coefficient and the initial species concentration in bulk solution. Hydrogen concentrations were calculated from solubility data[7].

Maximum G-L mass transfer rate for hydrogen = $(k_{GL,H2})\ a\ (C_{H2}^{*})$ (6.10)

Maximum L-S mass transfer rate for hydrogen = $(k_{LS,H2})\ a_p\ (C_{H2,L})$ (6.11)

Maximum L-S mass transfer rate for acids = $(k_{LS,Acid})\ a_p\ (C_{Acid,L})$ (6.12)

The results of mass transfer calculations (section 6.7) showed that the maximum rates of G-L and L-S mass transfer for each reactant are orders of magnitude larger than the observed reaction rates, indicating that mass transport resistances across phase boundaries were negligible at the experimental conditions studied.

6.6. Intraparticle mass transfer

The effect of mass transport inside the catalyst pores can be characterized by the Weisz-Prater criterion[8] via the observable modulus:

$$\eta\varphi^2 = \frac{-rL^2}{C_s D_e} \tag{6.13}$$

where:

$\eta\varphi^2$ = observable modulus

$-r$ = initial species reaction rate [mol / L · s]

L = characteristic length of the catalyst [m] = d_p / 6 for spherical particles

d_p = catalyst particle diameter [m]

C_s = liquid phase concentration at the catalyst surface [mol / L]

$D_e = \varepsilon^2 D_j$ = effective diffusivity [m^2 / s]

ε = support porosity = 0.6 for the 5 wt % Ru/C catalyst

D_j = diffusivity of reactant j in the liquid phase estimated using the Wilke-Chang equation[9]:

$$D_j = 7.4\times10^{-8}\frac{(\phi_B M_B)^{0.5} T}{\mu V_j^{0.6}} \tag{6.14}$$

where:

D_j = diffusivity of reactant j [cm^2 / s]

T = absolute temperature [K]

μ = viscosity of solution [cp]

V_j = molar volume of j as liquid at its normal boiling point [cm^3 / g mol]

ϕ_B = association parameter for solvent = 2.6 for water

M_B = molecular weight of solvent [g / mol]

The observable modulus is the ratio of the observed reaction rate to the effective diffusion rate inside the catalyst particle. If $\eta\varphi^2$ is less than 1, then the rate of mass transport is greater than the reaction rate and the reaction is not limited by intraparticle diffusion. As shown in Table 6.1, the observed modulus for each reactant is less than 0.1 (section 6.7), therefore mass-transport resistance inside the catalyst pores can be neglected.

The limiting reactant inside the catalyst particles was estimated by calculating the ratio of the observable modulus of hydrogen to that of the acid:

$$\frac{\eta\varphi_{H_2}^{\ 2}}{\eta\varphi_{Acid}^{\ 2}} = \frac{1}{b}\frac{C_{Acid}D_{e,Acid}}{C_{H_2}D_{e,H_2}} \tag{6.15}$$

where b is the stoichiometric ratio of hydrogen to acid (= 2.0). For all reactions we investigated, the ratio of observable moduli is much greater than 1, indicating that hydrogen is the limiting reactant.

6.7. Results of mass transfer calculations

Mass transfer coefficients and the maximum mass transfer rates were calculated for the experiment with the highest hydrogenation rate at which mass transfer is most likely to influence the reaction (50 ml 2 M lactic acid, 403 K, 6.9 MPa hydrogen pressure, and 0.5 g 5 wt % Ru/C catalyst). The results of mass transfer calculations are shown in Table 6.1: although G-L mass transfer of hydrogen is slower than L-S mass transfer of either acid or hydrogen, the maximum G-L and L-S mass transfer rates for both hydrogen and the acid are at least an order of magnitude larger than the observed maximum reaction rates, indicating that mass transport resistances across phase boundaries are negligible at the experimental conditions studied. This conclusion is supported by experiments represented in Figure 3.7 in which the acid conversion rate increases in proportion to the catalyst loading. This would not be the case if phase boundary mass transfer resistances limited reaction rate. Diffusion inside the catalyst pores is not limited because the observed modulus for each reactant is much less than one. The results of mass transfer analysis showed that surface reaction of the adsorbed species is the rate-limiting step. The experimental data collected represent intrinsic reaction kinetics and are suitable for kinetic model development.

Table 6.1. Results of Mass Transfer Analysis[a,b]

Description		Value
G-L mass transfer coefficient of H_2	$k_{GL}a$ [1/s]	7.1×10^{-2}
L-S mass transfer coefficient of H_2	$k_{LS,H2}$ [m/s]	3.5×10^{-5}
L-S mass transfer coefficient of LA	$k_{LS,LA}$ [m/s]	3.8×10^{-5}
L-S mass transfer area per volume fluid	a_p [1/m]	28000
Observed modulus for H_2	$\eta\varphi_{H2}^2$	4.2×10^{-2}
Observed modulus for LA	$\eta\varphi_{LA}^2$	4.9×10^{-4}
Maximum G-L mass transfer rate of H_2	$(k_{GL,H2})\ a\ (C_{H2}^*)$ [mol/cm^3/s]	3.8×10^{-6}
Maximum L-S mass transfer rate of H_2	$(k_{LS,H2})\ a_p\ (C_{H2,L})$ [mol/cm^3/s]	5.4×10^{-5}
Maximum L-S mass transfer rate of LA	$(k_{LS,Acid})\ a_p\ (C_{Acid,L})$ [mol/cm^3/s]	2.1×10^{-3}
Observed maximum reaction rate of H_2	$(-r_{H2})_{max}$ [mol/cm^3/s]	1.1×10^{-7}
Observed maximum reaction rate of LA	$(-r_{LA})_{max}$ [mol/cm^3/s]	5.5×10^{-8}

[a]Conditions: 50 ml 2 M lactic acid solution; 403 K; 6.9 MPa H_2; 0.5 g (5 wt % Ru/carbon)/50 ml aqueous solution; 1000 rpm.

[b]Mass transfer rates and reaction rates are reported on a unit fluid volume basis.

6.8. References

(1) Zwietering, T. N. Suspending of solids in liquid by agitators. *Chem. Eng. Sci.* **1958**, *8*, 244.

(2) Bern, L.; Lidefelt, J.; Schoon, N. Mass transfer and scaleup in fat hydrogenation. *J. Am. Oil Chem. Soc.* **1976**, *53*, 463.

(3) Yagi, H.; Yoshida, F. Gas absorption by Newtonian and non-Newtonian fluids in sparged agitated vessels. *Ind. Eng. Chem. Process Des. Dev.* **1975**, *14* (4), 488.

(4) Zhang, Z.; Jackson, J. E.; Miller, D. J. Kinetics of aqueous phase hydrogenation of lactic acid to propylene glycol. *Ind. Eng. Chem. Res.* **2002**, *41*, 691.

(5) Felder, R.M.; Rousseau, R.W., *Elementary Principles of Chemical Processes*, 2nd Ed., page 248, Wiley, New York, **1986**.

(6) Boon-Long, S.; Laguerie, C.; Couderc, J. Mass transfer from suspended solids to a liquid in agitated vessels. *Chem. Eng. Sci.* **1978**, *33* (7), 813.

(7) Hydrogen and Deuterium; Young, C. L., Ed.; *Solubility Data Series*; IUPAC, Pergamon Press; New York, **1981**; Vol. 5/6.

(8) Weisz, P.B.; Prater, C. D. Interpretation of measurements in experimental catalysis. *Adv. Catal.* **1954**, *6*, 143.

(9) Wilke, C.; Chang, P. Correlation of diffusion coefficients in dilute solution. *AIChE J.* **1955**, *1*, 264.

Chapter 7. Kinetic Modeling

7.1. Hydrogenation of organic acids over carbon-supported ruthenium catalyst

7.1.1. Introduction

The results of mass transfer analysis (Table 6.1) show that the acid conversion rates are not limited by mass-transport resistances over the ranges of temperature and acid feed concentrations investigated; therefore, the experimental data collected represent intrinsic reaction kinetics and are suitable for kinetic model development. To describe the hydrogenation reactions for LA, PA and their mixtures, a two-site Langmuir-Hinshelwood (L-H) kinetic model is postulated here in which acids adsorb on one type of surface catalytic site (S_1) and hydrogen dissociatively adsorbs on a second type of site (S_2). This two-site approach was first used in our group by Jere[1] for stereoretentive amino acid hydrogenation. The following set of elementary reactions is used to model both LA and PA hydrogenation:

$$\text{Acid} + S_1 = \text{Acid}\cdot S_1 \quad \text{(fast)} \tag{7.1a}$$

$$H_2 + 2S_2 = 2H\cdot S_2 \quad \text{(fast)} \tag{7.1b}$$

$$2H\cdot S_2 + \text{Acid}\cdot S_1 \rightarrow \text{Intermediate}\cdot S_1 + 2S_2 \quad \text{(slow)} \tag{7.1c}$$

$$\text{Intermediate}\cdot S_1 + 2H\cdot S_2 = \text{Alcohol}\cdot S_1 + 2S_2 \quad \text{(fast)} \tag{7.1d}$$

$$\text{Alcohol}\cdot S_1 = \text{Alcohol} + S_1 \quad \text{(fast)} \tag{7.1e}$$

The irreversible surface reaction of the adsorbed acid is assumed to be the rate-controlling step; all other steps are assumed to be rapid and close to equilibrium. The

adsorption of water is neglected. Several variations of the above L-H model were examined, including those with molecular hydrogen adsorption or same-site adsorption of the acid and hydrogen. Those models gave negative values of adsorption constants or a poor fit of data at high acid concentrations. Only the above two-site model gave positive values for all kinetic constants and reliably predicted the acid hydrogenation kinetics over a wide range of conditions.[2]

7.1.2. Hydrogenation of single acids over Ru/C catalyst

Combining the rate expressions for the above elementary reaction steps (Equations 7.1a-7.1e) and invoking the steady-state assumption for adsorbed intermediates yields the final rate expressions (Equations 7.12a and 7.12b) for single acid hydrogenation. The final rate equations are developed as follows:

Equilibrium constants for the adsorption of acid, hydrogen, and alcohol product are expressed as:

$$K_{Acid} = \frac{k_{Acid}}{k_{-Acid}} = \frac{C_{Acid \cdot S_1}}{C_{Acid} C_{v1}} \tag{7.2}$$

$$K_{H_2} = \frac{k_{H_2}}{k_{-H_2}} = \frac{\left(C_{H \cdot S_2}\right)^2}{P_{H_2} \left(C_{v2}\right)^2} \tag{7.3}$$

$$K_{Alcohol} = \frac{k_{Alcohol}}{k_{-Alcohol}} = \frac{C_{Alcohol \cdot S_1}}{C_{Alcohol} C_{v1}} \tag{7.4}$$

where $C_{Acid\cdot S1}$, $C_{H\cdot S2}$, $C_{Alcohol\cdot S1}$, C_{v1}, and C_{v2} represent the concentrations of acid-occupied sites, hydrogen-occupied sites, alcohol-occupied sites, vacant surface sites S_1, and vacant surface sites S_2, respectively.

The overall reaction rate is determined by the rate-limiting steps expressed in Equations (7.1c) and (7.1d). To simplify the model, desorption of the chemisorbed intermediate is neglected since the rate of consumption is much faster than that of formation for the intermediate at the present reaction conditions. The concentration of the adsorbed intermediate can be solved using the steady-state assumption by setting the rate of accumulation to zero. The surface reaction rate is expressed by Equation (7.5):

$$-r_{Acid} = k_s C_{Acid\cdot S_1} \left(C_{H\cdot S_2}\right)^2 \tag{7.5}$$

Substituting Equations (7.2) and (7.3) and rearrange the above rate equation:

$$-r_{Acid} = k_s \left(K_{Acid} C_{Acid} C_{v1}\right)\left(K_{H_2} P_{H_2} \left(C_{v2}\right)^2\right) \tag{7.6}$$

$$-r_{Acid} = k_s K_{Acid} K_{H_2} C_{v1} \left(C_{v2}\right)^2 C_{Acid} P_{H_2} \tag{7.7}$$

In addition, the relationships for the surface active sites are:

$$C_{t1} = C_{v1} + C_{Acid\cdot S_1} + C_{Alcohol\cdot S_1} \tag{7.8}$$

$$C_{t2} = C_{v2} + C_{H\bullet S_2} \tag{7.9}$$

where C_{t1} and C_{t2} represent the total concentrations of sites S_1 and S_2, respectively.

Substituting Equations (7.2), (7.3) and (7.4) to Equations (7.8) and (7.9), and solve for C_{v1} and C_{v2}:

$$C_{v1} = \frac{C_{t1}}{\left(1 + K_{Acid} C_{Acid} + K_{Alcohol} C_{Alcohol}\right)} \tag{7.10}$$

$$C_{v2} = \frac{C_{t2}}{\left(1 + \sqrt{K_{H_2} P_{H_2}}\right)} \tag{7.11}$$

Combining Equations (7.10) and (7.11) with Equation (7.7) give the following final rate expressions for single acid hydrogenation:

$$-r_{Acid}\,(kmol/kg\ catalyst/\sec)$$

$$= \frac{k_{Acid} C_{Acid} P_{H_2}}{\left(1 + K_{Acid} C_{Acid} + K_{Alcohol} C_{Alcohol}\right)\left(1 + \sqrt{K_{H_2} P_{H_2}}\right)^2} \tag{7.12a}$$

$$k_{Acid} = k_{sA} K_{Acid} K_{H_2} C_{t1} \left(C_{t2}\right)^2 \tag{7.12b}$$

where k_{Acid} = composite rate constant for each acid [m^3/kg catalyst/MPa/sec]

k_{sA} = surface reaction rate constant for each acid [(kg catalyst)^2/kmol^2/sec]

K_{Acid} = adsorption constant for each acid [m^3/kmol]

$K_{Alcohol}$ = adsorption constant for each alcohol product [m^3/kmol]

K_{H2} = adsorption constant for hydrogen [1/MPa]

C_{t1} = total catalyst site concentration for acid and alcohol adsorption [kmol/kg catalyst]

C_{t2} = total catalyst site concentration for hydrogen adsorption [kmol/kg catalyst]

The rate constants and equilibrium constants in Equations (7.12a) and (7.12b) for single acid hydrogenation were calculated by a least-squares regression analysis of kinetic data taken from 35 experiments (shown in Table 3.1) at 403 K. The values of these constants are reported in Table 7.1. The adsorption constant of LA on Ru/C catalyst is slightly higher than that of PA, indicating that these two acids compete relatively equally for catalytic surface sites. 1-PrOH has the highest affinity for active sites among these four reaction species, and PG is weakly adsorbed with an adsorption constant of 0.27 m^3/kmol. The relative magnitude of the kinetic parameters shown here are consistent with the results seen in Figures 3.15-3.18. Adding a second acid significantly decreased the conversion rate of the first acid because both compete relatively equally for surface reaction sites. The fact that PG has little effect on the reaction rate of both acids is consistent with its low adsorption constant. The presence of 1-PrOH in the starting solution decreases PA hydrogenation rate – evidence of strong adsorption onto catalyst sites.

Table 7.1. Kinetic Constants for Single Acid Hydrogenation over Ru/C at 403 K [a,b]

Kinetic Constants		Values at 403 K
Composite rate constant of LA	k_{LA} (m^3/kg catalyst/MPa/s)	1.0E-05
Composite rate constant of PA	k_{PA} (m^3/kg catalyst/MPa/s)	1.7E-06
Adsorption constant of LA	K_{LA} (m^3/kmol)	1.7
Adsorption constant of PA	K_{PA} (m^3/kmol)	1.4
Adsorption constant of PG	K_{PG} (m^3/kmol)	0.27
Adsorption constant of 1-PrOH	$K_{1\text{-}PrOH}$ (m^3/kmol)	2.9
Adsorption constant of H_2	K_{H2} (MPa^{-1})	0.21

[a]Conditions: 403 K; 0.5 g (5 wt % Ru/C)/50 ml solution; 1000 rpm.
[b]Use bulk solution concentrations.

Comparison of the experimental and predicted rates for individual LA and PA hydrogenation are shown in Figures 7.1 and 7.2. These parity plots illustrate the agreement between the observed rates and the rates predicted by the model. For both LA and PA hydrogenation, all of the data points are distributed near the y = x line in the parity plots, indicating that this two-site L-H model predicts single acid hydrogenation kinetics over a wide range of concentrations (0.1-5 M) with a high degree of reliability. Figures 7.3 and 7.4 compare experimental and predicted acid conversion versus time for experiments conducted at a typical reaction condition (0.5 M acid, 0.5 g Ru/C, 50 ml solution, 403 K, 6.9 MPa hydrogen). Clearly, the reaction trajectories are properly reproduced by the model.

For reaction conditions in Figures 7.1 and 7.2, the turnover frequency at a typical LA reaction rate of 3.3×10^{-6} kmol/kg of catalyst/s is ~ 270 mol of LA/mol of Ru surface atoms/hour; for PA at a rate of 0.7×10^{-6} kmol/kg of catalyst/s the turnover frequency is ~ 60/hour.

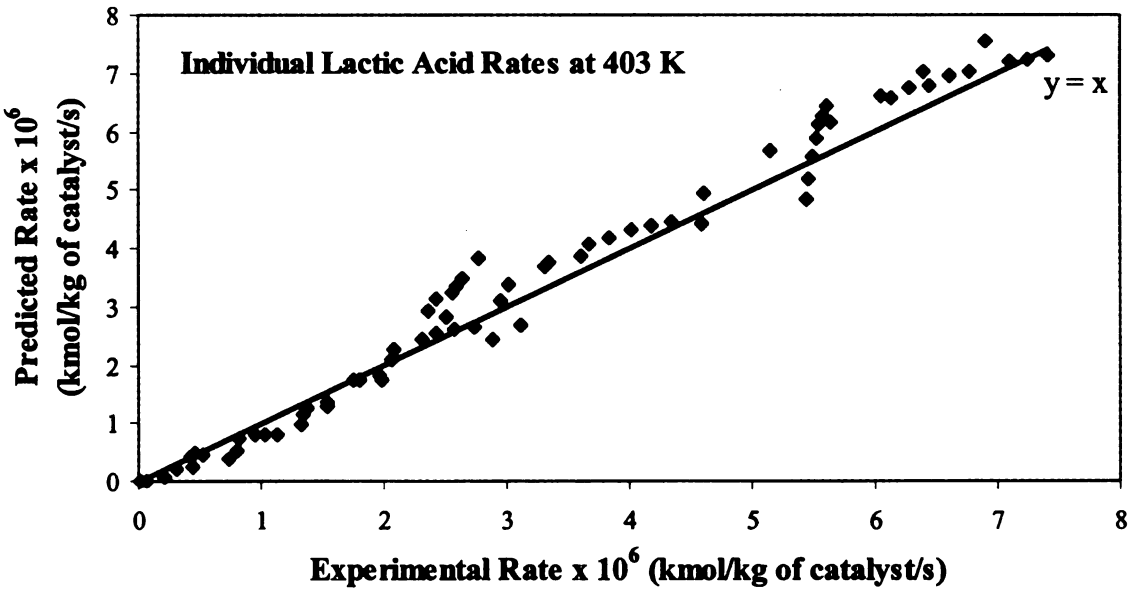

Figure 7.1. Experimental and predicted rates for individual lactic acid hydrogenation over Ru/C.
Conditions: T = 403 K, 0.5 g (5 wt % Ru/C)/50 ml solution, 1000 rpm.

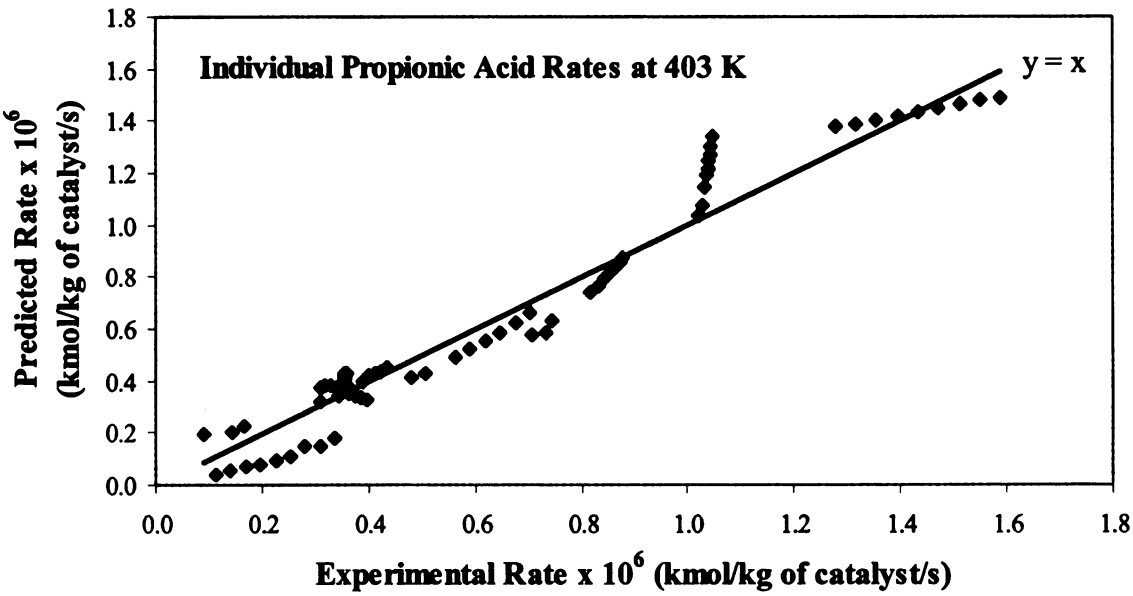

Figure 7.2. Experimental and predicted rates for individual propionic acid hydrogenation over Ru/C.
Conditions: T = 403 K, 0.5 g (5 wt % Ru/C)/50 ml solution, 1000 rpm.

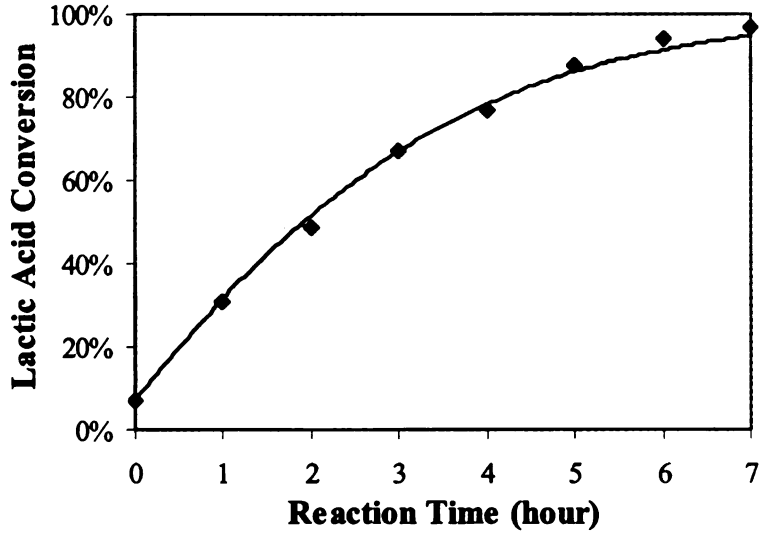

Figure 7.3. Experimental and predicted conversion rates for individual lactic acid hydrogenation over Ru/C.
Conditions: 0.5 M LA, 0.5 g (5 wt % Ru/C)/50 ml solution, T = 403 K, P_{H2} = 6.9 MPa, 1000 rpm.
The line represents reaction trajectory predicted by the model.

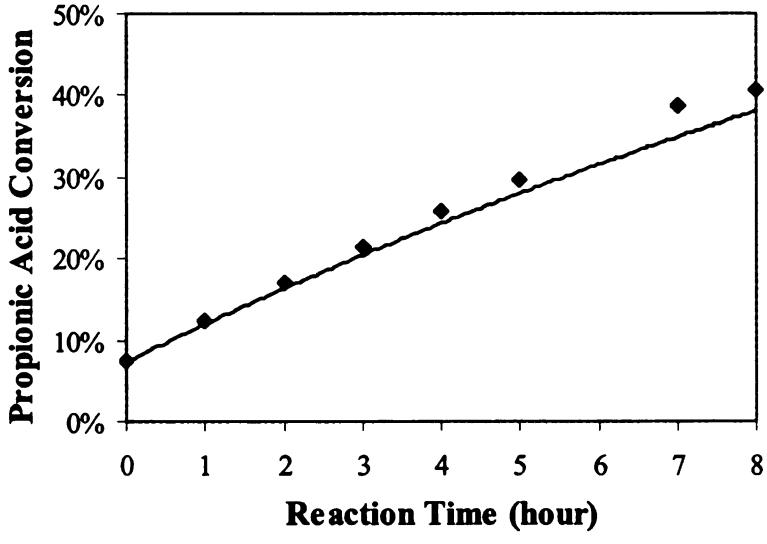

Figure 7.4. Experimental and predicted conversion rates for individual propionic acid hydrogenation over Ru/C.
Conditions: 0.5 M PA, 0.5 g (5 wt % Ru/C)/50 ml solution, T = 403 K, P_{H2} = 6.9 MPa, 1000 rpm.
The line represents reaction trajectory predicted by the model.

A sensitivity analysis (Table 7.2) of the kinetic constants, carried out by varying one constant while holding all others constant, shows that a ±20% change in k_{LA}, k_{PA}, K_{LA}, K_{PA}, and K_{H2} results in a substantial increase (50-700%) in the least squares error of predicted rate; the model is sensitive to these constants because they appear in the numerator of the kinetic rate expression. In contrast, the model is relatively insensitive to the adsorption constant K_{PG} and $K_{1\text{-}PrOH}$ of the alcohol products because of the low value of K_{PG} and because few experiments were conducted at significant concentrations of 1-PrOH.

Table 7.2. Sensitivity Analysis of the Kinetic Constants for Single Acid Hydrogenation over Ru/C at 403 K

Kinetic Constants	Change in the Constants	Change in the Sum of Deviation Squares (Π)[b]	
		Single LA	Single PA
k_{LA} (m^3/kg catalyst/MPa/s)	-20%	+195%	
	+20%	+705%	
k_{PA} (m^3/kg catalyst/MPa/s)	-20%		+193%
	+20%		+345%
K_{LA} (m^3/kmol)	-20%	+520%	
	+20%	+18%	
K_{PA} (m^3/kmol)	-20%		+250%
	+20%		+50%
K_{PG} (m^3/kmol)	-20%	+2%	
	+20%	+1%	
$K_{1\text{-}PrOH}$ (m^3/kmol)	-20%		+4%
	+20%		+4%
K_{H2} (MPa^{-1})	-20%	+307%	+138%
	+20%	+51%	+37%

[b]The sum of deviation squares:

$$\Pi = \sum_{i=1}^{n} (\text{Predicted Rate} - \text{Experimental Rate})^2$$

7.1.3. Hydrogenation of acid mixtures over Ru/C catalyst

In acid mixtures, competitive adsorption between LA and PA affects their relative hydrogenation rates. To quantify this effect, the two-site Langmuir-Hinshelwood model is extended to include adsorption of additional species in the denominator term. For two acid mixtures, the PG term in the denominator of the L-H rate expression is eliminated because PG is weakly adsorbed and thus has little effect on rate. The resulting kinetic rate expressions for mixed acid hydrogenation are given in Equations (7.13) and (7.14).

$$-r_{LA}(kmol/kg\ catalyst/\sec) = \frac{k_{LA}C_{LA}P_{H_2}}{\left(1+K_{LA}C_{LA}+K_{PA}C_{PA}+K_{1\text{-Pr}OH}C_{1\text{-Pr}OH}\right)\left(1+\sqrt{K_{H_2}P_{H_2}}\right)^2} \tag{7.13a}$$

$$k_{LA} = k_{sLA}K_{LA}K_{H_2}C_{t1}\left(C_{t2}\right)^2 \tag{7.13b}$$

$$-r_{PA}(kmol/kg\ catalyst/\sec) = \frac{k_{PA}C_{PA}P_{H_2}}{\left(1+K_{LA}C_{LA}+K_{PA}C_{PA}+K_{1\text{-Pr}OH}C_{1\text{-Pr}OH}\right)\left(1+\sqrt{K_{H_2}P_{H_2}}\right)^2} \tag{7.14a}$$

$$k_{PA} = k_{sPA}K_{PA}K_{H_2}C_{t1}\left(C_{t2}\right)^2 \tag{7.14b}$$

$$\frac{\left(-r_{LA}\right)}{\left(-r_{PA}\right)} = \left(\frac{k_{sLA}}{k_{sPA}}\right)\left(\frac{K_{LA}}{K_{PA}}\right)\left(\frac{C_{LA}}{C_{PA}}\right) \tag{7.15}$$

The terms in the denominator of the rate equations represent the relative concentrations of vacant (*1*), acid-occupied ($K_{LA}C_{LA}$ and $K_{PA}C_{PA}$), alcohol-occupied ($K_{1\text{-}PrOH}C_{1\text{-}PrOH}$), and hydrogen-occupied ($K_{H2}P_{H2}$) surface sites. For 0.5 M concentrations of LA and PA at 403 K, the site occupancies are 39.1% vacant, 34.3% LA, and 26.6% PA. With 0.5 M 1-PrOH present, the fractions change to 26.6% vacant, 23.3% LA, 18.1% PA, and 32.0% 1-PrOH. At the typical hydrogen pressure of 6.9 MPa, the fraction of hydrogen surface sites occupied is 60.1%. These results indicate that at much higher concentrations (>2 M), the surface is essentially saturated with reactants.

To examine how well the mixed acid L-H model predicts hydrogenation rates in acid mixtures, all kinetic parameters obtained from single acid reactions (Table 7.1) were used directly, without adjustment, in Equations (7.13) and (7.14) for prediction of mixed acid hydrogenation rates. Parity plots of LA and PA hydrogenation rates in acid mixtures are shown in Figures 7.5 and 7.6. From Figure 7.5, the two-site L-H model works quite well for LA in the two-acid hydrogenation over the concentration range 0.05-5 M, although some deviation is seen at the higher reaction rates. In Figure 7.6, most of the PA rate data follow the trend predicted by the model; however, discrepancy between the experimental and predicted rates arises at some reaction conditions. Comparisons of predicted and experimental acid conversions as a function of time for a typical reaction condition (mixture of 0.5M LA and 0.5M PA, 0.5 g Ru/C, 50 ml solution, 403 K, 7 MPa hydrogen) are shown in Figures 7.7 and 7.8. The model reliably predicts conversion rates of both acids for the hydrogenation of acid mixtures under this condition.

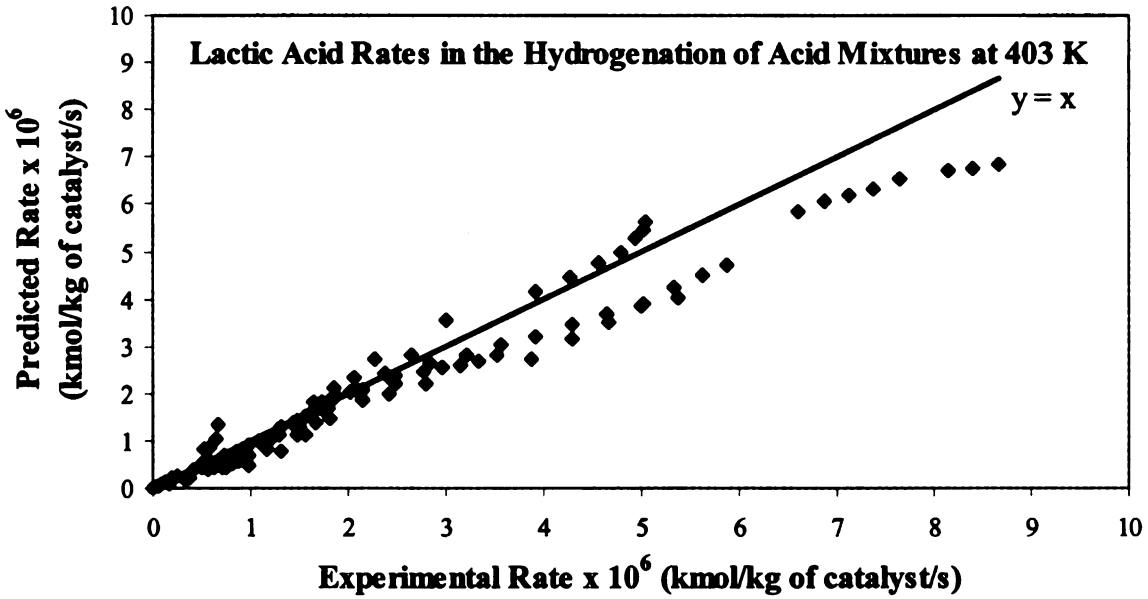

Figure 7.5. Experimental and predicted lactic acid rates in the hydrogenation of acid mixtures over Ru/C.
Conditions: T = 403 K, 0.5 g (5 wt % Ru/C)/50 ml solution, 1000 rpm.

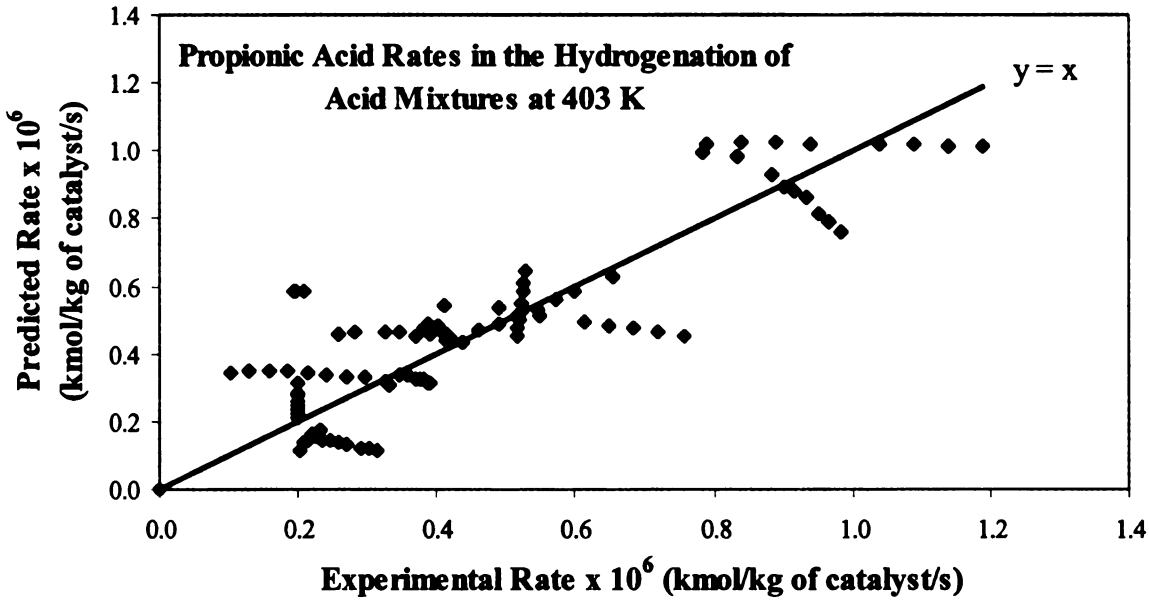

Figure 7.6. Experimental and predicted propionic acid rates in the hydrogenation of acid mixtures over Ru/C.
Conditions: T = 403 K, 0.5 g (5 wt % Ru/C)/50 ml solution, 1000 rpm.

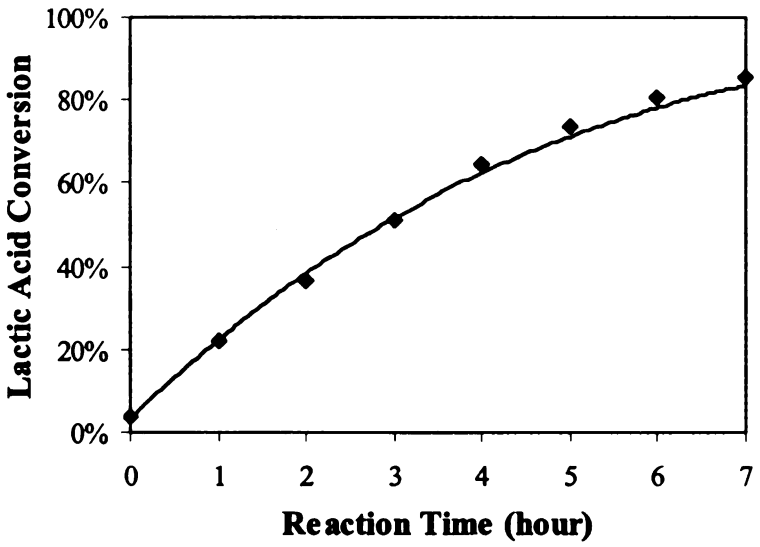

Figure 7.7. Experimental and predicted lactic acid conversion rates in the hydrogenation of acid mixtures over Ru/C.
Conditions: mixture of 0.5M LA and 0.5M PA, 0.5 g (5 wt % Ru/C)/50 ml solution, T = 403 K, P_{H2} = 6.9 MPa, 1000 rpm.
The line represents reaction trajectory predicted by the model.

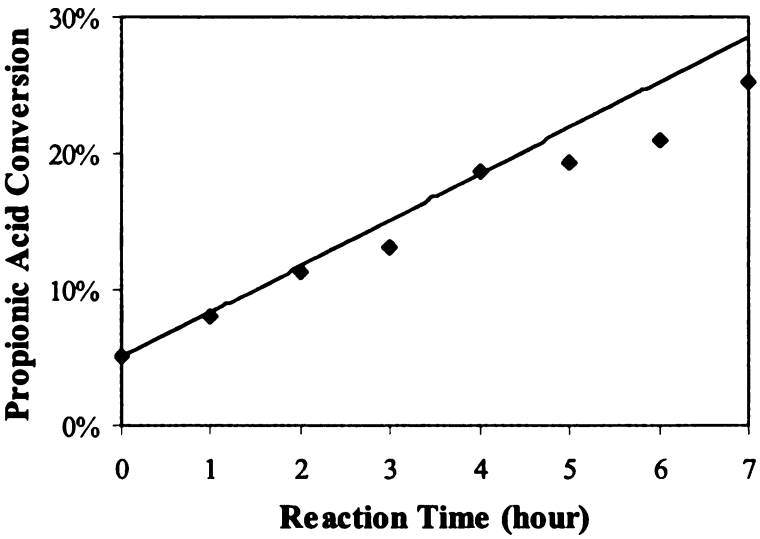

Figure 7.8. Experimental and predicted propionic acid conversion rates in the hydrogenation of acid mixtures over Ru/C.
Conditions: mixture of 0.5M LA and 0.5M PA, 0.5 g (5 wt % Ru/C)/50 ml solution, T = 403 K, P_{H2} = 6.9 MPa, 1000 rpm.
The line represents reaction trajectory predicted by the model.

7.1.4. Error analysis

The absolute value of percentage error in rate prediction for each data point was calculated via the expression in parenthesis in Equation (7.16a) below; the average was then determined over all individual data points. The average percent error in prediction of hydrogenation rates of LA and PA, both individually and in mixtures, are shown in Table 7.3.

$$Error\ \% = \frac{\sum_{n}\left(\frac{\left|Predicted\ Rate - Experimental\ Rate\right|}{Experimental\ Rate}\right)}{n} \times 100\% \qquad (7.16a)$$

The average absolute percent error for the single acid hydrogenation is within accepted range for kinetic modeling. It must be noted that the absolute percent error as described above weighs small values of reaction rate equally with large values, such that a small absolute deviation at low reaction rates can give a high percent error. This method of determining errors is thus conservative. If the error is taken relative to the average rate over all data points [a method that weighs small rates to a lesser extent, shown in Equation (7.16b) below], the average errors for LA and PA kinetic models are 9% and 11% respectively.

$$Error\ \% = \frac{\dfrac{\sum_{n} |Predicted\ Rate - Experimental\ Rate|}{n}}{\dfrac{\sum_{n} (Experimental\ Rate)}{n}} \times 100\%$$

$$= \frac{\sum_{n} |Predicted\ Rate - Experimental\ Rate|}{\sum_{n} (Experimental\ Rate)} \times 100\% \qquad (7.16b)$$

Percentage errors in mixed acid hydrogenation are similar for LA but larger for PA; the trend of PA hydrogenation in some experiments is unexplained at this point and even is opposite to that predicted by the kinetic model. Many of the experiments with these difficulties were conducted at relatively high concentrations (>2 M or >20 wt%) of acid, where the reaction environment may be substantially different from the aqueous phase media at lower concentrations.

Table 7.3. Average Error between Experimental and Predicted Rates over Ru/C at 403 K

Reaction System	Use Equation (7.16a)		Use Equation (7.16b)	
	Average Error (%)	Average Error of the Initial Rates (%)	Average Error (%)	Average Error of the Initial Rates (%)
Individual LA hydrogenation	15	14	9.5	11
Individual PA hydrogenation	18	17	11	13
LA in the hydrogenation of acid mixtures	17	13	15	16
PA in the hydrogenation of acid mixtures	30	17	22	19

7.1.5. Summary

Hydrogenation of LA and PA was carried out over a carbon-supported ruthenium catalyst for the acids alone in solution and for mixed acids in water. A two-site Langmuir-Hinshelwood kinetic model with surface reaction of the adsorbed acid as the rate-limiting step was developed to describe the hydrogenation of individual acids, acid mixtures, and acid mixtures with product alcohols. Competitive adsorption of the reacting species, reflected in the adsorption constants determined by fitting the L-H model, is postulated to be responsible for the strong effect of additional species on acid hydrogenation rates. The same kinetic and adsorption constants were used to characterize the hydrogenation of single acids and acid mixtures. The fit of the model was excellent for single acid hydrogenation, and reasonably good for mixed acids over a wide range of acid concentrations.

Finally, the activated carbon support may play a role in influencing relative rates of organic acid hydrogenation. Since the role of activated carbon is often to selectively adsorb organic species from water, the selective adsorption of acids or alcohols into the carbon micropores may result in higher concentrations in the catalyst vicinity and thus affects the observed reaction rates. We have characterized the adsorption behavior of the species presented here (LA, PA, PG, and 1-PrOH) on the activated carbon support (Chapter 5), and it is necessary to incorporate that information into an expanded reaction model for hydrogenation.

7.2. Hydrogenation of organic acids over ruthenium sponge catalyst

7.2.1. Introduction

The experimental data from acid hydrogenation over Ru sponge at 403 K were modeled using the same two-site Langmuir-Hinshelwood mechanism (Equations 7.1a-7.1e) postulated for acid hydrogenation over Ru/C catalyst: Acids adsorb on one type of surface catalytic site (S_1) and hydrogen dissociatively adsorbs on a second type of site (S_2); The irreversible surface reaction of the adsorbed acid is the rate-limiting step and all other steps are at equilibrium; The adsorption of water is neglected. The L-H rate expressions for the hydrogenation of single acid and acid mixtures are given in Equations 7.17-7.19. The PG and 1-PrOH terms in the denominator of the rate equations are eliminated because both products are weakly adsorbed on the ruthenium surface and thus have little effect on acid conversion rates (shown in Figures 4.10 and 4.11).

For single acid hydrogenations:

$$-r_{Acid}(kmol/kg\ catalyst/\sec) = \frac{k_{Acid}C_{Acid}P_{H_2}}{\left(1+K_{Acid}C_{Acid}\right)\left(1+\sqrt{K_{H_2}P_{H_2}}\right)^2} \tag{7.17a}$$

$$k_{Acid} = k_{sA}K_{Acid}K_{H_2}C_{t1}\left(C_{t2}\right)^2 \tag{7.17b}$$

For the hydrogenation of acid mixtures:

$$-r_{LA}(kmol/kg\ catalyst/\sec) = \frac{k_{LA}C_{LA}P_{H_2}}{\left(1+K_{LA}C_{LA}+K_{PA}C_{PA}\right)\left(1+\sqrt{K_{H_2}P_{H_2}}\right)^2} \quad (7.18a)$$

$$k_{LA} = k_{sLA}K_{LA}K_{H_2}C_{t1}\left(C_{t2}\right)^2 \quad (7.18b)$$

$$-r_{PA}(kmol/kg\ catalyst/\sec) = \frac{k_{PA}C_{PA}P_{H_2}}{\left(1+K_{LA}C_{LA}+K_{PA}C_{PA}\right)\left(1+\sqrt{K_{H_2}P_{H_2}}\right)^2} \quad (7.19a)$$

$$k_{PA} = k_{sPA}K_{PA}K_{H_2}C_{t1}\left(C_{t2}\right)^2 \quad (7.19b)$$

where k_{Acid} = composite rate constant for each acid [m^3/kg catalyst/MPa/sec]

k_{sA} = surface reaction rate constant for each acid [(kg catalyst)^2/kmol^2/sec]

K_{Acid} = adsorption constant for each acid [m^3/kmol]

K_{H2} = adsorption constant for hydrogen [1/MPa]

C_{t1} = total catalyst site concentration for acid and alcohol adsorption [kmol/kg catalyst]

C_{t2} = total catalyst site concentration for hydrogen adsorption [kmol/kg catalyst]

7.2.2. L-H model parameters for acid hydrogenation over Ru sponge catalyst

The hydrogenation of LA and PA (alone and mixed) over Ru sponge was modeled using Equations (7.17)-(7.19). The adsorption constants of LA and PA on Ru sponge were assigned according to the adsorption constants on Ru/C ($K_{LA,Ru/C}$ = 1.7 m^3/kmol, $K_{PA,Ru/C}$ = 1.4 m^3/kmol) to compensate for pore adsorption effects: as seen in Figure 4.1, the calculated pore concentration of PA at 100-150 °C is 7-8 times that of the bulk concentration of 0.25 M; in contrast, the pore concentration of LA is only 2-3 times the bulk concentration at those temperatures. The calculated values of $K_{LA,Ru\ sponge}$ and $K_{PA,Ru\ sponge}$ are 0.7 m^3/kmol and 0.18 m^3/kmol, respectively, based on Equations (7.20a) and (7.20b).

$$\frac{K_{\text{LA, Ru/C}}}{K_{\text{LA, Ru sponge}}} = \frac{\text{Pore Concentration}}{\text{Bulk Concentration}} = 2.5 \qquad (7.20a)$$

$$\frac{K_{\text{PA, Ru/C}}}{K_{\text{PA, Ru sponge}}} = \frac{\text{Pore Concentration}}{\text{Bulk Concentration}} = 7.5 \qquad (7.20b)$$

The rate constants $k_{LA,Ru\ sponge}$ and $k_{PA,Ru\ sponge}$ in Equations (7.17)-(7.19) were calculated by a least-squares regression analysis of the kinetic data taken from 19 experiments at 403 K (shown in Table 4.1; include the reactions of single acids and acid mixtures). The rate data from these experiments were normalized on the same basis of catalytic activity using the method discussed in Section 4.3.4. For the hydrogenation of LA, we observed catalyst deactivation after 24 hours of reaction; therefore, only the experimental data at t ≤ 24 hours were used for modeling. For the hydrogenation of PA, only the initial data (t = 0) were applied in modeling for most experiments due to the low acid conversions (PA conversion ≤ 10 %).

The values of all kinetic constants for acid hydrogenation over Ru sponge are reported in Table 7.4. The higher adsorption constant of LA compared to PA indicates that LA is adsorbed more readily on ruthenium surface sites. Figures 7.9 and 7.10 are parity plots of acid hydrogenation rates including all experimental data (single acids and acid mixtures); Figures 7.11 and 7.12 compare the experimental and predicted rates of individual LA and PA; Shown in Figures 7.13 and 7.14 are the parity plots of LA and PA rates in mixed acid hydrogenations. The two-site L-H model gives reasonably good fit of the conversion kinetics of mixed acid hydrogenations at 403 K, hydrogen pressures from 3.4 to 7.9 MPa, and total initial concentrations from 0.2 to 1.1 M. All of the rate data from single acid hydrogenation follow the trend predicted by the model although the conversion rates are under-predicted. The single acid experiments were all conducted at very low concentrations ($\leq$ 0.1 M), which may attribute to the discrepancy observed between experimental and predicted rates.

Table 7.4. Kinetic Constants for Acid Hydrogenation over Ru Sponge at 403 K[c]

Kinetic Constants		Values at 403 K
Composite rate constant of LA	k_{LA} (m^3/kg catalyst/MPa/s)	4.2E-07
Composite rate constant of PA	k_{PA} (m^3/kg catalyst/MPa/s)	3.6E-08
Adsorption constant of LA	K_{LA} (m^3/kmol)	0.7
Adsorption constant of PA	K_{PA} (m^3/kmol)	0.18
Adsorption constant of PG	K_{PG} (m^3/kmol)	0
Adsorption constant of 1-PrOH	$K_{1\text{-}PrOH}$ (m^3/kmol)	0
Adsorption constant of H_2	K_{H2} (MPa^{-1})	0.22

[c]Conditions: 403 K; 5 g Ru sponge/50 ml solution; 1000 rpm.

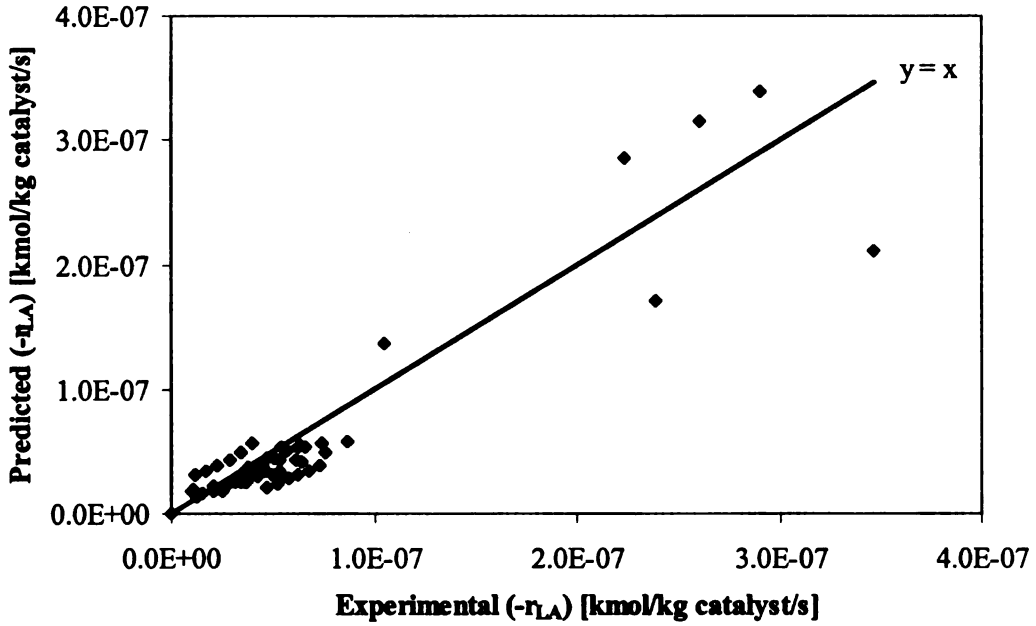

Figure 7.9. Experimental and predicted rates for lactic acid hydrogenation over Ru sponge (all data).
Conditions: 403 K; 5 g Ru sponge/50 ml solution; 1000 rpm.

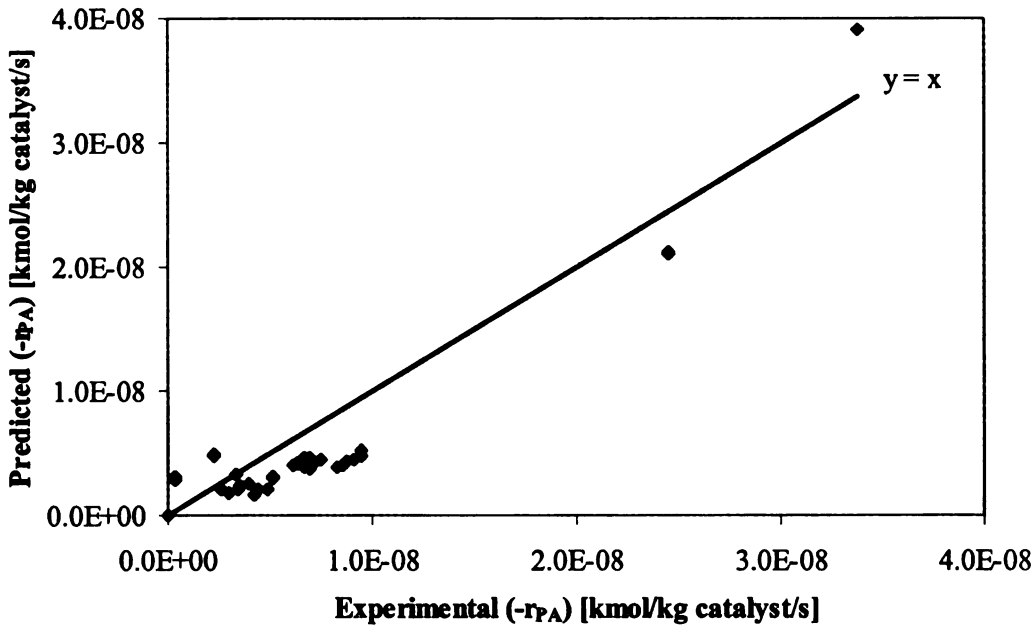

Figure 7.10. Experimental and predicted rates for propionic acid hydrogenation over Ru sponge (all data).
Conditions: 403 K; 5 g Ru sponge/50 ml solution; 1000 rpm.

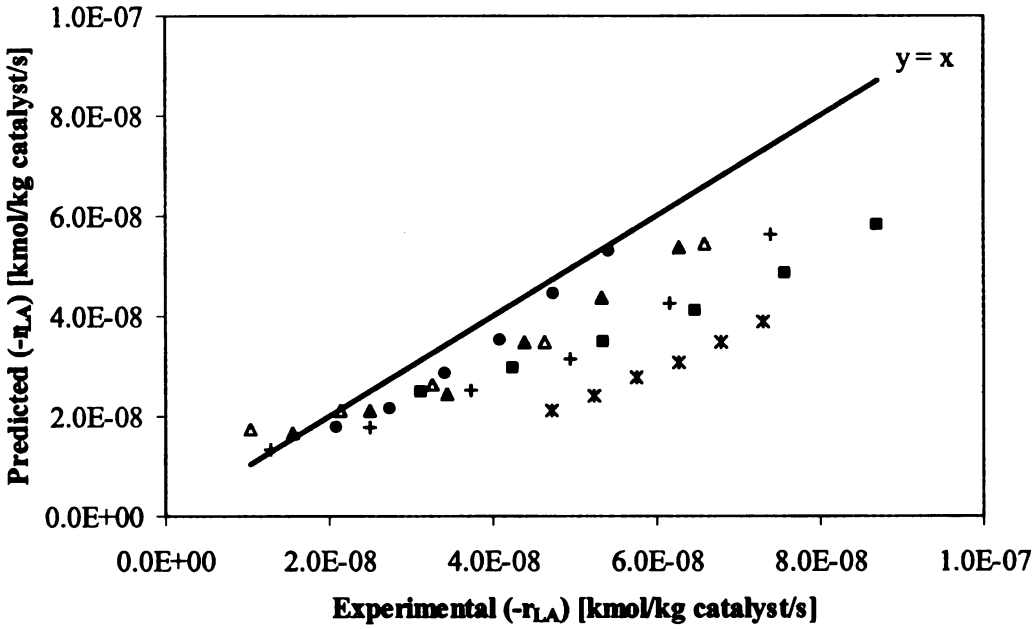

Figure 7.11. Experimental and predicted rates for individual lactic acid hydrogenation over Ru sponge.
Conditions: 403 K; 5 g Ru sponge/50 ml solution; 1000 rpm.

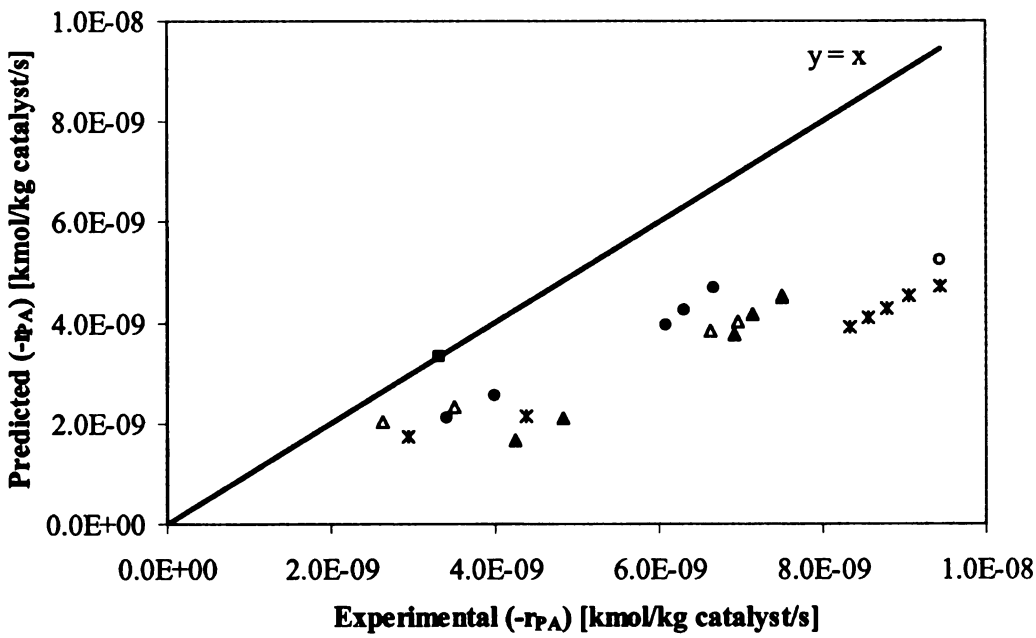

Figure 7.12. Experimental and predicted rates for individual propionic acid hydrogenation over Ru sponge.
Conditions: 403 K; 5 g Ru sponge/50 ml solution; 1000 rpm.

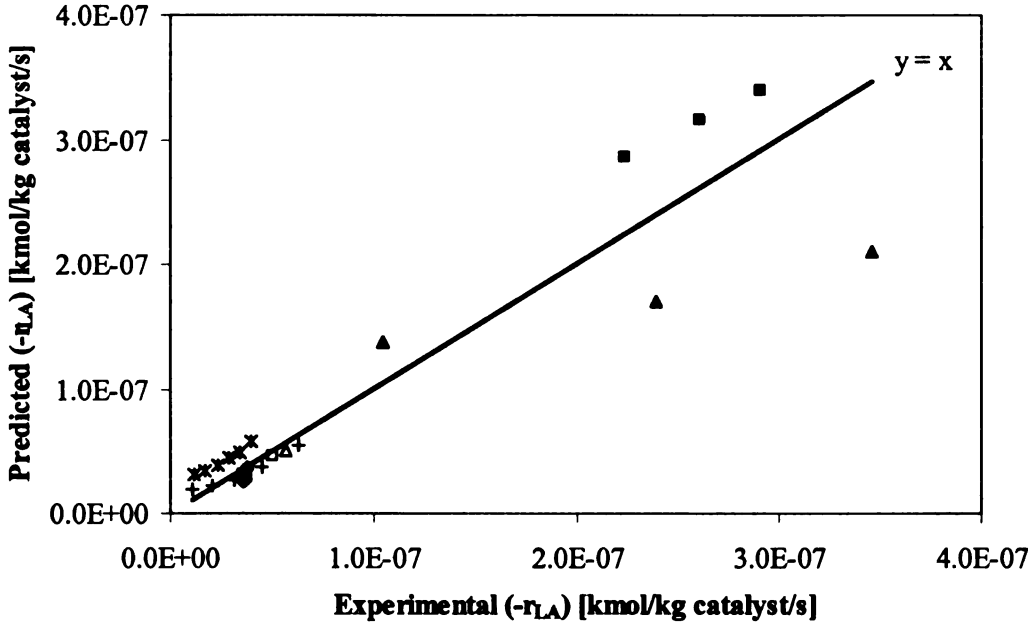

Figure 7.13. Experimental and predicted lactic acid rates in the hydrogenation of acid mixtures over Ru sponge.
Conditions: 403 K; 5 g Ru sponge/50 ml solution; 1000 rpm.

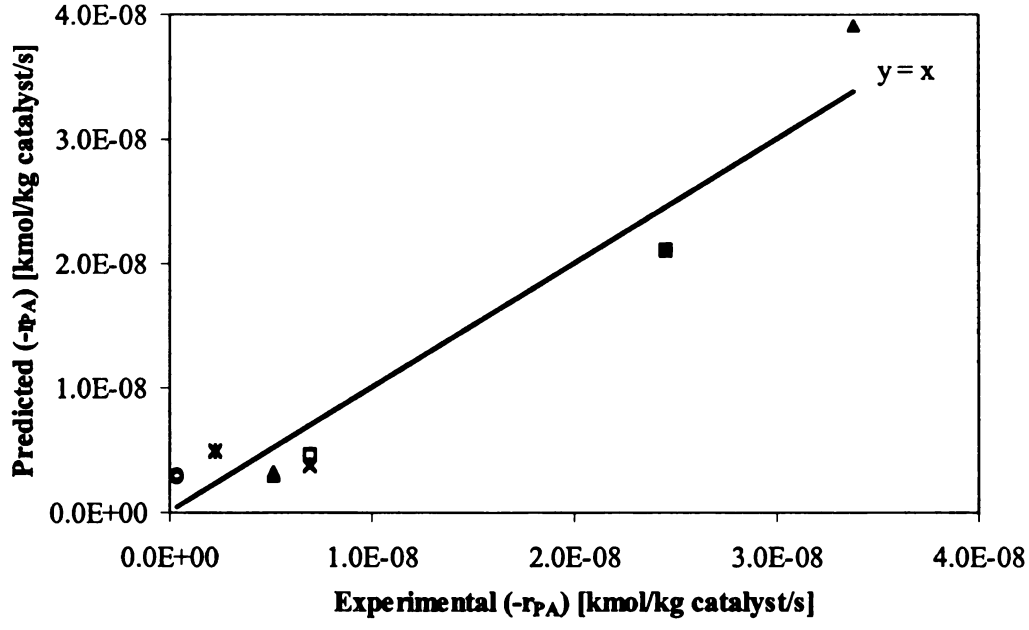

Figure 7.14. Experimental and predicted propionic acid rates in the hydrogenation of acid mixtures over Ru sponge.
Conditions: 403 K; 5 g Ru sponge/50 ml solution; 1000 rpm.

The average percent errors in prediction of hydrogenation rates of LA and PA, both individually and in mixtures, were calculated using Equations (7.16a) and (7.16b), and the results are shown in Table 7.5. The average percent errors for acid hydrogenations are within accepted range for kinetic modeling, considering the existence of uncertainty in measuring metal surface areas and normalizing ruthenium sponge activities.

Table 7.5. Average Error between Experimental and Predicted Rates over Ru Sponge at 403 K

Reaction System	Use Equation (7.16a)		Use Equation (7.16b)	
	Average Error (%)	Average Error of the Initial Rates (%)	Average Error (%)	Average Error of the Initial Rates (%)
Individual LA hydrogenation	28	23	30	25
Individual PA hydrogenation	41	34	43	38
LA in the hydrogenation of acid mixtures	34	20	27	25
PA in the hydrogenation of acid mixtures (all data)	**122**	**127**	**34**	**27**
PA in the hydrogenation of acid mixtures (omit PA rate data from Experiment 94) [d]	**34**	**30**	**25**	**21**

[d]The rate data of PA in Experiment 94 (mixture of 1M LA and 0.1M PA; 5g Ru-I-2; 403K; 7MPa H_2) were omitted in the error analysis. The PA conversion in this experiment was less than 4% after 50 hours of reaction. The polynomial fit of PA concentrations versus time can NOT give accurate prediction of experimental rates. The PA rate data are far off in the parity plot upon being fit, and thus introduce very large absolute percent errors (600-700%).

7.2.3. Comparison of the model parameters for acid hydrogenation over Ru/C and Ru sponge catalysts

A comparison of the model parameters for acid hydrogenation over Ru sponge with that determined from experiments over Ru/C is given in Table 7.6. The surface reaction rate constant for each acid was calculated on a metallic surface area basis (kmol acid/m^2 metal surface area/s) using Equation (7.21c):

$$k_{Acid} = k_{sA} C_{t1} (C_{t2})^2 \cdot K_{Acid} \cdot K_{H_2} \cdot S_{catalyst} \qquad (7.21a)$$

$$\left[\frac{m^3}{\text{kg catalyst} \cdot MPa \cdot s}\right] = \left[\frac{kmol}{\text{m}^2 \text{ metal} \cdot s}\right] \cdot \left[\frac{m^3}{kmol}\right] \cdot \left[\frac{1}{MPa}\right] \cdot \left[\frac{\text{m}^2 \text{ metal}}{\text{kg catalyst}}\right] \qquad (7.21b)$$

$$k_{sA} C_{t1} (C_{t2})^2 \left[\frac{kmol}{\text{m}^2 \text{ metal} \cdot s}\right] = \frac{k_{Acid}}{K_{Acid} K_{H_2} S_{catalyst}} \qquad (7.21c)$$

where $S_{catalyst}$ = metal surface area of the catalyst [m^2 metal / kg catalyst].

The surface reaction rate constants for LA and PA are about the same on the carbon-supported and un-supported ruthenium catalysts, given that we have substantial uncertainty (± 40%) in measuring the active surface area for the Ru sponge. The adsorption constant on Ru/C is 2.5 times that on Ru sponge for LA, and 7.5 times for PA. The relative magnitude of the adsorption constants on Ru/C and on Ru sponge were determined based on adsorption studies conducted on activated carbon support. The product 1-PrOH is responsible for inhibiting the PA hydrogenation rates on Ru/C due to

its strong competitive adsorption into the carbon micropore, while this effect is minimized on the nonporous Ru sponge. There is no difference in hydrogen adsorption affinity for the two catalyst cases.

Table 7.6. Comparison of the Kinetic Constants for Acid Hydrogenation over Ru/C and Ru Sponge at 403 K[e]

Kinetic Constants		Ru/C	Ru Sponge
Surface reaction rate constant for LA	$k_{sLA}C_{t1}(C_{t2})^2$ (kmol/m^2 metal surface area/s)	1.7E-08	1.7E-08 (± 6.8E-09)
Surface reaction rate constant for PA	$k_{sPA}C_{t1}(C_{t2})^2$ (kmol/m^2 metal surface area/s)	3.5E-09	5.7E-09 (± 2.3E-09)
Composite rate constant of LA	k_{LA} (m^3/kg catalyst/MPa/s)	1.0E-05	4.2E-07
Composite rate constant of PA	k_{PA} (m^3/kg catalyst/MPa/s)	1.7E-06	3.6E-08
Adsorption constant of LA	K_{LA} (m^3/kmol)	1.7	0.7
Adsorption constant of PA	K_{PA} (m^3/kmol)	1.4	0.18
Adsorption constant of PG	K_{PG} (m^3/kmol)	0.27	0
Adsorption constant of 1-PrOH	$K_{1\text{-}PrOH}$ (m^3/kmol)	2.9	0
Adsorption constant of H_2	K_{H2} (MPa^{-1})	0.21	0.22

[e]The metal surface areas are 1.6 m^2/g (Ru/C) and 0.16 m^2/g (Ru sponge), respectively.

7.3. Global model for the hydrogenation of organic acids over Ru/C catalyst – incorporating local pore concentrations into kinetic modeling

Adsorption of reactant and product species can have a major effect on local pore concentrations in activated carbon-supported metal catalysts. This is because the activated carbon micropores and functionalized carbon surfaces facilitate selective adsorption of organic species from water; at equilibrium this adsorption typically leads to local reactant and product concentrations in the catalyst vicinity (e.g. in activated carbon micropores) that are significantly different from those in bulk solution phase outside the carbon support.[3] Because chemical kinetics and mass transport are commonly represented in terms of concentration or mole fraction, a correct description of reaction kinetics must account for the difference in concentration between solution and pore. To gain a deeper understanding of aqueous-phase catalysis involving activated carbon-supported catalysts in general, Lars Peereboom[3] in Miller group conducted adsorption study on the carbon support for the prediction of local pore concentrations. We assume that reaction kinetics are the same for hydrogenations taking place on the surface of Ru sponge and inside the pore structures of Ru/C, if we compensate for pore effects of the carbon support. By incorporating local pore concentrations on Ru/C into the reaction kinetics on Ru sponge, we expect to be able to reliably predict hydrogenation rates of organic acids over Ru/C catalyst - the global model.

The local concentrations of reaction species LA, PA, PG, and 1-PrOH in the 3310 activated carbon micropores were calculated using the (extended) Langmuir adsorption model discussed in Chapter 5, based on the measured micropore volume of 0.17 cm^3/g carbon. The Langmuir adsorption model works well for bulk solution concentrations

below 0.5 M and temperatures from 298 K to 433 K. The kinetic data used in the global model were taken from all hydrogenation experiments performed over Ru/C at 403 K (shown in Table 3.1: P_{H2} = 3.4-10.3 MPa, and C_{acid} = 0.05-5 M). For the experiments with low initial concentrations ($\leq$ 0.5M) of acids, we applied pore concentrations instead of solution concentrations in the new modeling process. The pore concentrations are usually higher than the solution concentrations since organic species tends to fill the carbon pore. For the high concentration cases ($\geq$ 2M), we took bulk solution concentrations for modeling because the catalyst surface is saturated and there is no significant enhancement in local pore concentrations.

Kinetic parameters of the global model are given in Table 7.7. The surface reaction rate constants ($k_{sLA}C_{t1}(C_{t2})^2$ and $k_{sPA}C_{t1}(C_{t2})^2$) and equilibrium constants (K_{LA}, K_{PA}, K_{PG}, $K_{1\text{-}PrOH}$, and K_{H2}) were taken directly from the modeling results of Ru sponge shown in Table 7.6. The composite rate constants (k_{LA} and k_{PA}) for pore reactions on Ru/C were calculated based on surface reaction rate constants on Ru sponge by accounting for difference in metal surface area for the two catalyst cases (the metal surface area is 1.6 m^2/g for Ru/C, and 0.16 m^2/g for Ru sponge).

Figures 7.15-7.18 are parity plots of acid conversion rates for the hydrogenation of single and mixed acids on Ru/C catalyst. These parity plots illustrate the agreement between the experimental rates and the rates predicted by the global model. By incorporating local pore concentrations on Ru/C into the reaction kinetics on Ru sponge, the global model works reasonably well in prediction of the hydrogenation rates for single and mixed acids on Ru/C over a wide range of conditions (acid concentrations from 0.05 to 5M; hydrogen pressures from 3.4 to 10.3 MPa).

Table 7.7. Kinetic Constants for Acid Hydrogenation over Ru/C at 403 K (Global Model) [f,g]

Kinetic Constants		at 403 K
Composite rate constant of LA (calculated)	k_{LA} (m^3/kg catalyst/MPa/s)	4.2E-06
Composite rate constant of PA (calculated)	k_{PA} (m^3/kg catalyst/MPa/s)	3.6E-07
Surface reaction rate constant for LA	$k_{sLA}C_{t1}(C_{t2})^2$ (kmol/m^2 metal surface area/s)	1.7E-08
Surface reaction rate constant for PA	$k_{sPA}C_{t1}(C_{t2})^2$ (kmol/m^2 metal surface area/s)	5.7E-09
Adsorption constant of LA	K_{LA} (m^3/kmol)	0.7
Adsorption constant of PA	K_{PA} (m^3/kmol)	0.18
Adsorption constant of PG	K_{PG} (m^3/kmol)	0
Adsorption constant of 1-PrOH	$K_{1\text{-}PrOH}$ (m^3/kmol)	0
Adsorption constant of H_2	K_{H2} (MPa^{-1})	0.22

[f]Conditions: 403 K; 0.5 g (5 wt % Ru/C)/50 ml solution; 1000 rpm.
[g]Use pore concentrations.

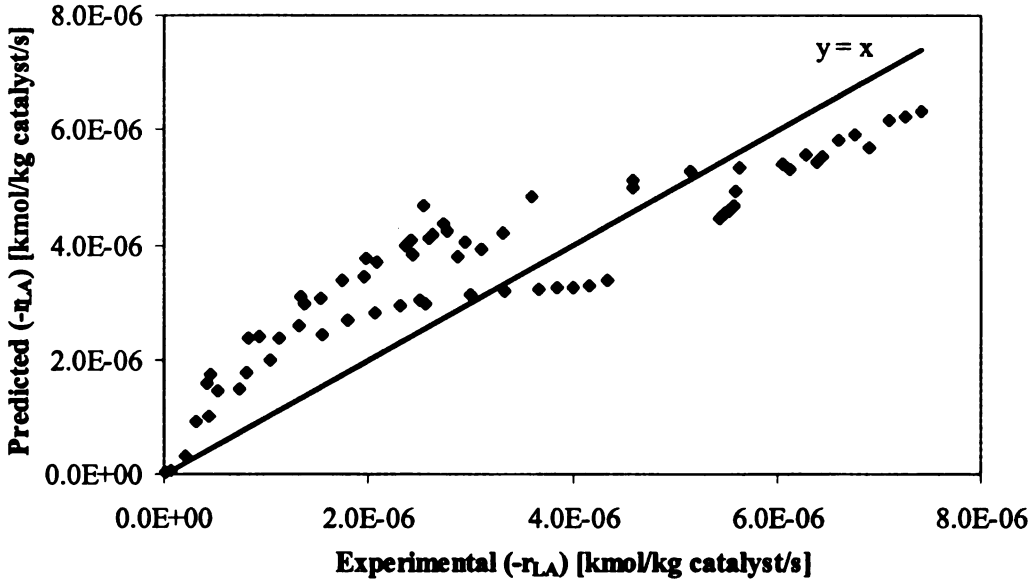

Figure 7.15. Experimental and predicted rates for individual lactic acid hydrogenation over Ru/C (global model; use pore concentrations).
Conditions: T = 403 K, 0.5 g (5 wt % Ru/C)/50 ml solution, 1000 rpm.

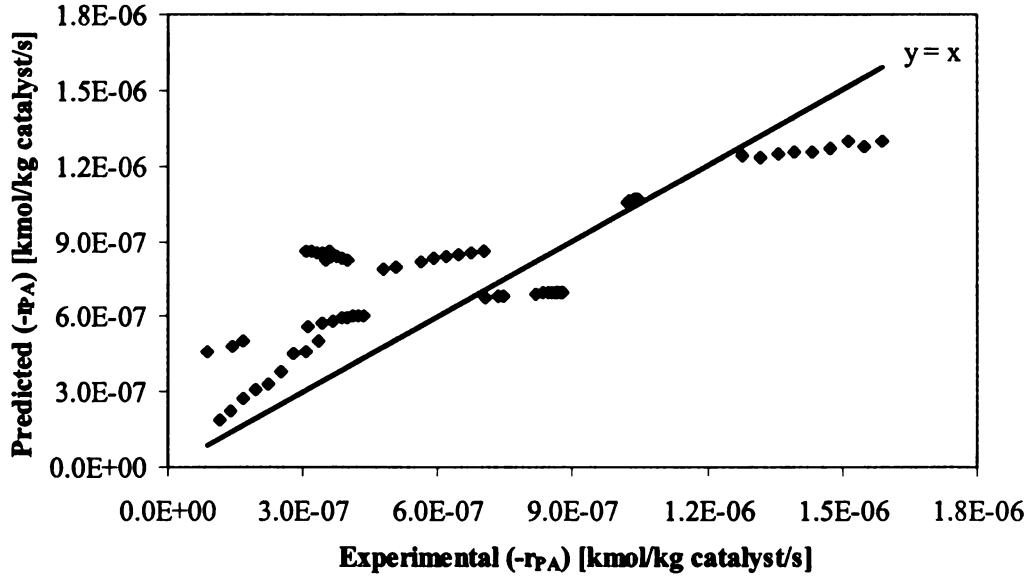

Figure 7.16. Experimental and predicted rates for individual propionic acid hydrogenation over Ru/C (global model; use pore concentrations).
Conditions: T = 403 K, 0.5 g (5 wt % Ru/C)/50 ml solution, 1000 rpm.

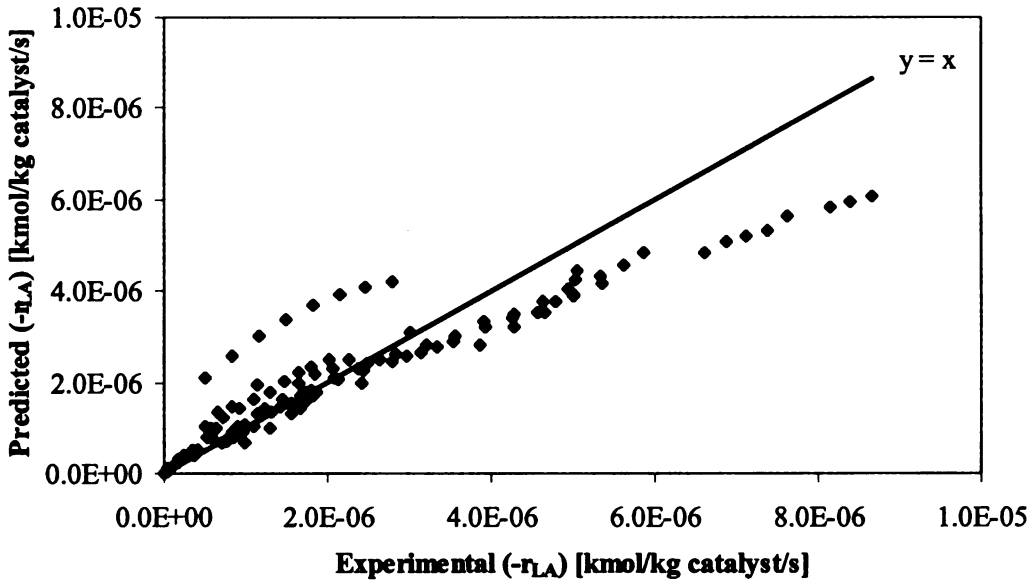

Figure 7.17. Experimental and predicted lactic acid rates in the hydrogenation of acid mixtures over Ru/C (global model; use pore concentrations).
Conditions: T = 403 K, 0.5 g (5 wt % Ru/C)/50 ml solution, 1000 rpm.

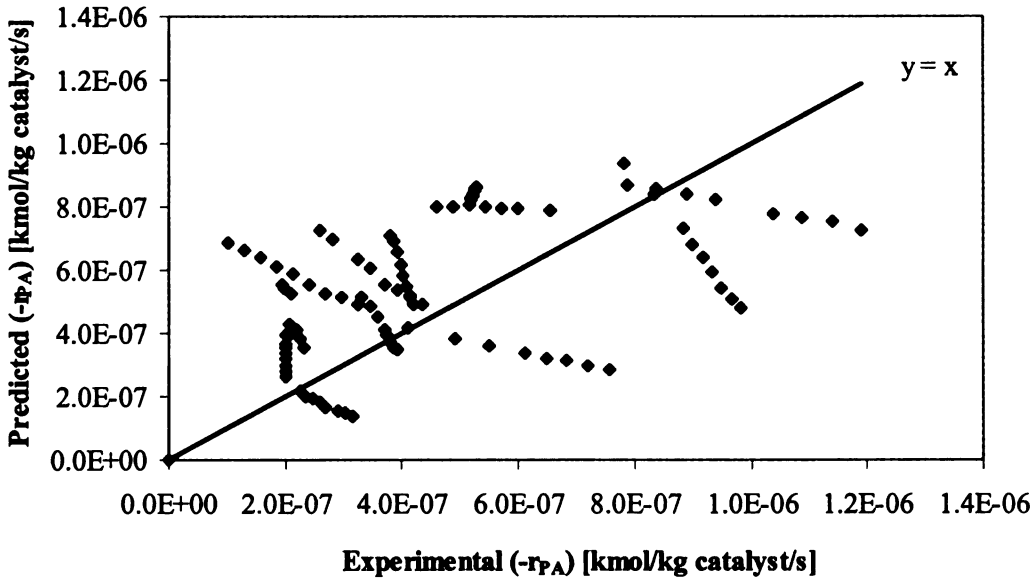

Figure 7.18. Experimental and predicted propionic acid rates in the hydrogenation of acid mixtures over Ru/C (global model; use pore concentrations).
Conditions: T = 403 K, 0.5 g (5 wt % Ru/C)/50 ml solution, 1000 rpm.

Table 7.8 shows the results of error analysis for the global model. The average percent errors in prediction of hydrogenation rates of LA and PA were calculated using Equations (7.16a) and (7.16b). The relatively large errors seen here are attributed to the uncertainty involved in measuring metal surface areas and the limited concentration range (less than 0.5M) applied to the adsorption model.

Table 7.8. Average Error between Experimental and Predicted Rates over Ru/C at 403 K (Global Model)

Reaction System	Use Equation (7.16a)		Use Equation (7.16b)	
	Average Error (%)	Average Error of the Initial Rates (%)	Average Error (%)	Average Error of the Initial Rates (%)
Individual LA hydrogenation	57	32	29	24
Individual PA hydrogenation	65	59	37	36
LA in the hydrogenation of acid mixtures	30	20	24	21
PA in the hydrogenation of acid mixtures	62	36	48	40

7.4. References

(1) Jere, F.; Jackson, J. E.; Miller, D. J. Kinetics of aqueous phase hydrogenation of L-alanine to L-alaninol. *Ind. Eng. Chem. Res.* **2004**, *43*, 3297.

(2) Yuqing Chen, Dennis J. Miller and James E. Jackson. Kinetics of Aqueous-Phase Hydrogenation of Organic Acids and Their Mixtures over Carbon Supported Ruthenium Catalyst. *Ind. Eng. Chem. Res.* **2007**, *46*, 3334-3340.

(3) Lars Peereboom, Benjamin Koenigsknecht, Margaret Hunter, James E. Jackson, and Dennis J. Miller. Aqueous-Phase adsorption of propylene glycol onto activated carbon. *Carbon* **2007**, *45*, 579-586.

Chapter 8. Conclusions and Future Work

Our research aims to develop an improved mechanistic understanding of organic acid hydrogenation on heterogeneous ruthenium catalysts in aqueous solution. We approach this goal by investigating the hydrogenation of LA and PA alone, together, and in mixtures with their alcohol products PG and 1-PrOH, over carbon-supported and un-supported ruthenium metal catalysts in a three-phase stirred batch reactor. The present study characterizes (competitive) adsorption and reaction by a generalized two-site L-H kinetic model that describes the hydrogenation rates of the acids (alone and mixed). The model includes effects of product adsorption and inhibition, and accounts for the difference in concentration between solution and carbon micropores. The model reliably predicted acid hydrogenation kinetics over a wide range of concentrations.

The future work:

(1) Hydrogenation of single acids over Ru sponge was investigated only at low concentrations ($\leq$ 0.1 M). For a more robust model, higher concentrations (0.5 M, 1 M, and 2 M) of initial feedstock may need to be included.

(2) We observed inconsistency in catalytic activity of the Ru sponge catalyst. Surface techniques, such as x-ray photoelectron spectroscopy (XPS), would provide insights into the changes to the catalyst due to different reaction conditions, surface defects, crystal faces, and the effects of foreign metals.

(3) Characterizing the configuration of species adsorbed on the ruthenium metal catalyst, and relate adsorption affinity and reactivity to substrate structure and feedstock composition, is still a major challenge of the present work. The continuous microreactor

system (Figure 2.4) designed by Lars Peereboom allows us to accurately measure the quantity of species adsorbed onto metal surfaces. Chemisorption of single acids and acid mixtures need to be observed at different concentrations (or concentration ratios) and temperatures for the purpose of characterizing their relative affinities for metal surface sites. The reversibility of species adsorption can be examined via temperature programmed desorption (TPD) technique. Attenuated total reflection infrared spectroscopy (ATR-IR) is a useful method to characterize substrates adsorption structures and their linkages with the catalyst surface in aqueous solution.[1] Isotopic labeling (H-D exchange) in combination with ^{13}C-NMR provides non-destructive measure of substrate-metal interactions, and helps us determine the reactivity of hydrogen atoms on different carbons of a specific organic acid. H-D exchange between D_2O and hydrogen yields important information about water-catalyst interaction and thus the role of water in aqueous phase hydrogenation.

References

(1) Dalavoy, T. S.; Jackson, J. E.; Swain, G. M.; Miller, D. J.; Li, J.; Lipkowski, J., Mild electrocatalytic hydrogenation of lactic acid to lactaldehyde and propylene glycol. *Journal of Catalysis* **2007**, *246*, (1), 15-28.